

**THE ROLE OF INFLAMMATION AND OXIDATIVE STRESS IN ADIPOCYTES
IN THE DEVELOPMENT OF INSULIN RESISTANCE**

A DISSERTATION
SUBMITTED TO THE FACULTY OF
UNIVERSITY OF MINNESOTA
BY

JOEL STEVEN BURRILL

IN PARTIAL FULFILLMENT OF THE REQUIREMENTS
FOR THE DEGREE OF
DOCTOR OF PHILOSOPHY

DR. DAVID A BERNLOHR, ADVISOR

AUGUST 2015

Acknowledgements

I would like to thank my graduate advisor Dr. David Bernlohr for his tremendous guidance and support over the past 6 years. His immense knowledge and patience make him a spectacular teacher. He has supported my interests and desires and has played a pivotal role in my development as a scientist.

I would like to thank the members and former members of my committee, Drs. Alex Lange, Eric Hendrickson, Do-Hyung Kim, Brian Fife and Xiaoli Chen, for their guidance during my time in graduate school. Their advice and expertise has helped mold my research.

To the members, both past and present, of the Bernlohr Laboratory, thank you for the help throughout the years. I must thank in particular Dr. Eric Long, a former post-doc in the laboratory, for teaching me, pushing me to think outside the box, for sarcastic interactions and for being a great friend. Thank you to Ann Hertzell for always having an open ear to conversations about science.

Thank you to the graduate students that have been a great support network, especially Adam Harvey, Jordan Becker, Frazer Heinis, Joe Belanto, Chris Braden and Melissa Ingram.

Dedication

This thesis is dedicated to the people that have supported me throughout this journey through graduate school

To my parents who have always been supportive and encouraging and for always loving me regardless of what has gone on.

To my brothers, Jeff, Pete and Tom, for always being someone to look up to.

To my extended family, thank you for everything you've done for me over the years.

To my girlfriend Bethany, for supporting me and putting up with my constant sarcasm and stress.

And to my friends Sean, Rob, Jason, Thomas, Cools and ARob for always being there when I need them.

TABLE OF CONTENTS

Acknowledgements	i
Dedication	ii
List of Tables	v
List of Figures	vi
Chapter 1	
Obesity, Inflammation, Oxidative Stress, Adipocyte Metabolism & Insulin Resistance	1
I. Metabolic Syndrome and Obesity Linked Insulin Resistance	2
II. Inflammation and Oxidative Stress	14
III. Metabolism and Mitochondrial Dysfunction	28
IV. Current Objectives	38
V. References	40
Chapter 2	
Proinflammatory cytokines differentially regulate adipocyte mitochondrial metabolism, oxidative stress, and dynamics	52
I. Summary	53
II. Introduction	55
III. Experimental Procedures	58
IV. Results	69
V. Discussion	89
VI. Acknowledgements	99
VII. Grants	99
VIII. Author Contributions	100
IX. References	101
Chapter 3	
Inflammation and ER Stress Regulate Branched-Chain Amino Acid Uptake and Metabolism in Adipocytes	106
I. Summary	107
II. Introduction	108
III. Research Design and Methods	110
IV. Results	116
V. Discussion	131
VI. Acknowledgements	135
VII. References	136
Chapter 4	

Rictor Oxidation and Disruption of the Mammalian Target of Rapamycin Complex 2 (mTORC2) Links Mitochondrial Oxidative Stress to Insulin Resistance in Adipocytes	140
I. Summary.....	141
II. Introduction	142
III. Methods	145
IV. Results	150
V. Discussion.....	165
VI. References.....	172
 Chapter 5	
Perspectives and Conclusions	177
I. References.....	183
 Complete Bibliography	184

List of Tables

Chapter 2: Proinflammatory Cytokines Differentially Regulate Adipocyte Mitochondrial Metabolism, Oxidative Stress and Dynamics	
Table 1: Primers used for quantitative real-time PCR (qPCR).....	67
Chapter 3: Inflammation and ER Stress Regulate Branched-Chain Amino Acid Uptake and Metabolism in Adipocytes	
Supplementary Table 1: Primers used for quantitative PCR to measure gene expression.....	112

List of Figures

Chapter 1

Adipocyte Metabolism, Oxidative Stress, Insulin Resistance & Mitochondrial Function

- Figure 1:** Adipocentric view of the development of obesity-linked insulin resistance.....12
- Figure 2:** Mitochondrial electron transport chain and ROS Production.....19
- Figure 3:** Formation of 4-HNE and 4-HHE.....22

Chapter 2

Proinflammatory Cytokines Differentially Regulate Adipocyte Mitochondrial Metabolism, Oxidative Stress, and Dynamics

- Figure 1:** Respiration profiling in chronic cytokine treatment of 3T3-L1 adipocytes.....70
- Figure 2:** Lipid and glucose metabolism following cytokine treatment of 3T3-L1 adipocytes.....72
- Figure 3:** Reactive oxygen species and protein carbonylation following cytokine treatment of 3T3-L1 adipocytes.....75
- Figure 4:** Sphingolipid profiles following cytokine treatment.....77
- Figure 5:** Expression of factors linked to mitochondrial biogenesis and function in response to cytokine treatment.....80
- Figure 6:** Mitochondrial morphology in cytokine-treated 3T3-L1 adipocytes.....83
- Figure 7:** Expression of proteins linked to mitochondrial fission and fusion in response to cytokine treatment.....85
- Figure 8:** Acute effects of TNF α on mitochondrial fragmentation.....87

Chapter 3

Inflammation and ER Stress Regulate Branched-Chain Amino Acid Uptake and Metabolism in Adipocytes

- Figure 1:** Obesity down-regulates the expression of genes of BCAA metabolism.....118
- Figure 2:** Inflammatory factors down-regulate the expression of genes of BCAA metabolism.....122
- Figure 3:** Obesity and inflammation down-regulate TCA cycle and anaplerotic reaction enzyme gene expression.....124
- Figure 4:** Leucine transport and metabolism in 3T3-L1 adipocytes.....126
- Figure 5:** Metabolomics analysis of 3T3-L1 cells.....128
- Figure 6:** ER stress down-regulates BCAA metabolism genes.....130

Chapter 4

Rictor Oxidation and Disruption of the Mammalian Target of Rapamycin Complex 2 (mTORC2) Links Mitochondrial Oxidative Stress to Insulin Resistance in Adipocytes

Figure 1: Obesity and inflammation down-regulate the expression of mitochondrial antioxidants.....	151
Figure 2: Prdx3 KD 3T3-L1 characterization.....	153
Figure 3: Oxidative stress in Prdx3 KD adipocytes.....	155
Figure 4: Mitochondrial function and morphology in Prdx3 KD adipocytes.....	157
Figure 5: Decreased insulin signaling in Prdx3 KD adipocytes.....	159
Figure 6: Prdx3 KD adipocytes do not exhibit ER stress or mtUPR....	161
Figure 7: Prdx3 KD induces protein oxidation and mTORC2 disruption.....	163

CHAPTER ONE

Obesity, Inflammation, Oxidative Stress, Adipocyte Metabolism & Insulin Resistance

Joel Burrill wrote this chapter in its entirety.

Metabolic Syndrome and Obesity Linked Insulin Resistance

Obesity is defined by the Center for Disease Control as an adult who has a BMI (Body Mass Index; calculated as weight in kilograms divided by height in meters squared) of 30 or higher. In recent years, the prevalence of obesity has risen in children and adolescents (ages 2-19) to 16.9% (1). The rise in the obesity epidemic has been linked to a general increase in caloric intake, coupled with a decrease in physical activity leading to weight gain.

The increased adiposity associated with poor nutritional decisions and the influence of genetic factors can lead to the development of tissue specific insulin resistance, especially in liver, skeletal muscle and adipose tissue (2). Insulin action in peripheral tissues plays a crucial role in maintaining blood glucose levels. When these tissues fail to respond to the insulin stimulus, blood glucose levels rise to a hyperglycemic state. In response to hyperglycemia, pancreatic β -cells produce and secrete more insulin. If β -cells fail to produce the amount of insulin required to control the glucose level at euglycemia, this can expose organs to toxic levels of glucose, called glucotoxicity. The elevations of glucose in many tissues, including the pancreas and liver, can alter function, decrease the ability to proliferate and even cause apoptosis (3). This link between glucotoxicity and apoptosis within the β -cell can lead to β -cell death and limits the amount of insulin produced. The timing of β -cell death also corresponds with the transition of insulin resistance to clinically diagnosed Type II Diabetes (T2D) (4).

Insulin resistant individuals are at a high risk of also developing coronary heart disease, hypertension and stroke. These diseases (hypertension, insulin resistance, stroke, heart disease) collectively are included in the definition of metabolic syndrome (5, 6). It is clear that weight loss, especially as a result of bariatric surgery, increases insulin sensitivity, but long-term lifestyle changes are challenging for obese insulin-resistant individuals (7, 8). Therefore, it is important to understand the molecular mechanisms behind insulin resistance and the development of T2D and this understanding could lead to new therapeutic approaches.

Insulin action within insulin-responsive tissues, such as muscle, liver and adipose, varies slightly. Although there is variation, insulin generally promotes glucose uptake and inhibits lipolysis and gluconeogenesis (9). Insulin is produced and secreted by pancreatic β -cells in response to the elevated blood glucose levels associated with food intake. In liver, insulin does not signal to increase glucose uptake, but rather signals to inhibit gluconeogenesis and stimulate glycogen synthesis. Glycogen is a branched chain polymer used to store glucose for later use. In addition to glycogen synthesis, insulin signals in liver to initiate lipogenesis through the activation of the transcription factor sterol regulatory element binding protein -1c (SREBP-1c). Lastly, insulin signals for lipoprotein uptake through the low-density lipoprotein (LDL) receptor. The insulin resistant

state in hepatocytes results in the inability to clear LDL from the blood stream and fasting hyperglycemia due to failure to suppress glucose output (10).

In contrast to the hepatocyte, one main role of insulin action in the adipocyte is to regulate glucose transporter type 4 (GLUT4) translocation allowing for increased glucose uptake. Furthermore, insulin action on the adipocyte is responsible for the inhibition of lipolysis, the process of liberating free fatty acids (FFAs) from the lipid droplet for use as energy in muscle, liver and brain during times of low glucose (11, 12). Lastly, failure of proper insulin signaling in the adipocyte can result in decreased lipogenesis through decreased activation of SREBP-1c (10). These insulin-stimulated pathways are critical not only for maintaining local tissue functions, but also affect whole body metabolism and the function of other tissues, such as muscle.

Skeletal muscle is the primary tissue for insulin-stimulated glucose metabolism. This glucose has three main fates; glycolysis for energy production in times of energy demand, glycogen synthesis for storage, and lipogenesis (10, 13). In mice lacking the insulin receptor in skeletal muscle, the muscle displays severe insulin resistance. However, glucose tolerance is normal due to up-regulation of insulin-independent glucose uptake as a compensatory mechanism. Furthermore, glucose uptake in other tissues, such as fat, is increased three fold

(14). Proper glucose uptake and gluconeogenesis in skeletal muscle is crucial for maintenance of euglycemia and insulin sensitivity.

The primary roles of insulin signaling are the control of cellular growth and differentiation as well as metabolism. Furthermore, insulin signaling and insulin sensitivity are required for control of blood glucose levels in the normal range of 4-7 mM (15). The maintenance of blood glucose levels requires insulin-responsive tissues to take up glucose from the blood upon an insulin stimulus. When insulin binds to the α -subunit of the insulin receptor, the tyrosine kinase domains of the β subunit are brought together and undergo transphosphorylation. Upon phosphorylation the receptor tyrosine kinases phosphorylate downstream targets including insulin receptor substrate (IRS), of which there are four isoforms. Tyrosine phosphorylated IRS1 creates docking sites for multiple Src homology 2- containing (SH2) proteins including the p85 regulatory subunit of phosphoinositide 3-kinase (PI3K) (16). This activation of PI3K leads to the production of phosphatidylinositol(3,4,5)-triphosphate (PtdIns-(3,4,5)-P3) which induces the activation of protein serine kinase cascades by recruitment of phosphoinositide-dependent kinase 1 (PDK1) and its substrate kinases, protein kinase B (PKB, or AKT), and atypical protein kinase Cs (PKCs) via their pleckstrin homology (PH) domains (17).

AKT plays a crucial role in insulin signaling. PDK1 phosphorylates AKT on Thr308 which activates AKT allowing for phosphorylation of downstream targets such as glycogen synthase kinase 3 α/β (GSK3 α/β), Akt substrate 160 kDa (AS160), Forkhead box O (FOXO) transcription factors, endothelial nitric oxide synthase (eNOS), phosphodiesterase 3b (PDE3b), tuberous sclerosis complex-2 (TSC2) and mammalian target of rapamycin (mTOR) (17, 18). Phosphorylation of GSK3 is critical for control for glycogen synthesis by decreasing the inhibitory phosphorylation levels of glycogen synthase (19). Phosphorylation of AS160 leads to the translocation of the glucose transporter GLUT4 to the plasma membrane (20). The phosphorylation of TSC2 on Ser939, Ser1130 and Thr1462 by AKT acts as a negative regulator of TSC complex activity allowing for mTOR translocation to the plasma membrane and mTOR complex 1 formation (mTORC1) (21-24). AKT can also be phosphorylated by mTOR complex 2 (mTORC2) on Ser473. Phosphorylation on Ser473 is required for full kinase activity of AKT and maximal FOXO phosphorylation (25-27). Failure for AKT to signal fully can result in decreased insulin signal transduction.

mTOR represents a complex node of signaling critical for metabolism and metabolic shifts within various tissues. mTORC1 and mTORC2 are large complexes with mTORC1 having six and mTORC2 having seven protein members, respectively. The atypical serine/threonine protein kinase mTOR is shared between both complexes. Furthermore, both complexes contain

mammalian lethal with sec-13 protein 8 (mLST8), DEP domain-containing mTOR-interacting protein (Deptor) and the Tti1/Tel2 complex. mTORC1 specific proteins include regulatory-associated protein of mammalian target of rapamycin (Raptor) and proline-rich Akt substrate 40 kDa (PRAS40). mTORC2 includes rapamycin-insensitive companion of mTOR (Rictor), mammalian stress-activated map kinase-interacting protein 1 (mSin1) and protein observed with rictor 1 and 2 (protor1/2) (28). These complexes play different roles but both are important for responding to environmental signals while maintaining metabolic homeostasis.

Upon insulin stimulation, downstream of mTORC1 are a number of signaling cascades that control protein synthesis, autophagy and energy homeostasis. mTORC1 phosphorylates transcriptional regulators eukaryotic translation initiation factor 4E-binding protein 1 (4E-BP1) and S6 kinase 1 (S6K1), which promote protein synthesis. Furthermore, mTORC1 promotes growth by negatively regulating autophagy. mTORC1 directly phosphorylates and suppresses the unc-51-like kinase 1 (ULK1)/mammalian autophagy-related gene 13 (Atg13)/focal adhesion kinase family-interacting protein of 200 kDa (FIP200) complex. Lastly, mTORC1 positively drives cellular metabolism by increasing hypoxia inducible factor 1 α (HIF1 α) expression and transcription, which is a positive regulator of many glycolytic genes and enzymes (28). The downstream targets of mTORC2 are distinct from mTORC1, in that AKT, Cullin 7 E3 ubiquitin ligase complex subunit F-box protein (Fbw8), and serum/glucocorticoid regulated

kinase 1 (SGK1) are targets for phosphorylation (28-30). mTORC2 directly phosphorylates AKT on serine 473 as mentioned earlier, resulting in full activation of AKT signaling (31). Fbw8 is part of an E3 ubiquitin ligase complex, and when phosphorylated by mTORC2 on serine 86 leads to the degradation of IRS1 (30). SGK1 activity is completely dependent on mTORC2, and this activity is responsible for control of ion transport and cell growth, as well as phosphorylation of FOXO1 and FOXO3a transcription factors (32).

mTOR as described above plays a critical role in normal metabolism, however in the lean to obese transition, mTOR signaling can be altered leading to disrupted signaling. In adipose tissue, mTOR plays a pivotal role in adipogenesis and central metabolism as mice with an adipose-specific loss of mTORC1 are lean, resistant to high-fat diet-induced obesity and have fewer adipocytes (33). Furthermore, loss of mTORC2 in adipose tissue results in normal fat distribution, but a defect in AKT phosphorylation leading to an increase in lipolysis and FFA in serum (34). Other studies in mice fed a high-fat diet have elevated levels of mTORC1 activity as seen by increased S6K1 phosphorylation resulting in the negative regulation of insulin signaling, thus perpetuating adipose tissue insulin resistance. One reason for this increased mTORC1 activity is due to the increased levels of circulating nutrients, such as the branched-chain amino acids and pro-inflammatory cytokines present locally in adipose tissue (35). The role

mTOR plays in signaling for adipogenesis and metabolic homeostasis is critical for proper adipocyte function.

Perhaps the greatest role of the adipocyte is the storage and release of lipids.

The adipocyte takes up glucose through the insulin-independent glucose transporter, GLUT1, and the insulin-dependent glucose transporter, GLUT4.

Glycolysis is responsible for breaking down glucose into two pyruvate molecules and generating two ATP molecules in the process. The acetyl-CoA produced has two fates, fatty acid synthesis and glycerol-3-phosphate synthesis. Both of these molecules are critical for triglyceride synthesis (36). For fatty acid synthesis, the pyruvate generated through glycolysis enters the mitochondria and is converted by pyruvate dehydrogenase to acetyl-CoA, where it enters the TCA cycle and is converted to citrate. This citrate can then be transported back to the cytoplasm and converted back to acetyl-CoA. Subsequently, cytoplasmic acetyl-CoA can be carboxylated, by acetyl-CoA carboxylase, to malonyl-CoA and produce fatty acyl-CoAs. Glycerol-3-phosphate acyltransferase (GPAT) adds the first fatty acyl-CoA to glycerol-3-phosphate. Following this addition, two more fatty acyl-CoAs are esterified into the glycerol-3-phosphate backbone, generating triglycerides (37). This process is referred to as *de-novo* lipogenesis and the triglycerides are then stored in the lipid droplet within adipocytes. It is important to note that a second source of acetyl-CoA comes from fatty acid uptake. Fatty acids can be liberated on the extracellular surface of the plasma membrane from lipoproteins by

lipoprotein lipase (LPL) and transported into the cell by fatty acid transport protein 1 (FATP1) and fatty acid translocase (CD36). Once inside the cell, these fatty acids are converted to acyl-CoAs by acyl-CoA synthase and then used for *de-novo* lipogenesis (36). Importantly, previous studies in adipocytes have shown that FATP1 is stimulated by insulin and that knockdown in adipocytes reduces intracellular TG (38). Lipogenesis plays a critical role in the lean-to-obese transition as storage of excess nutrients as fat is required for metabolic health and if nutrient uptake and lipogenesis is disrupted in the adipocyte, it can lead to development of major metabolic challenges in other tissues.

Opposing lipogenesis in adipocytes is the process of lipolysis. This is the process by which fatty acids are released from the lipid droplet and secreted into circulation to be used by other tissues as energy. Lipolysis is a good measure of adipose tissue insulin sensitivity as it is a process inhibited by insulin. In this process, insulin signaling through IRS1 to PI3K activates PDE3b, leading to a decrease in cyclic AMP (cAMP) and negative regulation of protein kinase A (PKA) activity. PKA is responsible for phosphorylation of two major lipases, adipose triglyceride lipase (ATGL), the lipase responsible for the initial and rate limiting cleavage of triglyceride to diglycerides, and hormone-sensitive lipase (HSL), which is responsible for the cleavage of diglycerides to monoglycerides. Furthermore PKA is responsible for phosphorylation of perilipin, a protein that coats the outer membrane of the lipid droplet. When perilipin is phosphorylated, a

conformation change occurs allowing for access of lipases to the lipid droplet (39, 40). During times of nutritional overload, tissues fail to respond to insulin properly, and in adipose tissue this can lead to unrepressed lipolysis and elevations in circulating free fatty acids that are a hallmark of metabolic disease.

The role of adipose tissue in central metabolism, as discussed throughout this chapter, has led to the development of the adipocentric view of systemic insulin resistance (Figure 1). In this model, through overnutrition and/or genetics, adipose tissue undergoes hypertrophy. Furthermore, the resident immune cells, such as macrophages, can be polarized by the FFAs secreted by adipocytes to an inflammatory state. These immune cells secrete pro-inflammatory factors that act as recruitment factors for further infiltration of immune cells or act back upon the adipocyte signaling, causing changes in metabolism and adipokine secretion. Those adipokines that are secreted systemically, like leptin and adiponectin, play major roles in metabolic signaling in other tissues. This model sets forth the idea that systemic insulin resistance occurs because of local adipose tissue insulin resistance. This model is supported by multiple lines of evidence. Firstly, the adipose-specific GLUT4 knockout mouse shows profound insulin resistance, especially in the skeletal muscle and liver, and develops glucose intolerance and hyperinsulinaemia (41). All of these changes are hallmarks of metabolic disease and support the model that adipose tissue is the initiating factor in development of insulin resistance and T2D. A second line of evidence supporting this model

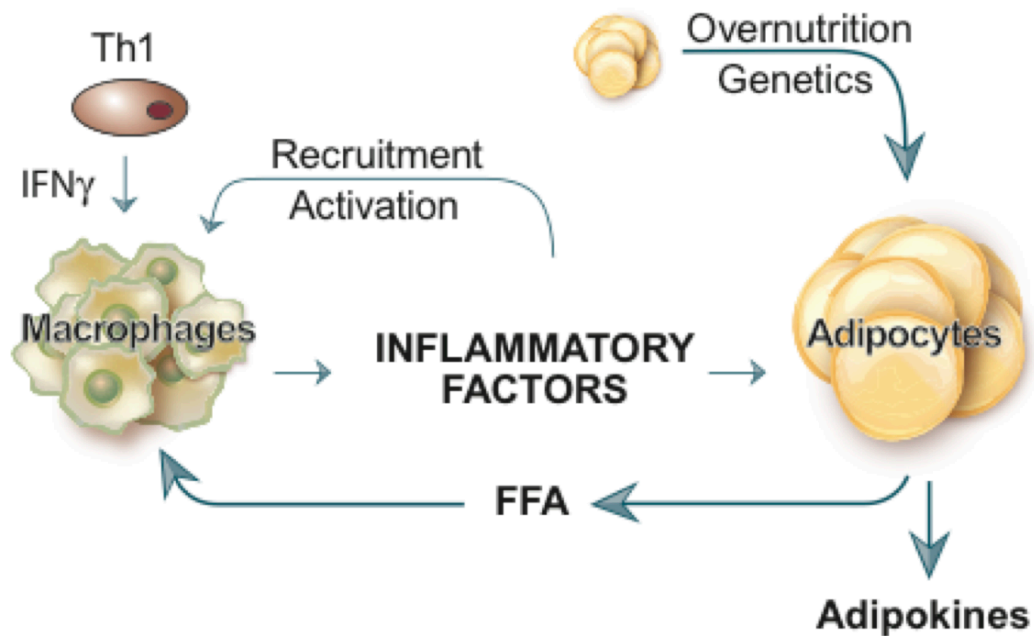


Figure 1: Adipocentric view of the development of obesity-linked insulin resistance. Accumulation of excess lipid in the adipocyte from over nutrition leads to inflammation in the adipose tissue, signaling for recruitment and polarization of macrophages to the inflammatory state. This propagates the inflammatory environment and contributes to local insulin resistance. Cytokines and lipids secreted from adipose tissue act in both a paracrine and autocrine manner to influence insulin sensitivity of other tissues, such as muscle and liver.

Credit to Tony Hertzal for creation of this figure for use by the Bernlohr Lab.

comes from the adipose-specific insulin receptor knockout mouse. These mice are protected from obesity-induced glucose intolerance and have reduced fat mass. Furthermore, these mice show a decrease in suppression of lipolysis and a decrease in triglyceride synthesis (42). Another piece of supporting evidence comes from the leptin-deficient mouse (*ob/ob*). Leptin is an adipokine, a circulating factor secreted from adipocytes, which acts via hypothalamic receptors to inhibit feeding (43). The *ob/ob* mouse has been highly studied since its discovery in 1949 and the primary characteristics of the mouse are hyperphagia, obesity, hyperinsulinaemia and hyperglycemia. These mice are highly insulin resistant and as such have been used as a model for obesity and T2D for many years (44). As leptin is solely derived from adipose tissue, this mouse model provides good evidence that adipocyte biology and signaling can drive the development of systemic insulin resistance. All of these models provide supporting evidence that proper signaling in adipose tissue is critical for whole body insulin sensitivity.

Inflammation and Oxidative Stress

The first evidence of a link between obesity, inflammation and insulin resistance came from the Spiegelman lab in the early 1990s when they identified that tumor necrosis factor alpha (TNF α) was expressed in adipose tissue of obese mice, and promoted insulin resistance by serine phosphorylation of IRS1 (45).

Furthermore, in 2003 two reports demonstrated obesity leads to the infiltration of macrophages into adipose tissue and that macrophages are primarily responsible for the inflammation observed (46, 47). It has since been observed that up to 45-60% of cells within adipose tissue of obese mice are macrophages, as identified by their surface marker F4/80, compared to adipose tissue of lean mice which 10-15% of cells are macrophages (48). Furthermore, the macrophages in lean animals have an alternatively activated (M2) phenotype. The M2 phenotype demonstrated by ARG1⁺CD206⁺CD301⁺ surface markers is less inflammatory as compared to adipose tissue macrophages from obese mice which display a classically activated, inflammatory (M1) phenotype as demonstrated by NOS2⁺TNF⁺ surface markers (49, 50).

Classically activated macrophages contribute to the pathogenesis of obesity-induced insulin resistance in a number of studies. Deletion of the CD11c, a transmembrane protein found on macrophages and dendritic cells, in macrophages reduces adipose tissue inflammation and improves insulin action without changing weight gain (51). Furthermore, mice deficient of IKK β (1 μ B

Kinase β) in myeloid cells (including macrophages) reduce the macrophage-mediated inflammation in adipose tissue, which results in prolonged insulin sensitivity (52). IKK β is critical for nuclear factor kappa-light-chain-enhancer of activated B cells (NF- κ B) signaling as it phosphorylates I κ B. When I κ B is phosphorylated it releases the NF- κ B dimer of RelA and p50 allowing nuclear translocation and activation of transcription of inflammatory genes (53). Adipose tissue fatty acid homeostasis, a hallmark of obesity, triggers the activation of resident macrophages by saturated fatty acids binding to the pattern-recognition receptor Toll-like receptor 4 (TLR4) (54). TLR4 signaling results in the activation of NF- κ B signaling leading to the production of pro-inflammatory cytokines such as tumor necrosis factor α (TNF α), monocyte chemoattractant protein 1 (MCP1) and interleukin-6 (IL-6) (55). These cytokines act upon adipocytes to initiate inflammatory signaling, as well as act in an autocrine manner perpetuating the inflammatory signal. Furthermore, cytokines like MCP1 are important for recruitment of monocytes and macrophages from circulation into the adipose tissue to further increase the level of inflammation (56). It is important to note that in normal inflammatory signaling, there is the induction of the innate immune system that corresponds with increased macrophage infiltration, followed by an induction of the adaptive immune response, and then resolution of inflammation. However in the obese state within adipose tissue, the inflammation does not resolve, resulting in a chronic-low grade inflammatory state (57).

Alternatively activated (M2) macrophages are primarily found in lean adipose tissue, especially subcutaneous adipose tissue, and generally protect against the negative effects seen with diet-induced obesity (58). These macrophages play an important role in tissue homeostasis and wound repair. Cytokines like interleukin-4 (IL-4) and interleukin-13 (IL-13) secreted from other immune cells, such as eosinophils, play an important role in activating M2 macrophages (48). Upon stimulation by IL-4 or IL-13, macrophages activate the IL-4 receptor, which in turn, activates the janus-activated kinase (JAK) and the signal transducer and activator of transcription (STAT) family of proteins (59, 60). IL-4 also stimulates macrophages to activate peroxisome proliferator-activated receptors (PPARs), specifically PPAR δ , which are ligand-dependent transcription factors that act as fatty acid sensors and control expression of glucose and lipid metabolism genes (61). PPAR δ and STAT6 working in parallel up regulate a number of genes critical for M2 polarization such as arginase 1 (Arg1), chitinase-like 3 (Ym1) and resistin like α (Fizz1) (62). Under lean conditions production of IL-13 promotes M2 activation and suppression of M1 polarization through the production of a second anti-inflammatory cytokine interleukin-10 (IL-10). However, in the case of obesity, inflammatory FFAs activate TLR4 signaling and decrease PPAR γ signaling enough to derepress the inflammatory program of macrophages leading to the polarization and further recruitment of M1 macrophages (56).

Many studies have demonstrated a link between inflammation, with pro-inflammatory cytokines like $\text{TNF}\alpha$, to both oxidative stress and insulin resistance (45, 63-65). While these studies are convincing, there is still debate as to the exact mechanism behind how inflammation leads to oxidative stress.

Oxidative stress is characterized as an imbalance between the production of reactive oxygen species (ROS) and the activity of the antioxidant defense system (66). The three main ROS within the cellular environment are superoxide anion ($\text{O}_2^{\cdot-}$), hydrogen peroxide (H_2O_2) and hydroxyl radical ($\cdot\text{OH}$). ROS play important roles in normal signaling within the cell, but an imbalance in production or detoxification can lead to negative effects. These ROS, if not metabolized, are capable of non-enzymatically modifying proteins, DNA, RNA and lipids in their biological environment. This enables them to act as signaling molecules in various metabolic pathways (61, 67-69).

ROS are produced basally as a byproduct of normal metabolic processes from many sources. These sources include xanthine oxidase, nitric oxide synthase and NADPH oxidase (70). Furthermore, within the mitochondria there are eight known sources of ROS production, including pyruvate dehydrogenase and 2-oxoglutarate dehydrogenase (71, 72). The largest source of mitochondria ROS come from the electron transport chain (ETC). Under physiological conditions electrons are passed between complexes in the ETC releasing a small amount of

energy that is used to pump hydrogen ions into the inter-mitochondrial membrane space. This electrochemical potential created across the inner mitochondrial membrane is then dissipated through the F_0F_1 ATP synthase, coupling its energy release to the formation of ATP. This process, termed oxidative phosphorylation (OxPhos), which will be discussed more in the next section, has the potential to leak electrons from Complexes I, II and III, and due to the molecularly oxygen-rich environment, these leaked electrons can readily react with molecular oxygen to form $O_2^{\cdot-}$ (Figure 2) (73). Superoxide anion is readily metabolized by superoxide dismutase (SOD). Mitochondrial SOD (SOD2, MnSOD) and cytoplasmic SOD (SOD1, Cu/Zn-SOD) catalyze the metabolism of $O_2^{\cdot-}$ to H_2O_2 at a rate of $\sim 10^9 M^{-1} s^{-1}$, which is $\sim 10^4$ faster than an uncatalyzed reaction (74, 75). This results in little free $O_2^{\cdot-}$ available to react with other biomolecules in the local environment.

H_2O_2 is the most stable and diffusible form of ROS produced in mammalian cells. It is required for many cellular functions, including differentiation of preadipocytes to adipocytes (76). Antioxidant enzymes such as catalase (CAT), peroxiredoxin (PRDX) and glutathione peroxidase (GPX) reduce H_2O_2 to O_2 and H_2O . Disruption of H_2O_2 metabolism can result in H_2O_2 accumulation, result in production of hydroxyl radical ($\cdot OH$) through the metal-catalyzed Fenton reaction (77, 78). As $\cdot OH$ cannot be metabolized, $\cdot OH$ can only be removed via damaging reactions with DNA, proteins and lipids.

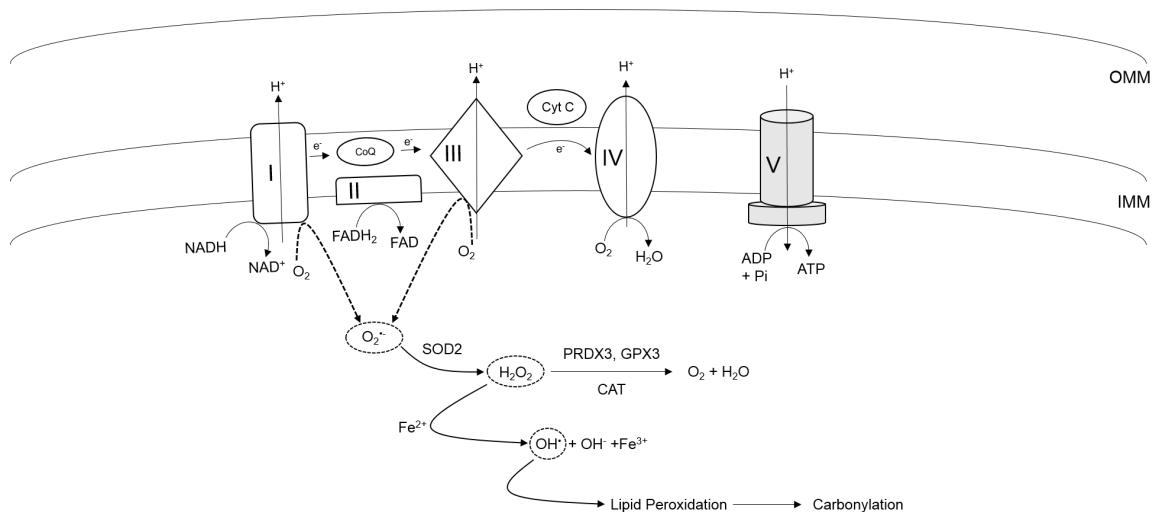


Figure 2: Mitochondrial Electron Transport Chain and ROS Production

A schematic representation of the electron transport chain. A potential is generated across the inner-mitochondrial membrane (IMM) by pumping H^+ through complexes I, III and IV. This potential is used to drive ATP synthesis through the F_0F_1 ATP Synthase. Electron leakage can occur from Complex I and III where they react with molecular oxygen to form superoxide anion. Further ROS generation can occur through metabolism of superoxide anion to hydrogen peroxide and Fenton chemistry to form hydroxyl radical. These species are circled in a dotted line.

Opposing the accumulation of ROS is the antioxidant response. The cell maintains basal levels of antioxidants and in response to elevated levels, the antioxidant response is initiated. This response is controlled through nuclear factor erythroid 2-related factor 2 (NRF2) and Kelch ECH associating protein 1 (KEAP1). NRF2 is, under conditions of low ROS, a cytoplasmic protein that is complexed to KEAP1. The complex of NRF2 and KEAP1 leads to the ubiquitination of NRF2 and targets it to the ubiquitin proteasome. Upon elevations of ROS, three cysteine residues on KEAP1 are oxidized, Cys151, Cys273 and Cys288. This oxidation of KEAP1 releases NRF2, allowing for nuclear translocation. NRF2 is the critical transcription factor that binds to the antioxidant response element (ARE), initiating the transcription of many antioxidants including SOD, GPXs, PRDXs and glutathione-s-transferases (GSTs) (79, 80). Aberrant antioxidant response can lead to ROS accumulation, overwhelming metabolic capacity leading to production of species like $\cdot\text{OH}$ that cannot be metabolized.

Damage to lipids via radical attack, termed lipid peroxidation, has been widely studied as a mechanism of radical-induced cellular damage. Polyunsaturated fatty acids (PUFAs) are particularly susceptible to lipid peroxidation. PUFA may be subject to multiple oxidation events followed by bond rearrangement and degradation to small, reactive, diffusible molecules. These small molecules include malondialdehyde (MDA), straight chain aldehydes and α,β -unsaturated

aldehydes such as 4-hydroxynonenal (4-HNE), 4-oxononenal (4-ONE), acrolein and 4-hydroxyhexenal (4-HHE) (81). The formation of specific α,β -unsaturated aldehydes species is dependent on the composition of fatty acids esterified into membranes. 4-HNE and 4-ONE are products of ω -6 PUFA such as arachidonic acid (AA) (20:4; ω -6) or linoleic acid (18:2; ω -6) (Figure 3A) (81). In contrast to 4-HHE, is a product of ω -3 PUFA such as docosahexaenoic acid (DHA) (22:6; ω -3) and α -linolenic acid (18:3; ω -3) (Figure 3B) (81). Tissues high in DHA and other ω -3 PUFA, such as brain, produce greater levels of 4-HHE compared to 4-HNE/4-ONE (82-86). Adipose tissue, both subcutaneous as well as visceral, is high in ω -6 PUFA and thus produces greater levels of 4-HNE/4-ONE compared to 4-HHE (87-90).

α,β -unsaturated aldehydes such as 4-HNE, 4-ONE, and 4-HHE, are metabolized and eliminated via a number of mechanisms including phase I metabolism, phase II metabolism, or chemical adduction to the side chains of histidine, lysine or cysteine. Phase I metabolism consists of a series of oxidation and reduction reactions that decrease the reactivity around the carbon 3 (C3) center of these aldehydes (91). For 4-HNE, aldehyde dehydrogenase (ALDH) results in the formation of *trans*-4-hydroxy-2-nonenic acid, which can be further oxidized by β -oxidation. Furthermore, aldo-keto reductase (AKR) can reduce the aldehyde in 4-HNE to form 1,4-dihydroxynonene. Lastly, alkenal/one oxidoreductase (AO), can

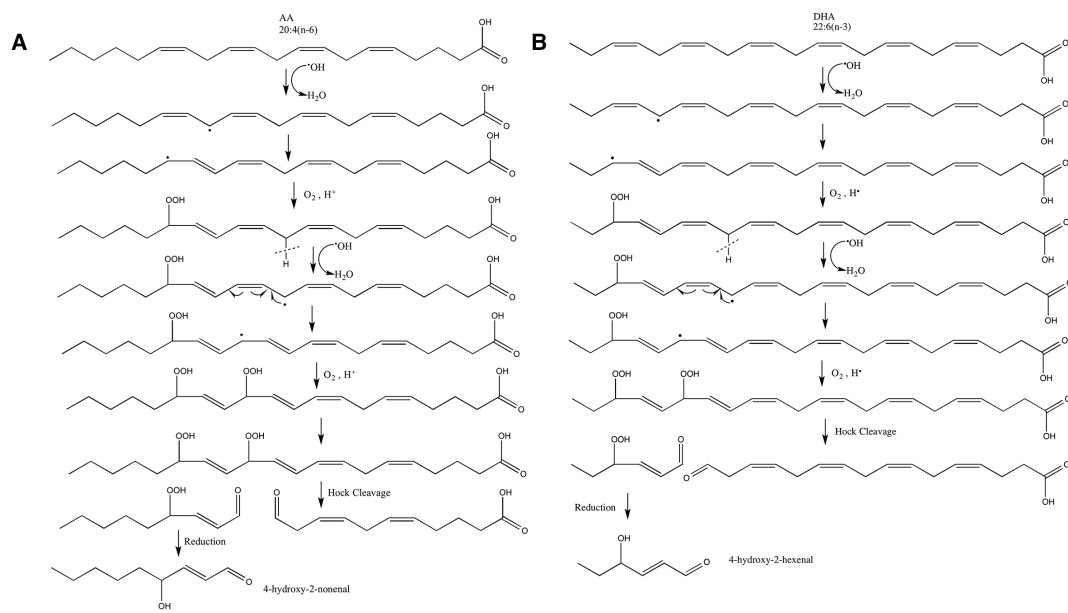


Figure 3: Formation of 4-HNE and 4-HHE

Mechanism of formation of A) 4-hydroxynonenal from arachidonic acid (AA) and B) 4-hydroxyhexenal from docosahexaenoic acid (DHA).

reduce the unsaturated 2,3 double bond which results in 4-hydroxynonanal (91). All three of these reactions reduce the likelihood of Michael addition of aldehydes to cysteine, histidine or lysine.

Phase II metabolism results in the glutathionylation of these aldehydes at C3.

The primary enzyme for glutathionylation of 4-HNE is glutathione-S-transferase A 4 (GSTA4) (92, 93). GSTA4 is selective for 4-HNE with a catalytic activity of $k > 3 \times 10^6 \text{ M}^{-1} \text{ s}^{-1}$ which is 10-fold higher than its activity towards 4-HHE (94).

Glutathionylated molecules, such as glutathionylated-4-HNE (GS-HNE), are further metabolized by AKR or ALDH, which represents phase I metabolism. The glutathionylated metabolites of 4-HNE are then actively exported from the cell by RLIP76 or multidrug resistance protein 1 (MRP1) with subsequent urinary excretion (95). Disruption of metabolism of 4-HNE and other α,β -unsaturated aldehydes can result in accumulation and increased adduction to amino acid side chains on proteins to form Schiff bases or Michael adducts in a process called protein carbonylation.

Protein carbonylation is a chemically non-reversible, covalent modification and the residues affected, histidine, lysine and cysteine, when modified can cause alterations in protein function. It is believed that Michael addition, the nucleophilic attack at the C3 carbon of the lipid by the side chain of the amino acid, represents ~80% of all carbonyl adducts with Schiff bases, whereas the addition

of the lipid to the primary amine of lysine, representing the other 20% (96).

Protein carbonylation plays a role in many disease states including liver steatosis, obesity, and some neurodegenerative diseases (97-101).

The role of adipose tissue carbonylation in obesity has been investigated in both murine and human models (67, 99). In rodent models, many proteins in both the cytoplasm and mitochondria are carbonylated (67, 98). Adipocyte fatty acid binding protein (AFABP) is carbonylated at Cys117 resulting in a decreased ability to bind fatty acids (98). Moreover, many proteins within the mitochondrial oxidative phosphorylation chain (OxPhos), tricarboxylic acid (TCA) cycle and branched chain amino acid (BCAA) metabolism are carbonylated (67).

Furthermore, in cases of obesity and inflammation within adipose tissue, Gsta4, Prdx3, Gpx3 and Aldh2 are transcriptionally down regulated which can lead to inability to metabolize ROS and lipid peroxidation products (87, 99, 102). Taken together, these data provide strong evidence for the role of carbonylation and oxidative stress in the development of obesity-induced insulin resistance.

In addition to lipid peroxidation, ROS have the ability to directly alter the redox status of proteins. These alterations, play an important role in physiology as well as in disease states (103-106). H_2O_2 can oxidize a variety of targets within the cell, resulting in altered protein function and signaling. Specifically, H_2O_2 can oxidize cysteine- or methionine-containing proteins. It is estimated that

approximately 10% of all cysteine residues within the proteome are redox sensitive. Furthermore, the sulfur atom found on cysteine residues can exist in many states, including the thiolate anion ($-S^-$), a free sulfhydryl ($-SH$), sulfenic acid ($-SOH$), sulfinic acid ($-SO_2H$) and sulfonic acid ($-SO_3H$) or a disulfide ($-S-S-$) (104). Although H_2O_2 is capable of oxidizing free sulfhydryls found on cysteine residues, this reaction is unfavorable under physiological conditions. However, H_2O_2 is much more reactive with the thiolate anion, but under physiological conditions the pKa of a solvent-exposed cysteine residue is about 8.3, and therefore exists in the protonated form (106). Some proteins are capable of shielding their cysteine residues in the thiolate form, which allows for targeted specificity for oxidation by H_2O_2 resulting in formation of sulfenic acid (104).

Sulfenic acid is important in some physiological processes, particularly with regard to protein phosphatases (107). Nearly all tyrosine phosphatases contain conserved redox sensitive cysteine residues that become oxidized in the presence of low levels of hydrogen peroxide. This oxidation temporarily decreases the activity of the enzyme allowing for propagation of phosphorylation signaling cascades. In adipose tissue, binding of insulin to the insulin receptor initiates not only the insulin signaling cascade, but also the activation of NADPH oxidase (108). Upon activation, the NADPH oxidase releases superoxide anion into the extracellular compartment. SOD present on the outer membrane converts $O_2^{\cdot-}$ to H_2O_2 . Increases in extracellular hydrogen peroxide levels create

a favorable concentration gradient allowing for its diffusion back into the cell (104). Intracellular H_2O_2 is then capable of oxidizing cysteines on the tyrosine protein phosphatase PTEN (phosphatase and tensin homolog) to sulfenic acid on Cys124 rendering it inactive (109). Inactivation of PTEN under insulin-stimulating conditions is favorable to the cell because it amplifies the insulin signal by allowing for the phosphorylation cascade to occur in an uninhibited manner (110). Because the formation of sulfenic acids are reversible, PTEN does not remain permanently inactivated. Enzymes like thioredoxin are able to reduce these oxidized cysteines in a glutathione-dependent manner resulting in recycling the protein back to its active state (58, 108, 111, 112).

Glutathione plays a central role in oxidative stress and oxidative damage.

Glutathione (GSH), or γ -glutamylcysteinylglycine, is a tripeptide that serves many roles within the cell. γ -Glutamylcysteine ligase followed by glutathione synthetase catalyze the formation of glutathione from glutamate, cysteine and glycine.

Glutathione plays a critical role in maintaining the proper redox balance within the cells as it can be used as a cofactor for enzymatic reductions and as a result glutathione can cycle between the oxidized GSSG state and the reduced GSH (113). N-acetylcysteine (NAC) is an antioxidant commonly used in experimental contexts and performs this role by replenishing the free GSH pools and scavenging aldehydes (114). Maintaining a normal pool of GSH is critical for normal cellular antioxidant function, and in the case of obesity, elevated levels of

ROS shift the balance in the GSH/GSSG ratio to the more oxidized state which is linked to impaired insulin action (115). Given the importance of GSH in the antioxidant response and its role in insulin action, increasing the levels of GSSG may be one way ROS directly affect insulin resistance in adipocytes.

It is clear that inflammation and oxidative stress are linked within adipose tissue. Driven by obesity, adipose tissue maintains a chronic, low-grade, irresolvable inflammatory state that drives ROS levels past the natural antioxidant capacity leading to a state of oxidative stress and damage. This thesis aims to understand the molecular mechanisms that link these two states.

Metabolism and Mitochondrial Dysfunction

While the adipocyte has long been thought to primarily store energy, it has become clear that the metabolism that occurs within the adipocyte plays an important role in whole body physiology. Much of this metabolism occurs within the mitochondria. As the organelle that is critical for energy production within the cell, many studies have investigated the role mitochondria play in metabolic syndrome. As the mitochondria are responsible for a large amount of the ROS production and lipid peroxidation within the cell, mitochondrial biogenesis and dynamics are important to understand, as well as the mitochondrial metabolic pathways.

Mitochondrial biogenesis is the process by which new mitochondria are formed. The mitochondria contain more than 1000 proteins but the mitochondrial DNA (mtDNA) only encodes 13 proteins, 22 tRNAs and 2 rRNAs. Many of the proteins of the mitochondria are encoded by the nuclear genome (116). A number of critical transcription factors and co-activators have been identified that are responsible for mitochondrial biogenesis, including nuclear respiratory factor 1 and 2 (NRF-1, NRF-2), peroxisome proliferator-activated receptor γ (PPAR γ), and PPAR γ coactivator-1 α (PGC1 α) expression (117). NRF-1 controls the expression of a number of proteins that make up the OxPhos chain, as well as proteins responsible for mitochondrial protein import and heme biosynthesis. Furthermore NRF-1 controls the level of transcription factor A mitochondrial

(TFAM), which is a major regulator of mitochondrial DNA transcription and replication (118). PPAR γ activation by rosiglitazone, a PPAR agonist, leads to increased expression of mitochondrial proteins and an increase in oxygen consumption in white adipose tissue (119). Perhaps the most important transcriptional regulator of mitochondrial biogenesis is PGC1 α , which is sufficient to increase mitochondrial mass, OxPhos components, mitochondrial metabolic pathway proteins and proteins involved in mitochondrial fission and fusion (120-123). Production of mitochondrial proteins is one critical step in the mitochondrial biogenesis process.

Mitochondria are a very dynamic organelle and while often pictured as a single organelle, they exist in a network that are undergoing constant fission and fusion (124). Mitochondrial fission is controlled by dynamin-related protein-1 (DRP-1) and fission protein 1 (FIS1). FIS1 is a single-pass transmembrane protein that is anchored in the outer mitochondrial membrane (OMM) by its C-terminal domain, and interacts with DRP-1, a cytosolic protein, when recruited to the mitochondria under conditions for mitochondrial fission. Mitochondrial fusion on the other hand is controlled by optic atrophy protein 1 (OPA1), and mitofusin (MFN1/2), a dynamin-related GTPase. OPA1 is localized to the inner-mitochondrial membrane (IMM) and participates in the tethering and fusing of the IMM, as well as, cristae remodeling. Furthermore, MFN1/2 interact with one another coordinating OMM fusion (125). Generally, a fragmented network of mitochondria

is present in times of low energy demand whereas hyperfused mitochondria are present during conditions of stress and starvation where energy demands are high. These processes work in concert to maintain functioning and healthy mitochondria.

Disruptions of normal mitochondrial fission and fusion can lead to altered mitochondrial dynamics, resulting in changes in mitochondrial membrane potential, changes in mitochondrial metabolism and increased oxidative stress. One proposed role of mitochondrial fission is to eliminate damaged mitochondria from the network by removal via mitophagy. Mitophagy is defined as the autophagy of mitochondria and is critically regulated by Parkin, an E3 ubiquitin ligase and PTEN-induced putative kinase 1 (PINK1). Parkin is a cytoplasmically localized protein that translocates to the mitochondria upon reductions in membrane potential and ubiquitinates its target proteins. The adaptor protein p62 can then bind both ubiquitinated mitochondrial proteins as well as LC3 on autophagosomes. This binding recruits the autophagosome membrane to the mitochondria for mitochondrial clearance via autophagy (126). Furthermore, PINK1, a serine/threonine kinase, is responsible for recruitment of Parkin to the depolarized mitochondrial membrane through phosphorylation of MFN2, which then acts as a mitochondrial receptor for Parkin (127). Failure of clearance of damaged or dysfunctional mitochondria can lead to a mitochondrial dysfunction phenotype.

Mitochondrial dysfunction is a hallmark of metabolic disease. There are many causes of mitochondrial dysfunction including oxidative damage, both direct oxidation and carbonylation, as well as accumulation of unfolded proteins within the mitochondria, which activates the mitochondrial unfolded protein response (mtUPR). For carbonylation, many proteins within the mitochondria have been identified as targets under conditions of elevated oxidative stress, including proteins in the OxPhos, tricarboxylic acid cycle (TCA) and branched chain amino acid (BCAA) metabolism pathways (67). Unlike carbonylation, cysteine oxidation has been less studied in its role in changing activity of proteins. Understanding of how oxidative modifications can alter the activity of these metabolic pathways is crucial for development of new treatments.

One of the key metabolic pathways of the mitochondria is the TCA cycle, which is critical for energy storage and metabolism. The process starts with glucose uptake through the glucose transporter GLUT4 and through a series of enzymatic steps, referred to as glycolysis, glucose is broken down into pyruvate, generating 2 ATP in the process. Pyruvate is then transported into the mitochondria by the mitochondrial pyruvate carrier where upon pyruvate dehydrogenase uses it to form acetyl-CoA. Acetyl-CoA feeds into the first step of the TCA cycle where oxaloacetate and acetyl-CoA combine to form citrate by citrate synthase. Aconitase then converts citrate to isocitrate. Isocitrate dehydrogenase oxidizes

isocitrate to α -ketoglutarate (α KG) in a NAD^+ dependent reaction. Subsequently, α -ketoglutarate dehydrogenase decarboxylates α KG to form succinyl-CoA whereupon succinyl-CoA synthetase converts it to succinate producing ATP or GTP in the process. Succinate dehydrogenase, also known as Complex II of the electron transport chain, then converts succinate, in a FAD-dependent mechanism, to fumarate. Fumarase acts on fumarate to produce malate, and malate dehydrogenase converts malate to oxaloacetate, thus restarting the cycle. This cycle provides the electron acceptors and donors required for the electron transport chain, as well as production of some energy. As two acetyl-CoAs are produced from one glucose molecule, it requires two turns of the TCA cycle to fully metabolize glucose. After two turns, two GTP or ATPs, six NADH, two FADH_2 and four CO_2 molecules are produced (128). The TCA cycle is a key metabolic process that occur within the mitochondria.

Oxidative phosphorylation, or mitochondrial respiration, is the primary source of ATP generation within a cell. As discussed earlier, the electron transport chain (ETC) is one of the largest sources of ROS within a cell, but the primary role of the ETC is to generate ATP. Electron transfer through the ETC is coupled to proton translocation from the matrix of the mitochondria into the inter-membrane space. This proton translocation generates an electrochemical gradient of protons, deriving the proton motive force. The proton motive force drives ATP synthesis through the F_0F_1 -ATP synthase (Figure 2) (129, 130). The mechanism

behind the ATP generation lies in the five large complexes that make up the ETC (Figure 2). The two entry points for electrons within the ETC are in Complexes I and II. Complex I is an IMM spanning NADH-ubiquinone oxidoreductase which transfers electrons from mitochondrial NADH to ubiquinone (Q) to ubiquinol (QH₂) within the IMM. During this process four protons are pumped from the matrix to the inter-membrane space of the mitochondria (129). Complex II on the other hand is embedded in the matrix side of the IMM and is the succinate-quinone oxidoreductase, which uses succinate as a substrate and converts it to fumarate while transferring electrons from FADH₂ to Q producing QH₂ and FAD⁺ in the process (131). The electrons that have been passed to QH₂ are then transferred to cytochrome *c* in Complex III, a CoenzymeQ: Cytochrome *c* oxidoreductase otherwise referred to as cytochrome *bc*₁ complex. This electron transfer within Complex III relies on the four redox cofactors that make up some of its subunits, two *b*-type hemes, one *c*-type heme and one [2Fe-2S] cluster. These redox clusters allow for translocation of the electrons through the IMM to cytochrome *c*, which resides on the outer surface of the IMM as well as transfer of 4 protons across the IMM (132). Cytochrome *c* then passes electrons to the terminal enzyme of the electron transport chain, cytochrome *c* oxidase. Four electrons are used to reduce molecular oxygen to form water. This process occurs across the IMM and in the process transports four protons into the inter-membrane space (133). The passing of electrons through the ETC creates the proton motive force necessary for ATP generation. Complex V, also known as

the F_0F_1 ATP synthase, uses this proton gradient created through electron transfer to run the ATPase function in reverse, thus creating ATP from ADP and inorganic P_i (134). This process generates the large majority of ATP required for cellular functions.

Branched-chain amino acid metabolism is a third important metabolic pathway that occurs within the mitochondria. The branched chain amino acids, leucine, isoleucine and valine, are elevated in cases of obesity, and the increased levels correlate better than BMI with development of T2D (135). While BCAA metabolism is a mitochondrial process that occurs in the mitochondrial matrix, the uptake of BCAAs from circulation occurs through two sets of plasma membrane transporters. Solute carrier family 1, member 5 (SLC1A5) is a transporter that transports the BCAAs as well as other amino acids such as glutamate and this transporter is highly expressed in adipocytes (136, 137). Working alongside SLC1A5 is the heterodimeric complex made up of solute carrier family 3, member 2 (SLC3A2) and solute carrier family 7, member 5 (SLC7A5). This complex works as an exchanger, exchanging intracellular glutamine and asparagine for extracellular BCAAs (138, 139). The BCAAs, once inside the mitochondria, can be metabolized to acetyl-CoA and succinyl-CoA through a series of enzymatic reactions. Briefly, the BCAAs can be transaminated by branched-chain amino acid transaminase 2, mitochondrial (BCAT2) to form the branched-chain α -keto acids, then metabolized by the

branched-chain α -ketoacid dehydrogenase (BCKDH complex) followed by 4-6 subsequent enzymatic steps to produce succinyl-CoA from valine, succinyl-CoA and acetyl-CoA from isoleucine and acetyl-CoA from leucine (140). Metabolism of BCAAs plays an important role in anapleuratically replenishing the TCA cycle. In the case of adipose tissue, the metabolites of acetyl-CoA and succinyl-CoA feed in to lipogenesis for storage of the energy for future use (140). As discussed earlier, through the TCA cycle, citrate is produced and can be transported into the cytoplasm and metabolized to acetyl-CoA. Further steps of lipogenesis result in generation of triglyceride, which are then stored within the lipid droplet. When metabolism of BCAAs is abnormal, it can be characterized as a type of mitochondrial dysfunction.

While mitochondrial dysfunction has often been thought to refer specifically to dysregulated oxidative phosphorylation and ATP production, it can refer to any mitochondrial process that is altered. The TCA cycle, OxPhos and BCAA metabolism are critical for proper mitochondrial function and proper oxygen consumption, but when any of these pathways, or other mitochondrial pathways are dysregulated, it can be characterized as mitochondrial dysfunction.

In many systems, mitochondrial dysfunction is linked with endoplasmic reticulum (ER) stress (141, 142). Furthermore, the inflammation described within white adipose tissue during obesity and T2D can induce ER stress (143, 144). ER

Stress, also known as the unfolded protein response (UPR), is induced when misfolded proteins accumulate. The ER stress response is then induced to restore normal ER function. The UPR is made up of three arms of signaling, activating transcription factor (ATF) 6, inositol-requiring enzyme 1 (IRE1) and double-stranded RNA-activated protein kinase (PKR)-like ER kinase (PERK). ATF6 is known to be cleaved by site-1 protease upon induction of ER stress. This cleavage results in translocation of the α fragment to the nucleus and initiates transcription of target genes, such as C/EBP homologous protein (CHOP) and x-box binding protein 1 (XBP1). Activation of IRE1 leads to the activation of the RNase domain, and subsequent cleavage of XBP1 RNA to the spliced form (sXBP1). sXBP1 can then translocate to the nucleus and increase the transcription of protein chaperones and other proteins involved in protein folding. Upon induction of the UPR, PERK is able to homodimerize and autophosphorylates, leading to activation of the kinase domain. This activation allows for phosphorylation of eukaryotic initiation factor 2 α (eIF2 α) leading to a decrease in protein synthesis (145, 146). These three axes of ER stress in concert work to decrease protein synthesis and work to reduce the misfolded or unfolded proteins. It is clear that ER stress plays a role in the development of insulin resistance, especially within the adipocyte. However, the molecular mechanisms linking ER stress and mitochondrial dysfunction are still unknown.

During the development of obesity and T2D, the hypertrophy of adipocytes within white adipose tissue can induce mitochondrial dysfunction (147). Hypertrophy of adipocytes is casually linked with obesity through the excess of nutrients, and this hypertrophy increases adipose tissue inflammation as discussed earlier in this chapter. Furthermore, increased oxidative damage, including carbonylation, is known to play a role in the development of mitochondrial dysfunction (148). These factors all taken together link obesity, insulin resistance, oxidative stress and mitochondrial dysfunction.

Current Objectives

This thesis sets forth to investigate the link between adipose tissue inflammation, mitochondrial function and obesity. These three topics are clearly linked but the molecular mechanisms behind them are still unclear. Oxidative stress is causally linked to insulin resistance in the adipocyte and down-regulation of GSTA4 along with increases in carbonylation affect mitochondrial function (66, 102). With these observations, it is possible that GSTA4 could be responsible for the increased oxidative stress observed, but that inflammation can drive this process as well. The question remains what exactly is inflammation doing to mitochondrial bioenergetics and metabolic pathways and how does this relate to the development of insulin resistance in the adipocyte?

The central hypothesis of this research is that inflammation induces changes in mitochondrial dynamics and increases in oxidative stress that result in changes in central metabolic processes within the mitochondria. These changes within the mitochondria are associated with decreased metabolic capacity and decreased antioxidant response and contribute to oxidative modifications that directly modulate insulin signaling and lead to the development of insulin resistance within the adipocyte.

The studies presented herein aim to answer the following questions: How does adipose tissue inflammation impact mitochondrial dynamics within the adipocyte?

How do obesity and inflammation affect specific mitochondrial metabolism pathways? And what is a direct mechanism for mitochondrial oxidative stress to induce insulin resistance within the adipocyte? Using a combination of techniques including metabolic, proteomic and genetic assays, this thesis sets forth to investigate the role of inflammation and oxidative stress in mitochondrial function and insulin resistance in the adipocyte.

References

1. Ogden, C. L., Carroll, M. D., Kit, B. K., and Flegal, K. M. (2012) Prevalence of Obesity and Trends in Body Mass Index Among US Children and Adolescents, 1999-2010. *JAMA*. **307**, 483–490
2. DeFronzo, R. A. (1988) Lilly lecture 1987. The triumvirate: beta-cell, muscle, liver. A collusion responsible for NIDDM. *Diabetes*. **37**, 667–687
3. Muoio, D. M., and Newgard, C. B. (2008) Mechanisms of disease: Molecular and metabolic mechanisms of insulin resistance and beta-cell failure in type 2 diabetes. *Nat. Rev. Mol. Cell Biol.* **9**, 193–205
4. Poitout, V., and Robertson, R. P. (2002) Minireview: Secondary β -Cell Failure in Type 2 Diabetes—A Convergence of Glucotoxicity and Lipotoxicity. *Endocrinology*. **143**, 339–342
5. Ford, E. S., Li, C., and Sattar, N. (2008) Metabolic Syndrome and Incident Diabetes: Current state of the evidence. **31**, 1898–1904
6. Wannamethee, S. G., Shaper, A. G., Lennon, L., and Morris, R. W. (2005) Metabolic Syndrome vs Framingham Risk Score for Prediction of Coronary Heart Disease, Stroke, and Type 2 Diabetes Mellitus. *Archives of Internal Medicine*. **165**, 2644–2650
7. Hamman, R. F., Wing, R. R., Edelstein, S. L., Bray, G. A., Delahanty, L., Hoskin, M., Kriska, A. M., Mayer-Davis, E. J., Pi-Sunyer, X., Regensteiner, J., Venditti, B., and Wylie-Rosett, J. (2006) Effect of weight loss with lifestyle intervention on risk of diabetes. *Diabetes Care*. **29**, 2102–7–2107
8. Ikramuddin, S., Korner, J., Lee, W.-J., Connett, J. E., Inabnet, W. B., Billington, C. J., Thomas, A. J., Leslie, D. B., Chong, K., Jeffery, R. W., Ahmed, L., Vella, A., Chuang, L.-M., Bessler, M., Sarr, M. G., Swain, J. M., Laqua, P., Jensen, M. D., and Bantle, J. P. (2013) Roux-en-Y Gastric Bypass vs Intensive Medical Management for the Control of Type 2 Diabetes, Hypertension, and Hyperlipidemia. *JAMA*. **309**, 2240–2249
9. Epstein, F. H., Shepherd, P. R., and Kahn, B. B. (1999) Glucose Transporters and Insulin Action — Implications for Insulin Resistance and Diabetes Mellitus. *N. Engl. J. Med.* **341**, 248–257
10. Rask-Madsen, C., and Kahn, C. R. (2012) Tissue-Specific Insulin Signaling, Metabolic Syndrome, and Cardiovascular Disease. *Arterioscler. Thromb. Vasc. Biol.* **32**, 2052–2059
11. Cahill, G. F., Jr. (2006) Fuel Metabolism in Starvation. *Annu. Rev. Nutr.* **26**, 1–22
12. Langin, D. (2006) Control of fatty acid and glycerol release in adipose tissue lipolysis. *C. R. Biol.* **329**, 598–607
13. Guo, S. (2014) Insulin signaling, resistance, and the metabolic syndrome: insights from mouse models into disease mechanisms. *J. Endocrinol.* **220**, T1–T23
14. Brüning, J. C., Brüning, J. C., Michael, M. D., Winnay, J. N., Michael, M.

- D., Winnay, J. N., Hayashi, T., Hayashi, T., Hörsch, D., Accili, D., Hörsch, D., Accili, D., Goodyear, L. J., Kahn, C. R., Goodyear, L. J., and Kahn, C. R. (1998) A Muscle-Specific Insulin Receptor Knockout Exhibits Features of the Metabolic Syndrome of NIDDM without Altering Glucose Tolerance. *Mol. Cell.* **2**, 559–569
15. Saltiel, A. R., and Kahn, C. R. (2001) Insulin signalling and the regulation of glucose and lipid metabolism. *Nature.* **414**, 799–806
 16. Siddle, K. (2011) Signalling by insulin and IGF receptors: supporting acts and new players. *J. Mol. Endocrinol.* **47**, R1–R10
 17. Cheng, Z., Tseng, Y., and White, M. F. (2010) Insulin signaling meets mitochondria in metabolism. *Trends Endocrinol Metab.* **21**, 589–598
 18. Taniguchi, C. M., Emanuelli, B., and Kahn, C. R. (2006) Critical nodes in signalling pathways: insights into insulin action. *Nat. Rev. Mol. Cell Biol.* **7**, 85–96
 19. Frame, S., and Cohen, P. (2001) GSK3 takes centre stage more than 20 years after its discovery. *Biochem. J.* **359**, 1–16
 20. Sano, H., Kane, S., Sano, E., Miinea, C. P., Asara, J. M., Lane, W. S., Garner, C. W., and Lienhard, G. E. (2003) Insulin-stimulated Phosphorylation of a Rab GTPase-activating Protein Regulates GLUT4 Translocation. *Journal of Biological Chemistry.* **278**, 14599–14602
 21. Harris, T. E., and Lawrence, J. C. (2003) TOR Signaling. *Sci Signal.* **2003**, re15–re15
 22. Inoki, K., Li, Y., Zhu, T., Wu, J., and Guan, K.-L. (2002) TSC2 is phosphorylated and inhibited by Akt and suppresses mTOR signalling. *Nat. Cell Biol.* **4**, 648–657
 23. Manning, B. D., Tee, A. R., Logsdon, M. N., Blenis, J., and Cantley, L. C. (2002) Identification of the Tuberous Sclerosis Complex-2 Tumor Suppressor Gene Product Tuberin as a Target of the Phosphoinositide 3-Kinase/Akt Pathway. *Mol. Cell.* **10**, 151–162
 24. Potter, C. J., Pedraza, L. G., and Xu, T. (2002) Akt regulates growth by directly phosphorylating Tsc2. *Nat. Cell Biol.* **4**, 658–665
 25. Sarbassov, D. D., Guertin, D. A., Ali, S. M., and Sabatini, D. M. (2005) Phosphorylation and regulation of Akt/PKB by the rictor-mTOR complex. *Science.* **307**, 1098–1101
 26. Guertin, D. A., Stevens, D. M., Thoreen, C. C., Burds, A. A., Kalaany, N. Y., Moffat, J., Brown, M., Fitzgerald, K. J., and Sabatini, D. M. (2006) Ablation in Mice of the mTORC Components raptor, rictor, or mLST8 Reveals that mTORC2 Is Required for Signaling to Akt-FOXO and PKC α , but Not S6K1. *Dev. Cell.* **11**, 859–871
 27. Jacinto, E., Facchinetti, V., Liu, D., Soto, N., Wei, S., Jung, S. Y., Huang, Q., Qin, J., and Su, B. (2006) SIN1/MIP1 maintains rictor-mTOR complex integrity and regulates Akt phosphorylation and substrate specificity. *Cell.* **127**, 125–137
 28. Laplante, M., and Sabatini, D. M. (2012) mTOR Signaling in Growth

- Control and Disease. *Cell*. **149**, 274–293
29. Oh, W. J., and Jacinto, E. (2014) mTOR complex 2 signaling and functions. *Cell Cycle*. **10**, 2305–2316
 30. Kim, S. J., DeStefano, M. A., Oh, W. J., Wu, C.-C., Vega-Cotto, N. M., Finlan, M., Liu, D., Su, B., and Jacinto, E. (2012) mTOR complex 2 regulates proper turnover of insulin receptor substrate-1 via the ubiquitin ligase subunit Fbw8. *Mol. Cell*. **48**, 875–887
 31. Breuleux, M., Klopfenstein, M., Stephan, C., Doughty, C. A., Barys, L., Maira, S. M., Kwiatkowski, D., and Lane, H. A. (2009) Increased AKT S473 phosphorylation after mTORC1 inhibition is rictor dependent and does not predict tumor cell response to PI3K/mTOR inhibition. *Mol. Cancer Ther.* **8**, 742–753
 32. García-Martínez, J. M., and Alessi, D. R. (2008) mTOR complex 2 (mTORC2) controls hydrophobic motif phosphorylation and activation of serum- and glucocorticoid-induced protein kinase 1 (SGK1). *Biochem. J.* **416**, 375
 33. Polak, P., Cybulski, N., Feige, J. N., Auwerx, J., Ruegg, M. A., and Hall, M. N. (2008) Adipose-Specific Knockout of raptor Results in Lean Mice with Enhanced Mitochondrial Respiration. *Cell Metab.* **8**, 399–410
 34. Kumar, A., Lawrence, J. C., Jung, D. Y., Ko, H. J., Keller, S. R., Kim, J. K., Magnuson, M. A., and Harris, T. E. (2010) Fat cell-specific ablation of rictor in mice impairs insulin-regulated fat cell and whole-body glucose and lipid metabolism. *Diabetes*. **59**, 1397–1406
 35. Um, S. H., Frigerio, F., Watanabe, M., Picard, F., Joaquin, M., Sticker, M., Fumagalli, S., Allegrini, P. R., Kozma, S. C., Auwerx, J., and Thomas, G. (2004) Absence of S6K1 protects against age- and diet-induced obesity while enhancing insulin sensitivity. *Nature*. **431**, 200–5
 36. Shi, Y., and Burn, P. (2004) Lipid metabolic enzymes: emerging drug targets for the treatment of obesity. *Nat Rev Drug Discov.* **3**, 695–710
 37. Ahmadian, M., E Duncan, R., Jaworski, K., Sarkadi-Nagy, E., and Sul, H. S. (2007) Triacylglycerol metabolism in adipose tissue. *Future Lipidol.* **2**, 229–237
 38. Lobo, S., Wiczler, B. M., Smith, A. J., Hall, A. M., and Bernlohr, D. A. (2007) Fatty acid metabolism in adipocytes: functional analysis of fatty acid transport proteins 1 and 4. *J. Lipid Res.* **48**, 609–620
 39. Choi, S. M., Tucker, D. F., Gross, D. N., Easton, R. M., DiPilato, L. M., Dean, A. S., Monks, B. R., and Birnbaum, M. J. (2010) Insulin Regulates Adipocyte Lipolysis via an Akt-Independent Signaling Pathway. *Mol. Cell. Biol.* **30**, 5009–5020
 40. Langin, D., and Arner, P. (2006) Importance of TNF α and neutral lipases in human adipose tissue lipolysis. *Trends in Endocrinology & Metabolism.* **17**, 314–320
 41. Abel, E. D., Peroni, O., Kim, J. K., Kim, Y.-B., Boss, O., Hadro, E., Minnemann, T., Shulman, G. I., and Kahn, B. B. (2001) Adipose-selective

- targeting of the GLUT4 gene impairs insulin action in muscle and liver. *Nature*. **409**, 729–733
42. Blüher, M., Michael, M. D., Peroni, O. D., Ueki, K., Carter, N., Kahn, B. B., and Kahn, C. R. (2002) Adipose tissue selective insulin receptor knockout protects against obesity and obesity-related glucose intolerance. *Dev. Cell*. **3**, 25–38–38
 43. Klok, M. D., Jakobsdottir, S., and Drent, M. L. (2007) The role of leptin and ghrelin in the regulation of food intake and body weight in humans: a review. **8**, 21–34
 44. Lindström, P. (2007) The Physiology of Obese-Hyperglycemic Mice [ob/obMice]. *ScientificWorldJournal*. **7**, 666–685
 45. Hotamisligil, G. S., Shargill, N. S., and Spiegelman, B. M. (1993) Adipose expression of tumor necrosis factor- α : direct role in obesity-linked insulin resistance. *Science*. **259**, 87–91
 46. Xu, H., Barnes, G. T., Yang, Q., Tan, G., Yang, D., Chou, C. J., Sole, J., Nichols, A., Ross, J. S., Tartaglia, L. A., and Chen, H. (2003) Chronic inflammation in fat plays a crucial role in the development of obesity-related insulin resistance. *J. Clin. Invest*. **112**, 1821–1830
 47. Weisberg, S. P., McCann, D., Desai, M., Rosenbaum, M., Leibel, R. L., and Ferrante, A. W. (2003) Obesity is associated with macrophage accumulation in adipose tissue. *J. Clin. Invest*. **112**, 1796–1808
 48. Chawla, A., Nguyen, K. D., and Goh, Y. P. S. (2011) Macrophage-mediated inflammation in metabolic disease. *Nat. Rev. Immunol*. **11**, 738–749
 49. Lumeng, C. N., DelProposto, J. B., Westcott, D. J., and Saltiel, A. R. (2008) Phenotypic switching of adipose tissue macrophages with obesity is generated by spatiotemporal differences in macrophage subtypes. *Diabetes*. **57**, 3239–3246
 50. Lumeng, C. N., Bodzin, J. L., and Saltiel, A. R. (2007) Obesity induces a phenotypic switch in adipose tissue macrophage polarization. *J. Clin. Invest*. **117**, 175–184
 51. Patsouris, D., Li, P.-P., Thapar, D., Chapman, J., Olefsky, J. M., and Neels, J. G. (2008) Ablation of CD11c-Positive Cells Normalizes Insulin Sensitivity in Obese Insulin Resistant Animals. *Cell Metab*. **8**, 301–309
 52. Arkan, M. C., Hevener, A. L., Greten, F. R., Maeda, S., Li, Z.-W., Long, J. M., Wynshaw-Boris, A., Poli, G., Olefsky, J., and Karin, M. (2005) IKK- β links inflammation to obesity-induced insulin resistance. *Nat. Med*. **11**, 191–198
 53. Perkins, N. D. (2007) Integrating cell-signalling pathways with NF- κ B and IKK function. *Nat. Rev. Mol. Cell Biol*. **8**, 49–62
 54. Shi, H., Kokoeva, M. V., Inouye, K., Tzameli, I., Yin, H., and Flier, J. S. (2006) TLR4 links innate immunity and fatty acid-induced insulin resistance. *J. Clin. Invest*. **116**, 3015–25–3025
 55. Watanabe, Y., Nagai, Y., and Takatsu, K. (2013) Activation and

- regulation of the pattern recognition receptors in obesity-induced adipose tissue inflammation and insulin resistance. *Nutrients*. **5**, 3757–78–3778
56. Olefsky, J. M., and Glass, C. K. (2010) Macrophages, inflammation, and insulin resistance. *Annu. Rev. Physiol.* **72**, 219–246
 57. Esser, N., Legrand-Poels, S., Piette, J., Scheen, A. J., and Paquot, N. (2014) Inflammation as a link between obesity, metabolic syndrome and type 2 diabetes. *Diabetes Res. Clin. Pract.* **105**, 141–150
 58. Odegaard, J. I., and Chawla, A. (2010) Alternative macrophage activation and metabolism. *Annu Rev Pathol.* **6**, 275–97
 59. Takeda, K., Kamanaka, M., Tanaka, T., Kishimoto, T., and Akira, S. (1996) Impaired IL-13-mediated functions of macrophages in STAT6-deficient mice. *J. Immunol.* **157**, 3220–2
 60. Shimoda, K., van Deursen, J., Sangster, M. Y., Sarawar, S. R., Carson, R. T., Tripp, R. A., Chu, C., Quelle, F. W., Nosaka, T., Vignali, D. A., Doherty, P. C., Grosveld, G., Paul, W. E., and Ihle, J. N. (1996) Lack of IL-4-induced Th2 response and IgE class switching in mice with disrupted Stat6 gene. *Nature*. **380**, 630–3
 61. Evans, M. D., Dizdaroglu, M., and Cooke, M. S. (2004) Oxidative DNA damage and disease: induction, repair and significance. *Mutation Research/Reviews in Mutation Research*. **567**, 1–61
 62. Raes, G., De Baetselier, P., Noël, W., Beschin, A., Brombacher, F., and Gh, G. H. (2002) Differential expression of FIZZ1 and Ym1 in alternatively versus classically activated macrophages. *J. Leukoc. Biol.* **71**, 597–602–602
 63. Shimomura, I., Funahashi, T., Takahashi, M., Maeda, K., Kotani, K., Nakamura, T., Yamashita, S., Miura, M., Fukuda, Y., Takemura, K., Tokunaga, K., and Matsuzawa, Y. (1996) Enhanced expression of PAI-1 in visceral fat: possible contributor to vascular disease in obesity. *Nat. Med.* **2**, 800–3
 64. Uysal, K. T., Wiesbrock, S. M., Marino, M. W., and Hotamisligil, G. S. (1997) Protection from obesity-induced insulin resistance in mice lacking TNF-alpha function. *Nature*. **389**, 610–614
 65. Furukawa, S., Fujita, T., Shimabukuro, M., Iwaki, M., Yamada, Y., Nakajima, Y., Nakayama, O., Makishima, M., Matsuda, M., and Shimomura, I. (2004) Increased oxidative stress in obesity and its impact on metabolic syndrome. *J. Clin. Invest.* **114**, 1752–1761
 66. Houstis, N., Rosen, E. D., and Lander, E. S. (2006) Reactive oxygen species have a causal role in multiple forms of insulin resistance. *Nature*. **440**, 944–948
 67. Curtis, J. M., Hahn, W. S., Stone, M. D., Inda, J. J., Drouillard, D. J., Kuzmich, J. P., Donoghue, M. A., Long, E. K., Armién, A. G., Lavandro, S., Arriaga, E., Griffin, T. J., and Bernlohr, D. A. (2012) Protein carbonylation and adipocyte mitochondrial function. *J. Biol. Chem.* **287**, 32967–32980

68. Curtis, J. M., Hahn, W. S., Long, E. K., Burrill, J. S., Arriaga, E. A., and Bernlohr, D. A. (2012) Protein carbonylation and metabolic control systems. *Trends Endocrinol Metab.* **23**, 399–406
69. Barzilai, A., and Yamamoto, K.-I. (2004) DNA damage responses to oxidative stress. *DNA Repair (Amst.)*. **3**, 1109–1115
70. Thannickal, V. J., and Fanburg, B. L. (2000) Reactive oxygen species in cell signaling. *Am. J. Physiol. Lung Cell Mol. Physiol.* **279**, L1005–28–L1028
71. Brand, M. D. (2010) The sites and topology of mitochondrial superoxide production. *Exp. Gerontol.* **45**, 466–472
72. Sena, L. A., and Chandel, N. S. (2012) Physiological roles of mitochondrial reactive oxygen species. *Mol. Cell.* **48**, 158–167
73. Hamanaka, R. B., and Chandel, N. S. (2010) Mitochondrial reactive oxygen species regulate cellular signaling and dictate biological outcomes. *Trends Biochem. Sci.* **35**, 505–513
74. Liochev, S. I., and Fridovich, I. (2007) The effects of superoxide dismutase on H₂O₂ formation. *Free Radical Biology and Medicine.* **42**, 1465–1469
75. Fridovich, I. (1995) Superoxide Radical and Superoxide Dismutases. *Annu. Rev. Biochem.* **64**, 97–112
76. Lee, H., Lee, Y. J., Choi, H., Ko, E. H., and Kim, J. W. (2009) Reactive Oxygen Species Facilitate Adipocyte Differentiation by Accelerating Mitotic Clonal Expansion. *Journal of Biological Chemistry.* **284**, 10601–10609
77. Liochev, S. I., and Fridovich, I. (1994) The role of O₂⁻ in the production of HO₂· in vitro and in vivo. *Free Radical Biology and Medicine.* **16**, 29–33
78. Lloyd, R. V., Hanna, P. M., and Mason, R. P. (1997) The origin of the hydroxyl radical oxygen in the Fenton reaction. *Free Radical Biology and Medicine.* **22**, 885–8
79. Kansanen, E., Kuosmanen, S. M., Leinonen, H., and Levonen, A.-L. (2013) The Keap1-Nrf2 pathway: Mechanisms of activation and dysregulation in cancer. *Redox Biol.* **1**, 45–49
80. Surh, Y.-J., Kundu, J. K., and Na, H.-K. (2008) Nrf2 as a master redox switch in turning on the cellular signaling involved in the induction of cytoprotective genes by some chemopreventive phytochemicals. *Planta Med.* **74**, 1526–1539
81. Esterbauer, H., Zollner, H., and Schaur, R. J. (1990) Aldehydes Formed by Lipid Peroxidation: Mechanisms of Formation, Occurrence and Determination. in *Membrane Lipid Oxidation* (Vigo-Pelfrey, C. ed), pp. 239–268, Boca Raton, Florida, **1**, 239–268
82. Pawlosky, R. J., Bacher, J., and Salem, N. (2001) Ethanol consumption alters electroretinograms and depletes neural tissues of docosahexaenoic acid in rhesus monkeys: nutritional consequences of a low n-3 fatty acid diet. *Alcohol. Clin. Exp. Res.* **25**, 1758–1765

83. Salem, N., Litman, B., Kim, H. Y., and Gawrisch, K. (2001) Mechanisms of action of docosahexaenoic acid in the nervous system. *Lipids*. **36**, 945–959
84. Lim, S.-Y., Doherty, J. D., and Salem, N. (2005) Lead exposure and (n-3) fatty acid deficiency during rat neonatal development alter liver, plasma, and brain polyunsaturated fatty acid composition. *J. Nutr.* **135**, 1027–1033
85. Long, E. K., Murphy, T. C., Leiphon, L. J., Watt, J., Morrow, J. D., Milne, G. L., Howard, J. R. H., and Picklo, M. J. (2008) Trans-4-hydroxy-2-hexenal is a neurotoxic product of docosahexaenoic (22:6; n-3) acid oxidation. *J. Neurochem.* **105**, 714–724
86. Long, E. K., and Picklo, M. J. (2010) Trans-4-hydroxy-2-hexenal, a product of n-3 fatty acid peroxidation: make some room HNE... *Free Radical Biology and Medicine*. **49**, 1–8
87. Long, E. K., Olson, D. M., and Bernlohr, D. A. (2013) High-fat diet induces changes in adipose tissue trans-4-oxo-2-nonenal and trans-4-hydroxy-2-nonenal levels in a depot-specific manner. *Free Radical Biology and Medicine*. **63**, 390–398
88. Ahn, B.-H., Kim, H.-S., Song, S., Lee, I. H., Liu, J., Vassilopoulos, A., Deng, C.-X., and Finkel, T. (2008) A role for the mitochondrial deacetylase Sirt3 in regulating energy homeostasis. *Proc. Natl. Acad. Sci. U.S.A.* **105**, 14447–14452
89. Kontrová, K., Zídková, J., Bartos, B., Skop, V., Sajdok, J., Kazdová, L., Mikulík, K., Mlejnek, P., Zídek, V., and Pravenec, M. (2007) CD36 regulates fatty acid composition and sensitivity to insulin in 3T3-L1 adipocytes. *Physiol Res*. **56**, 493–496
90. Malcom, G. T., Bhattacharyya, A. K., Velez-Duran, M., Guzman, M. A., Oalman, M. C., and Strong, J. P. (1989) Fatty acid composition of adipose tissue in humans: differences between subcutaneous sites. *Am. J. Clin. Nutr.* **50**, 288–291
91. Schaur, R. J. (2003) Basic aspects of the biochemical reactivity of 4-hydroxynonenal. *Mol. Aspects Med.* **24**, 149–59
92. Engle, M. R., Singh, S. P., Czernik, P. J., Gaddy, D., Montague, D. C., Ceci, J. D., Yang, Y., Awasthi, S., Awasthi, Y. C., and Zimniak, P. (2004) Physiological role of mGSTA4-4, a glutathione S-transferase metabolizing 4-hydroxynonenal: generation and analysis of mGsta4 null mouse. *Toxicol. Appl. Pharmacol.* **194**, 296–308
93. Bruns, C. M., Hubatsch, I., Ridderström, M., Mannervik, B., and Tainer, J. A. (1999) Human glutathione transferase A4-4 crystal structures and mutagenesis reveal the basis of high catalytic efficiency with toxic lipid peroxidation products. *J. Mol. Biol.* **288**, 427–439
94. Hubatsch, I., Ridderström, M., and Mannervik, B. (1998) Human glutathione transferase A4-4: an alpha class enzyme with high catalytic efficiency in the conjugation of 4-hydroxynonenal and other genotoxic

- products of lipid peroxidation. *Biochem. J.* **330** (Pt 1), 175–179
95. Singhal, S. S., Yadav, S., Roth, C., and Singhal, J. (2009) RLIP76: A novel glutathione-conjugate and multi-drug transporter. *Biochem. Pharmacol.* **77**, 761–769
 96. Poli, G., Biasi, F., and Leonarduzzi, G. (2008) 4-Hydroxynonenal–protein adducts: A reliable biomarker of lipid oxidation in liver diseases. *Mol. Aspects Med.* **29**, 67–71
 97. Seki, S., Kitada, T., Sakaguchi, H., Nakatani, K., and Wakasa, K. (2003) Pathological significance of oxidative cellular damage in human alcoholic liver disease. *Histopathology.* **42**, 365–371
 98. Grimsrud, P. A., Picklo, M. J., Griffin, T. J., and Bernlohr, D. A. (2007) Carbonylation of adipose proteins in obesity and insulin resistance: identification of adipocyte fatty acid-binding protein as a cellular target of 4-hydroxynonenal. *Molecular & Cellular Proteomics.* **6**, 624–637
 99. Frohnert, B. I., Sinaiko, A. R., Serrot, F. J., Foncea, R. E., Moran, A., Ikramuddin, S., Choudry, U., and Bernlohr, D. A. (2011) Increased adipose protein carbonylation in human obesity. *Obesity.* **19**, 1735–1741
 100. Liu, Q., Smith, M. A., Avilá, J., DeBernardis, J., Kansal, M., Takeda, A., Zhu, X., Nunomura, A., Honda, K., Moreira, P. I., Oliveira, C. R., Santos, M. S., Shimohama, S., Aliev, G., la Torre, de, J., Ghanbari, H. A., Siedlak, S. L., Harris, P. L. R., Sayre, L. M., and Perry, G. (2005) Alzheimer-specific epitopes of tau represent lipid peroxidation-induced conformations. *Free Radical Biology and Medicine.* **38**, 746–754
 101. Perluigi, M., Fai Poon, H., Hensley, K., Pierce, W. M., Klein, J. B., Calabrese, V., De Marco, C., and Butterfield, D. A. (2005) Proteomic analysis of 4-hydroxy-2-nonenal-modified proteins in G93A-SOD1 transgenic mice—A model of familial amyotrophic lateral sclerosis. *Free Radical Biology and Medicine.* **38**, 960–968
 102. Curtis, J. M., Grimsrud, P. A., Wright, W. S., Xu, X., Foncea, R. E., Graham, D. W., Brestoff, J. R., Wiczer, B. M., Ilkayeva, O., Cianflone, K., Muoio, D. E., Arriaga, E. A., and Bernlohr, D. A. (2010) Downregulation of adipose glutathione S-transferase A4 leads to increased protein carbonylation, oxidative stress, and mitochondrial dysfunction. *Diabetes.* **59**, 1132–1142
 103. Sies, H. (2014) Role of metabolic H₂O₂ generation: redox signaling and oxidative stress. *J. Biol. Chem.* **289**, 8735–8741
 104. Fisher-Wellman, K. H., and Neuffer, P. D. (2012) Linking mitochondrial bioenergetics to insulin resistance via redox biology. *Trends Endocrinol Metab.* **23**, 142–153
 105. Rhee, S. G., Bae, Y. S., Lee, S. R., and Kwon, J. (2000) Hydrogen peroxide: a key messenger that modulates protein phosphorylation through cysteine oxidation. *Sci Signal.* **2000**, pe1–pe1
 106. Poole, L. B., Karplus, P. A., and Claiborne, A. I. (2004) Protein sulfenic acids in redox signaling. *Annu. Rev. Pharmacol. Toxicol.* **44**, 325–47

107. Hertog, den, J., Groen, A., and van der Wijk, T. (2005) Redox regulation of protein-tyrosine phosphatases. *Arch. Biochem. Biophys.* **434**, 11–15
108. Loh, K., Deng, H., Fukushima, A., Cai, X., Boivin, B., Galic, S., Bruce, C., Shields, B. J., Skiba, B., Ooms, L. M., Stepto, N., Wu, B., Mitchell, C. A., Tonks, N. K., Watt, M. J., Febbraio, M. A., Crack, P. J., Andrikopoulos, S., and Tiganis, T. (2009) Reactive oxygen species enhance insulin sensitivity. *Cell Metab.* **10**, 260–272
109. Cho, S.-H., Lee, C.-H., Ahn, Y., Kim, H., Kim, H., Ahn, C.-Y., Yang, K.-S., and Lee, S.-R. (2004) Redox regulation of PTEN and protein tyrosine phosphatases in H₂O₂ mediated cell signaling. *FEBS Letters.* **560**, 7–13–13
110. Tang, X., Powelka, A. M., Soriano, N. A., Czech, M. P., and Guilherme, A. (2005) PTEN, but not SHIP2, suppresses insulin signaling through the phosphatidylinositol 3-kinase/Akt pathway in 3T3-L1 adipocytes. *Journal of Biological Chemistry.* **280**, 22523–9–22529
111. Finkel, T. (2011) Signal transduction by reactive oxygen species. *J. Cell Biol.* **194**, 7–15–15
112. Gupta, V., and Carroll, K. S. (2014) Sulfenic acid chemistry, detection and cellular lifetime. *Biochim. Biophys. Acta.* **1840**, 847–875
113. Meister, A. (1988) Glutathione metabolism and its selective modification. *Journal of Biological Chemistry.* **263**, 17205–8–17208
114. Rushworth, G. F., and Megson, I. L. (2014) Existing and potential therapeutic uses for N-acetylcysteine: The need for conversion to intracellular glutathione for antioxidant benefits. *Pharmacol. Ther.* **141**, 150–159
115. Kobayashi, H., Matsuda, M., Fukuhara, A., Komuro, R., and Shimomura, I. (2009) Dysregulated glutathione metabolism links to impaired insulin action in adipocytes. *Am. J. Physiol. Endocrinol. Metab.* **296**, E1326–34
116. Calvo, S. E., and Mootha, V. K. (2010) The Mitochondrial Proteome and Human Disease. *Annu Rev Genomics Hum Genet.* **11**, 25–44
117. Dominy, J. E., and Puigserver, P. (2013) Mitochondrial Biogenesis through Activation of Nuclear Signaling Proteins. *Cold Spring Harb Perspect Biol.* **5**, a015008–a015008
118. Scarpulla, R. C. (2008) Transcriptional Paradigms in Mammalian Mitochondrial Biogenesis and Function. *Physiol. Rev.* **88**, 611–638
119. Wilson-Fritch, L., Nicoloso, S., Chouinard, M., Lazar, M. A., Chui, P. C., Leszyk, J., Straubhaar, J., Czech, M. P., and Corvera, S. (2004) Mitochondrial remodeling in adipose tissue associated with obesity and treatment with rosiglitazone. *J. Clin. Invest.* **114**, 1281–1289
120. Mootha, V. K., Lindgren, C. M., Eriksson, K.-F., Subramanian, A., Sihag, S., Lehar, J., Puigserver, P., Carlsson, E., Ridderstråle, M., Laurila, E., Houstis, N., Daly, M. J., Patterson, N., Mesirov, J. P., Golub, T. R., Tamayo, P., Spiegelman, B., Lander, E. S., Hirschhorn, J. N., Altshuler, D., and Groop, L. C. (2003) PGC-1 α -responsive genes involved in

- oxidative phosphorylation are coordinately downregulated in human diabetes. *Nat. Genet.* **34**, 267–273
121. Uldry, M., Yang, W., St-Pierre, J., Lin, J., Seale, P., and Spiegelman, B. M. (2006) Complementary action of the PGC-1 coactivators in mitochondrial biogenesis and brown fat differentiation. *Cell Metab.* **3**, 333–341
 122. Cunningham, J. T., Rodgers, J. T., Arlow, D. H., Vazquez, F., Mootha, V. K., and Puigserver, P. (2007) mTOR controls mitochondrial oxidative function through a YY1-PGC-1 α transcriptional complex. *Nature.* **450**, 736–740
 123. Rasbach, K. A., Gupta, R. K., Ruas, J. L., Wu, J., Naseri, E., Estall, J. L., and Spiegelman, B. M. (2010) PGC-1 regulates a HIF2 -dependent switch in skeletal muscle fiber types. *Proceedings of the National Academy of Sciences.* **107**, 21866–21871
 124. Westermann, B. (2010) Mitochondrial fusion and fission in cell life and death. *Nat. Rev. Mol. Cell Biol.* **11**, 872–884
 125. Parra, V., Verdejo, H., Del Campo, A., Pennanen, C., Kuzmicic, J., Iglewski, M., Hill, J. A., Rothermel, B. A., and Lavandro, S. (2011) The complex interplay between mitochondrial dynamics and cardiac metabolism. *J. Bioenerg. Biomembr.* **43**, 47–51
 126. Thomas, R. L., and Gustafsson, A. B. (2013) Mitochondrial autophagy-- an essential quality control mechanism for myocardial homeostasis. *Circ. J.* **77**, 2449–54
 127. Chen, Y., and Dorn, G. W. (2013) PINK1-Phosphorylated Mitofusin 2 Is a Parkin Receptor for Culling Damaged Mitochondria. *Science.* **340**, 471–475
 128. Dashty, M. (2013) A quick look at biochemistry: Carbohydrate metabolism. *Clin. Biochem.* **46**, 1339–1352
 129. Sazanov, L. A. (2015) A giant molecular proton pump: structure and mechanism of respiratory complex I. *Nat. Rev. Mol. Cell Biol.* **16**, 375–388
 130. Watt, I. N., Montgomery, M. G., Runswick, M. J., Leslie, A. G. W., and Walker, J. E. (2010) Bioenergetic cost of making an adenosine triphosphate molecule in animal mitochondria. *Proceedings of the National Academy of Sciences.* **107**, 16823–16827
 131. Cecchini, G. (2003) FUNCTION AND STRUCTURE OF COMPLEX II OF THE RESPIRATORY CHAIN*. *Annu. Rev. Biochem.* **72**, 77–109
 132. Crofts, A. R., and Berry, E. A. (1998) Structure and function of the cytochrome bc₁ complex of mitochondria and photosynthetic bacteria. *Curr. Opin. Struct. Biol.* **8**, 501–9
 133. Michel, H., Behr, J., Harrenga, A., and Kannt, A. (1998) CYTOCHROME COXIDASE: Structure and Spectroscopy. *Annu Rev Biophys Biomol Struct.* **27**, 329–356
 134. Yoshida, M., Muneyuki, E., and Hisabori, T. (2001) ATP synthase--a

- marvellous rotary engine of the cell. *Nat. Rev. Mol. Cell Biol.* **2**, 669–677
135. Wang, T. J., Larson, M. G., Vasan, R. S., Cheng, S., Rhee, E. P., McCabe, E., Lewis, G. D., Fox, C. S., Jacques, P. F., Fernandez, C., O'Donnell, C. J., Carr, S. A., Mootha, V. K., Florez, J. C., Souza, A., Melander, O., Clish, C. B., and Gerszten, R. E. (2011) Metabolite profiles and the risk of developing diabetes. *Nat. Med.* **17**, 448–453
 136. Fuchs, B. C., and Bode, B. P. (2005) Amino acid transporters ASCT2 and LAT1 in cancer: partners in crime? *Semin. Cancer Biol.* **15**, 254–266
 137. Utsunomiya-Tate, N., Endou, H., and Kanai, Y. (1996) Cloning and functional characterization of a system ASC-like Na⁺-dependent neutral amino acid transporter. *J. Biol. Chem.* **271**, 14883–14890
 138. Segawa, H., Fukasawa, Y., Miyamoto, K., Takeda, E., Endou, H., and Kanai, Y. (1999) Identification and functional characterization of a Na⁺-independent neutral amino acid transporter with broad substrate selectivity. *Journal of Biological Chemistry.* **274**, 19745–19751
 139. Fotiadis, D., Kanai, Y., and Palacín, M. (2013) The SLC3 and SLC7 families of amino acid transporters. *Mol. Aspects Med.* **34**, 139–158
 140. Newgard, C. B. (2012) Interplay between Lipids and Branched-Chain Amino Acids in Development of Insulin Resistance. *Cell Metab.* **15**, 606–614
 141. Yuzefovych, L. V., Musiyenko, S. I., Wilson, G. L., and Rachek, L. I. (2013) Mitochondrial DNA Damage and Dysfunction, and Oxidative Stress Are Associated with Endoplasmic Reticulum Stress, Protein Degradation and Apoptosis in High Fat Diet-Induced Insulin Resistance Mice. *PLoS ONE.* **8**, e54059
 142. Lim, J. H., Lee, H. J., Ho Jung, M., and Song, J. (2009) Coupling mitochondrial dysfunction to endoplasmic reticulum stress response: a molecular mechanism leading to hepatic insulin resistance. *Cell. Signal.* **21**, 169–177
 143. Todd, D. J., Lee, A.-H., and Glimcher, L. H. (2008) The endoplasmic reticulum stress response in immunity and autoimmunity. *Nat. Rev. Immunol.* **8**, 663–674
 144. Xue, X., Piao, J.-H., Nakajima, A., Sakon-Komazawa, S., Kojima, Y., Mori, K., Yagita, H., Okumura, K., Harding, H., and Nakano, H. (2005) Tumor necrosis factor alpha (TNFalpha) induces the unfolded protein response (UPR) in a reactive oxygen species (ROS)-dependent fashion, and the UPR counteracts ROS accumulation by TNFalpha. *J. Biol. Chem.* **280**, 33917–33925
 145. Senft, D., and Ronai, Z. A. (2015) UPR, autophagy, and mitochondria crosstalk underlies the ER stress response. *Trends Biochem. Sci.* **40**, 141–148
 146. Salvadó, L., Palomer, X., Barroso, E., and Vázquez-Carrera, M. (2015) Targeting endoplasmic reticulum stress in insulin resistance. *Trends in Endocrinology & Metabolism.* **0**, In Press

147. Kusminski, C. M., and Scherer, P. E. (2012) Mitochondrial dysfunction in white adipose tissue. **23**, 435–443
148. Frohnert, B. I., and Bernlohr, D. A. (2013) Protein carbonylation, mitochondrial dysfunction, and insulin resistance. *Adv Nutr.* **4**, 157–163

CHAPTER TWO

Proinflammatory cytokines differentially regulate adipocyte mitochondrial metabolism, oxidative stress, and dynamics

Hahn WS, Kuzmicic J, Burrill JS, Donoghue MA, Foncea R, Jensen MD, Lavadero S, Arriaga, EA, Bernlohr DA. *Am J Physiol Endocrinol Metab* 306: E1033-E1045, 2014.

This chapter contains an original research article previously published.

Reproduced with permission from American Journal of Physiology – Endocrinology and Metabolism, Copyright 2014.

Joel Burrill performed experiments in Figure 5A, and confirmed results in Figure 2C.

Summary

Wendy S. Hahn, Jovan Kuzmicic, Joel S. Burrill, Margaret A. Donoghue, Rocio Foncea, Michael D. Jensen, Sergio Lavandero, Edgar A. Arriaga, David A. Bernlohr. Pro-inflammatory cytokines differentially regulate adipocyte mitochondrial metabolism, oxidative stress and dynamics –Macrophage infiltration of adipose tissue and the chronic low-grade production of inflammatory cytokines have been mechanistically linked to the development of insulin resistance, the forerunner of type 2 diabetes mellitus. In this study we evaluated the chronic effects of TNF α , IL-6 and IL-1 β on adipocyte mitochondrial metabolism and morphology using the 3T3-L1 model cell system. TNF α treatment of cultured adipocytes led to significant changes in mitochondrial bioenergetics including increased proton leak, decreased $\Delta\Psi_m$, increased basal respiration and decreased ATP turnover. In contrast, while IL-6 and IL-1 β decreased maximal respiratory capacity, they had no effect on $\Delta\Psi_m$ and varied effects on ATP turnover, proton leak and basal respiration. Only TNF α treatment of 3T3-L1 cells led to an increase in oxidative stress (as measured by superoxide anion production and protein carbonylation) and C16 ceramide synthesis. Treatment of 3T3-L1 adipocytes with cytokines led to decreased mRNA expression of key transcription factors and control proteins implicated in mitochondrial biogenesis including PGC1 α and eNOS as well as decreased expression of COXIV and Cyt C. Whereas each cytokine led to effects on expression of mitochondrial markers, TNF α exclusively led to mitochondrial

fragmentation, decreased the total level of Opa1 while increasing Opa1 cleavage without affecting expression of levels of mitofusin 2, DRP1 or mitofilin. In sum, these results indicate that inflammatory cytokines have unique and specialized effects on adipocyte metabolism but each leads to decreased mitochondrial function and a re-programming of fat cell biology.

Introduction

THE ADIPOSE ORGAN is highly specialized in storage and release of energy in times of nutrient excess and deficit respectively (1, 2). It also plays a vital role in communicating to the brain and other tissues as to the energy status of the entire organism, and hence can influence feeding behavior and energy utilization (3-5). Low-grade chronic inflammation of adipose tissue has been characterized as a hallmark of obesity and insulin resistance (6-8). Current models of obesity-linked adipose inflammation include leukocyte infiltration, increased levels of pro-inflammatory cytokines such as monocyte chemoattractant protein-1 (MCP-1), tumor necrosis factor α (TNF α), interleukin 6 (IL-6) and interleukin 1 β (IL-1 β) and increased oxidative stress (8, 9). The dysfunction of the adipose tissue that occurs in the metabolic syndrome includes increased lipolysis in a fed state (10, 11) and alterations in adipokine secretion (12, 13), promoting the hypothesis that adipose inflammation underlies the metabolic syndrome and forms a platform for systemic dysfunction.

In adipose tissue macrophage infiltration leads to the production of reactive oxygen species (ROS) and increased oxidative stress in visceral adipose depots (14-16). Production of ROS (and related reactive nitrogen species) results in oxidative damage to phospholipids, proteins and DNA. Pathways for ROS formation are numerous and include superoxide ($O_2^{\cdot-}$) production via activation of NADPH oxidase (NOX), the 5/12/15 lipoxygenase system, xanthine oxidase (XO)

and mitochondrial complex I and complex III (6, 17). Hydrogen peroxide production occurs at numerous sites such as peroxisomal fatty acid oxidation, lysyl oxidase and several dihydrolipoamide dehydrogenase containing enzyme systems such as pyruvate dehydrogenase, α -ketoglutarate dehydrogenase and branch chain keto acid dehydrogenase (18, 19) as well as via mitochondrial and cytoplasmic superoxide dismutase (20). As such, ROS generation occurs in multiple locations and can be regulated by a large number of metabolic, hormonal and genetic determinants.

Although it is broadly appreciated that pro-inflammatory cytokines lead to adipocyte insulin resistance and mitochondrial dysfunction, the specific effects of such cytokines on mitochondrial dynamics have not been fully characterized. Mitochondria are highly dynamic and move along microtubules, fuse and fragment in response to stress stimuli and energy demands (21, 22). Fission proteins dynamin related protein 1 (DRP-1), MiD49/50 and fission protein 1 (FIS1) mediate biogenesis of new organelles as well as quality control and mitophagy through mitochondrial fragmentation (22). Conversely, fusion of mitochondria is mediated by mitofusin1/2 (MFN1/2) and optic atrophy 1 (OPA1) localized on the outer and inner membranes, respectively. Mitochondrial fusion is thought to be a mechanism for quality control where mitochondria can share DNA, proteins and metabolic substrates under conditions of stress or nutrient deprivation (23).

The current study was undertaken to characterize the role(s) of inflammatory cytokines on mitochondrial activity, morphology and dynamics with the goal of identifying molecular mechanisms that link inflammation and oxidative stress to cellular function. As opposed to an *in-vivo* approach using high fat fed animals where multiple cytokines concurrently affect cellular function we undertook a more focused approach using specific cytokines and their chronic effect in the 3T3-L1 adipocyte model cell system. In this report we define the role(s) of individual cytokines on key parameters affecting adipocyte mitochondrial function—respiration, dynamics and morphology.

Experimental Procedures

Reagents. Mouse recombinant TNF α , IL-1 β and IL-6 were purchased from R&D Systems (Minneapolis, MN). Oligomycin, carbonylcyanide p-trifluoromethoxyphenylhydrazone (FCCP) and Antimycin A were purchased from Sigma (St. Louis, MO). Trizol was purchased from Invitrogen (Grand Island, NY). EZ-link Biotin Hydrazide and IR-800 Streptavidin were purchased from Thermo Scientific (Rockford IL). Antibodies were purchased from the following companies; manganese superoxide dismutase (MnSOD), mitofillin and cleaved caspase 3 were from R&D Systems (Minneapolis, MN); MFN2 and OPA1 were from Abcam (Cambridge, MA); DRP1 was from BD Transduction Laboratories (San Jose, CA); FIS1 antibody was purchased from Alexis/ Enzo (Farmingdale, NY); Cytochrome c oxidase subunit IV (COXIV) antibody was from Cell Signaling Technology (Danvers, MA); Perilipin N-terminus antibody was from American Research Products (Belmont, MA) and β -actin was from Sigma (St. Louis, MO). Mitotracker green FM, TPP-HE (MitoSOX) and TMRM were purchased from Molecular Probes (Grand Island, NY).

Cell culture. 3T3-L1 fibroblasts were grown to confluence in DMEM containing 25 mM glucose, 1X Glutamax (Invitrogen, Carlsbad CA), supplemented with penicillin, streptomycin, and 10% calf serum. At 2 days post confluence (day 0) cells were switched to differentiation media containing; DMEM with 25 mM glucose and 1X glutamax, 10% fetal bovine serum (FBS), 1 μ g/mL insulin, 100

ng/mL dexamethasone, 115 µg/mL isobutylmethylxanthine, and 5 µM troglitazone (Sigma, St. Louis MO) for 2 days. After 2 days the dexamethasone, isobutylmethylxanthine and troglitazone are withdrawn. Beginning on day 4 the differentiated adipocytes are maintained in high glucose DMEM with 10% FBS. Differentiation was evaluated by the acquisition of the adipocyte morphology, expression of adipocyte marker proteins such as FABP4 and lipid accumulation.

Cytokine treatment. Each cytokine was reconstituted in 0.1% fatty acid-free BSA (Sigma, St. Louis MO) to a working concentration of 10 ng/ml. Beginning on day 6, 3T3-L1 adipocytes were treated with 1 nM TNF α , IL-6, or IL-1 β in DMEM containing 10% FBS for 96, 48, or 24 h. Media with cytokines was refreshed daily and assays were performed 8-11 days post differentiation.

Cell respiratory control. Cellular respiration and proton efflux was analyzed using the XF24 Analyzer and system software (Seahorse Bioscience, Billerica, MA). 3T3-L1 fibroblasts were grown and differentiated as described above in XF24 V7 culture dishes coated with 0.2% gelatin (Sigma, St. Louis MO). Adipocytes were treated with or without (control) 1 nM of each cytokine for 24-96 h in complete media prior to the assay (24). On day 10 post differentiation, cells were washed with and switched to serum-free modified, no bicarbonate, low phosphate DMEM (D5030) supplemented with 1X Glutamax (Invitrogen, Carlsbad, CA), 1 mM sodium pyruvate, 25 mM glucose, 0-1 nM cytokine and allowed to equilibrate for

1 h in non-CO₂ 37° C incubator. After cartridge calibration, cells were placed in the XF24 analyzer where cellular oxygen consumption and extracellular acidification rate were measured 4 times under basal conditions, then 3 times after the addition of 2.5 μM oligomycin through port A, 3 times after 2.5 μM FCCP addition through port B, and twice after 4 μM antimycin A addition through port C. Measurement protocol for each condition was mix 2 min, wait 2 min and measure 2 min. Time points (N=4) for each cytokine were assayed simultaneously. Oxygen consumption rate (OCR) (pmol/ min) and extracellular acidification rate (ECAR) (mpH/min) data obtained from the Seahorse XF24 Software were normalized to the untreated control (100%) for graphing purposes.

2-Deoxyglucose uptake assay. Cellular uptake of 2-deoxyglucose was assessed in 3T3-L1 adipocytes treated for 24 h with 1 nM of indicated cytokine in complete media beginning at day 9 of differentiation. On day 10 cells were washed in PBS and incubated for 2 h in serum-free HEPES buffer (3.8 mM HEPES, 2 mM NaHCO₃, 120 mM NaCl, 4.7 mM KCl, 1.2 mM pyruvate, 3.2 mM CaCl₂, 0.5% fatty acid free BSA, pH 7.4) supplemented with 1 nM cytokine. Uptake assay was initiated by adding 2-deoxyglucose to a final concentration of 100 μM at 0.5μCi ³H-2-deoxyglucose /mL. Cells were incubated for 5 minutes at 37°C, 5% CO₂. Uptake was terminated by washing 3 times with ice cold PBS. Cells were lysed in 1% triton X-100 and lysate was subjected to scintillation counting.

Intracellular ^3H -2-deoxyglucose was determined by linear regression of a standard curve of known concentrations.

Non-esterified fatty acid efflux. Fatty acid efflux from adipocytes treated with cytokines was assessed in similar nutrient conditions to those used in respiration studies. Serum-free modified DMEM (Sigma, St. Louis MO D5030) supplemented with 1 mM Glutamax, 1mM sodium pyruvate, 25 mM glucose, 0-1 nM cytokine with 2% fatty acid-free BSA was placed on washed cells after a 24 h cytokine treatment. Assay media was collected after 1 h and replicate measures of free fatty acids were determined spectrophotometrically using the NEFA-C kit (Wako Chemicals, Richmond VA) according to manufacturer's protocol.

Cellular NAD^+ / NADH levels. 3T3-L1 adipocytes were grown in 6-well plates and treated with cytokine as described earlier. Cells were washed twice in ice cold PBS, pelleted by centrifugation, all liquid was removed and resultant pellet was frozen on liquid nitrogen. Cell pellets were thawed and replicate samples were used to determine NAD^+ or NADH levels using the EnzyChromTM NAD^+ / NADH Assay Kit (BioAssay Systems; Hayward CA) according to manufacture's instructions. Levels of nicotinamide adenine dinucleotide were normalized to protein content determined by Bicinchoninic Acid Assay (Sigma, St Louis MO).

Mitochondrial superoxide analysis. Production of superoxide was measured in differentiated 3T3-L1 cells based on previously described procedures (25, 26). The media containing cytokines was removed and replaced with fresh media containing 10% FBS, 10 μ M Triphenylphosphonium hydroethidine (TPP-HE) and 100 nM rhodamine 123 (R123) for 60 min. at 37°C. Cells were then washed with PBS, suspended in 15 μ g/mL digitonin, and incubated on ice for 20 min. to remove residual cytoplasmic probe. The resultant cell pellet was lysed, treated with 2 mg/mL proteinase K for 45 min. followed by 400 U/mL DNase I for 30 min at 37 °C to digest the DNA present in the sample. Samples were diluted 1:5 in run buffer (10 mM borate/1 mM CTAB, pH 9.3) and analyzed by micellar electrokinetic chromatography with laser-induced fluorescence detection (MEKC-LIF) to measure OH-TPP-E⁺ and R123.

Mitochondrial membrane potential ($\Delta\Psi_m$). 3T3-L1 adipocytes grown in 12-well plates were treated for 24 h with or without 1 nM cytokine (N = 4-7). Live cells were stained by addition of 200 nM TMRM (Invitrogen, Carlsbad, CA) and incubated in complete media with or without cytokine for 30 min. at 37°C, 5% CO₂. A depolarization control was included by adding 500 nM of FCCP 5 min. prior to TMRM staining. Cells were then washed 3 times in PBS and removed from culture dish by incubation with 1X phenol red-free trypsin in KRH for 5 min. at room temperature, followed by inactivation with 10% v/v FBS. Cells were then transferred to a FACS tube while passing through a 70 μ m cell strainer. Cell

samples were run on a Becton Dickinson cell analyzer with FACSDiva software (BD Biosciences San Jose, CA) using the following parameters; PE 220V, FSC 500V, SSC 230V. Counts were gated and mean PE fluorescence from 10,000 cells was used to calculate average TMRM fluorescence/ sample. Data is reported as mean \pm SEM and statistical significance determined using the student's *t* test.

Protein carbonylation. Protein carbonyls were detected as described previously (26, 27). Briefly, cells were washed and scraped into buffer containing 100 mM sodium acetate, 10 mM sodium chloride, 0.1 mM EDTA, pH 5.5, complete mini protease inhibitors (Roche), pepstatin, and phosphatase inhibitors (Sigma, St. Louis MO). Cells were lysed by sonication and lipid was separated by low speed centrifugation. After removing the lipid cake, lysates were supplemented with 1% SDS, mixed and centrifuged at 100K x *g* for 1 h. Protein concentration was determined by bicinchoninic acid (BCA) method and 25 μ g total protein was incubated with 0.5 mM biotin hydrazide (Pierce, Rockford, IL) for 3 h at room temperature. The reaction mixture was subjected to SDS-PAGE using a 5-20% acrylamide gel and proteins were transferred to PVDF- immobilon FL membrane (Millipore, Billerica, MA). The membrane was blocked in Licor blocking buffer, incubated with IR-800 Streptavidin (Pierce) diluted 1:15,000 in PBS with 0.1% tween-20 for 1 h, washed thoroughly and carbonylated proteins were visualized

using LI-COR Odyssey infrared imager (LI-COR, Lincoln, NE) and quantified with the software provided by the manufacturer.

Sphingolipid analysis. The cellular content of sphingolipids was measured using a UPLC/MS/MS approach as describe previously (28, 29). Briefly, the cells were washed three times in ice cold PBS and centrifuged at 700 x g, the resultant pellet was flash frozen in liquid nitrogen. Cell pellets were thawed and homogenized in 100 µL PBS, pH 7.4. Homogenates were supplemented with internal standard solution consisting of ¹⁷C-sphingosine, ¹⁷C-S1P and ¹⁷C16-Cer (Avanti Polar Lipids) as well as extraction mixture (isopropanol: water: ethyl acetate, 30:10:60; vol:vol:vol). The mixture was vortexed, sonicated, and centrifuged for 10 min at 12,000 rpm at 4° C. The supernatant was transferred to new tube and evaporated under nitrogen. The dried sample was reconstituted in 100 µl of LC Solvent A (1 mM ammonium formate, 0.1% formic acid in methanol) for UPLC/MS/MS analysis on a Waters Acquity UPLC system (Milford, MA,USA) coupled with Thermo TSQ Quantum Ultra mass spectrometer (Waltham, MA, USA).

Mitochondrial isolation. 3T3-L1 adipocytes were scraped on ice-cold isolation buffer (20 mM Tris-HCl, 220 mM mannitol, 70 mM sucrose, 1mM EDTA, 0.1 mM EGTA; pH 7.4) containing protease inhibitors (Invitrogen, Carlsbad, CA). Cells were lysed with 20 strokes of a glass/ teflon homogenizer, and the resulting

homogenate was centrifuged at 700 x *g* for 10 min at 4° C. The supernatant was transferred to a new tube and centrifuged at 10,000 x *g* for 20 min, and the cytosolic fraction was collected. The pellet was washed once with isolation buffer, centrifuged again at 10,000 × *g* for 10 min and re-suspended in fresh isolation buffer supplemented with 1 % Triton X-100 and 0.1 % SDS. This fraction represents a mitochondrial enriched extract.

mRNA expression. Expression of mRNAs was measured by quantitative RT-PCR. Total RNA was isolated using TRIzol reagent according to manufacturer's protocol. RNA was treated with DNase I and cDNA was synthesized using iScript cDNA synthesis kit (Bio-Rad, Hercules, CA). Amplification was monitored with iQ SYBRgreen Supermix and the MyiQ detection system (Bio-Rad, Hercules, CA). Table 1 contains the primer sequences used to amplify and detect target transcripts. Relative expression was calculated using the $2^{-(\Delta\Delta Ct)}$ method. Data is reported as mean ± SEM and statistical significance determined using the student's *t* test.

Western blot. Cells treated with cytokine as previously stated were washed 3 times in ice-cold PBS, and lysed in buffer containing 50 mM NaCl, 1 mM EDTA, 1 mM EGTA, 50 mM NaF, 1 mM NaP₂O₇, 1% triton-X100, 0.1% SDS, 1X Complete mini Protease Inhibitor (Roche), 1x Phosphatase Inhibitor I and 1x Phosphatase Inhibitor II (Sigma).

Equal amounts of protein were separated by SDS-PAGE, transferred to PDVF Immobilon-FL (Millipore, Billerica, MA) membrane and blocked with 50% Licor Blocking buffer in phosphate-buffered saline (PBS). Blocked membranes were incubated with indicated primary antibodies overnight, and re-blotted with anti-rabbit or anti-mouse secondary antibodies conjugated to LI-COR IRDye for 1 h at room temperature. The bands were detected using a LI-COR Odyssey infrared imager (LI-COR Biotechnologies) and quantified with the software provided by the manufacturer. Protein content was normalized to an internal loading control such as β -actin or Mitofilin.

mRNA	Accession #	Forward (F) and Reverse (R) Primers
Tfam	NM_009360	F: CACTGGGAAACCCACAGCATACAG R: GGACATCTGAGGAAAAGCCTTGC
PGC1 α *	NM_008904	F: CACGAAAGGCTCAAGAGGGATG R: CACCAAAAACCTTCAAAGCGGTCTC
eNOS	NM_008713	F: TGTCTGCGGCGATGTCACTATG R: CGAAAATGTCCTCGTGGTAGCG
NRF1	NM_010938	F: TGGTCCAGAGAGTGCTTGTGAAG R: GGAGGCTGAGGAACGATTTCTTG
TFIIE	NM_026584	F: CAAGGCTTTAGGGGACCAGATAC R: CATCCATTGACTCCACAGTGACAC

* All PGC-1 α splice variants are recognized by this primer set.

Table 1: Primers used for quantitative real-time PCR (qPCR). The forward (F) and reverse (R) primers for the *mus musculus* mRNAs quantified by qPCR are indicated.

Mitochondrial imaging. Cells were grown and differentiated in a 6 well plate containing 25-mm round glass coverslips. For mitochondrial staining, cells were incubated in 300 nM Mitotracker green in KRH buffer at 37° C for 30 min. The cells were washed and maintained in KRH supplemented with 1% BSA and observed under an Olympus Deltavision PersonalDV microscope using a 100x/1.4 Oil objective at 25° C. The software SoftWoRx v.4.1.2 was used to acquire and de-convolve the images. 30 to 35 Z-stacks of 0.30 µm thickness were obtained per cell. The ImageJ plug-in VolumeJ was used to volume-reconstitute the Z-stacked images. Cell showing a fragmented pattern of mitochondria were manually counted and changes in mitochondrial number and mean volume were quantified using the ImageJ-3D Object counter plug-in for ImageJ. Each experiment was performed six times and 16–25 cells per condition were quantified. An increase in fragmentation pattern and in mitochondrial number, together with a decrease in mean mitochondrial volume were considered fission criteria (30).

Statistical analysis. Data are means ± SE of the indicated sample size (n). Student's t-test was performed for comparisons between two groups. Multiple groups were analyzed using one-way ANOVA followed by a protected Tukey's test. Statistical significance was defined as $P < 0.05$.

Results

Pro-inflammatory cytokines have distinct effects on adipocyte respiration profiles.

Chronic treatment of 3T3-L1 adipocytes with each of the pro-inflammatory cytokines TNF α , IL-1 β and IL-6 led to distinct changes in mitochondrial respiration. Oxygen consumption in intact 3T3-L1 adipocytes was measured in a basal state and after cells were challenged with oligomycin to inhibit ATP synthase, FCCP to depolarize the inner mitochondrial membrane, and antimycin A to inhibit complex III and thus oxygen utilization by the electron transport chain. The concentration dependence of TNF α on mitochondrial respiration was evaluated (10 pM to 1 nM) and effects on basal respiration were detected only on the highest concentration (result not shown) and consequently 1 nM cytokine was adopted for all of the studies reported herein. Fig. 1 profiles the respiration of cells that were treated for 24, 48 or 96 h with 1 nM of indicated cytokine as compared to untreated control.

TNF α treatment led to an increase in basal respiration at 24 h that then declined at 48 and 96 h. IL-1 β did not change the basal respiration at 24 or 48 h treatment but did decrease respiration significantly at 96 h. IL-6 treatment was accompanied by an increase in basal respiration only at the 96 h time point (Fig. 1A). Respiration measured after treatment with oligomycin reflects electron flow allowed by proton leak across the inner mitochondrial membrane, thus we

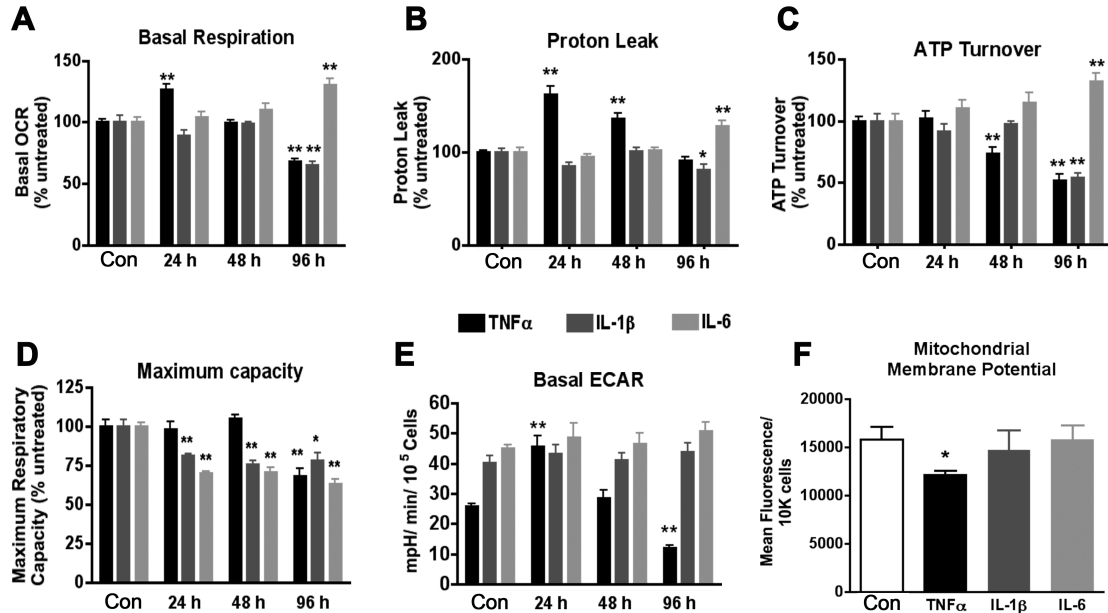


Fig 1. Respiration profiling in chronic cytokine treatment of 3T3-L1

adipocytes. 3T3-L1 adipocytes were treated with 1 nM of the indicated cytokine

in complete media for 24-96 h beginning on day 6 of differentiation and

parameters linked to respiration and other biological processes measured using

the Seahorse XF24 Analyzer. Values were used to calculate total oxygen

consumption due to basal respiration (A), inner mitochondrial membrane proton

leak (B), cellular ATP demand (C), as well as the maximum respiratory capacity

(D). ECAR was compared in cytokine treatments of varying duration under basal

respiration conditions (E). $\Delta\Psi_m$ was determined in 3T3-L1 adipocytes treated for

24 h with 1 nM cytokine (N=3) by TMRM staining and flow cytometry of 10,000

cells (F). All data are represented as mean \pm SEM, statistical significance of ** P

< 0.005, or * P < 0.05 was determined by student's *t*-test compared to untreated

0 h control. N = 5 unless noted.

calculated the proton leak and ATP turnover. $\text{TNF}\alpha$ significantly increased the proton leak at 24 and 48 h, IL-1 β caused a modest decrease in the proton leak at 96 h, and IL-6 elevated the proton leak only at the latest 96 h time point (Fig. 1B). Respiration coupled to ATP synthesis (ATP turnover) was unchanged by any of the cytokines tested at 24 h. However $\text{TNF}\alpha$ lowered ATP turnover at 48 and 96 h, a decrease that was also observed after 96 h of IL-1 β , and an increase was measured after 96 h of IL-6 treatment (Fig. 1C). The addition of the proton ionophore FCCP collapses the $\Delta\Psi_m$ and allows for the measurement of maximal oxygen consumption. Fig. 1D shows that the respiratory capacity remains intact in $\text{TNF}\alpha$ treatment at 24 and 48 h, but declines after 96 h. IL-1 β and IL-6 conversely decrease the maximum capacity at all time points measured.

The extra cellular acidification rate (ECAR) is an indicator of lactate efflux and indirectly assess reliance of the cells on anaerobic glycolysis. While the interleukins produced no measurable change in this parameter, $\text{TNF}\alpha$ increased ECAR by 1.7 fold at 24 h and then decreased the level by half at 96 h (Fig. 1E). Since basal lipolysis from 3T3-L1 adipocytes can be enhanced by pro-inflammatory cytokines, we hypothesized that the increased ECAR could be due in part to efflux of free fatty acids. We therefore measured the non-esterified free fatty acids (NEFAs) after 24 h of cytokine treatment. Fig. 2A demonstrates that while $\text{TNF}\alpha$ increased NEFAs in the media as expected, IL-1 β had a similar effect without the concomitant increase in ECAR (Fig. 1E). Both $\text{TNF}\alpha$ and IL-1 β

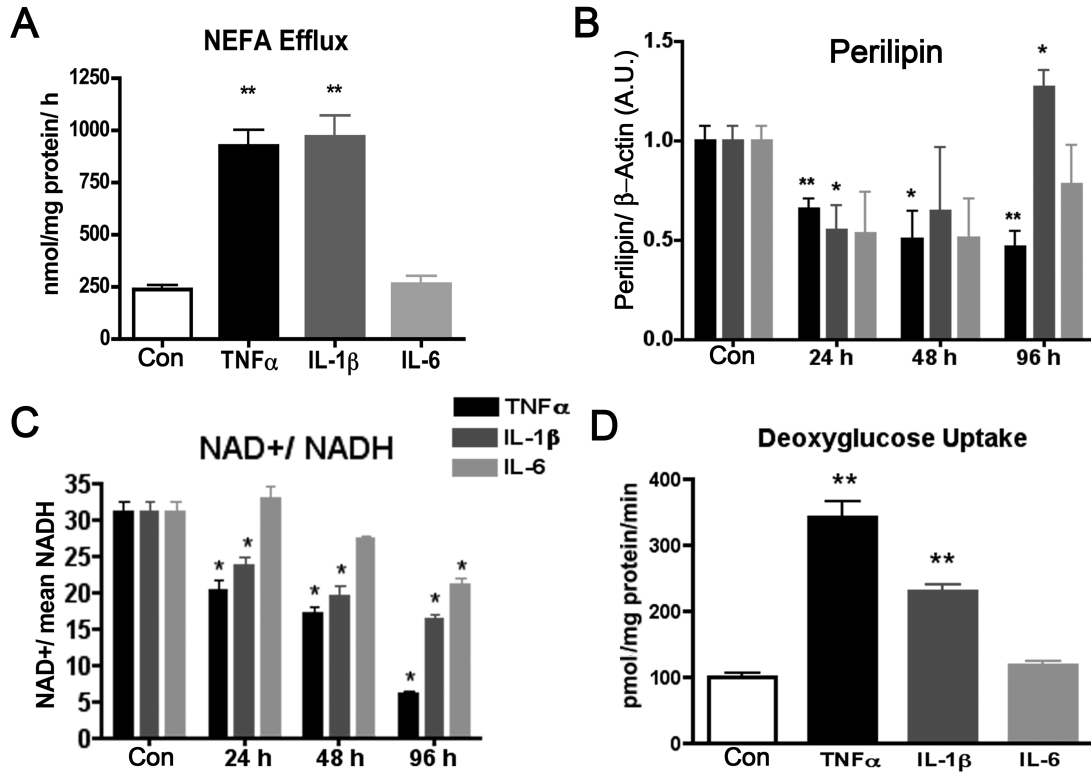
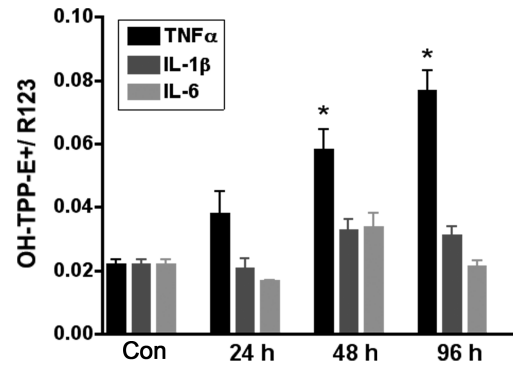
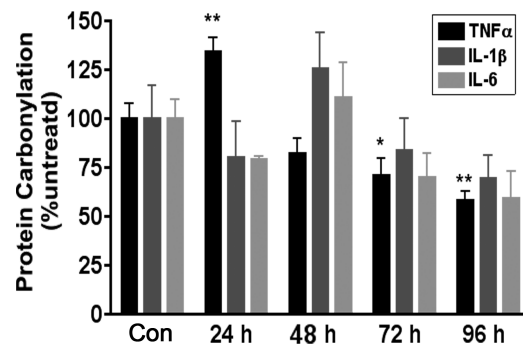
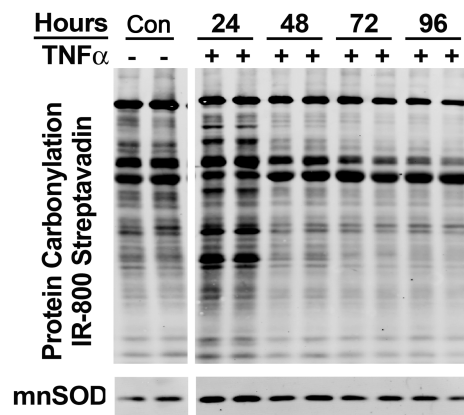


Fig 2. Lipid and glucose metabolism following cytokine treatment of 3T3-L1 adipocytes. Non-esterified fatty acid efflux (A), perilipin abundance (B), NAD⁺/NADH (C) and 2-deoxyglucose uptake (D) were measured following 24 h treatment of adipocytes with 1 nM cytokine. In panel B, Western blot quantitation of perilipin protein signal was normalized to β -actin protein signal (N = 6). For all panels * $P < 0.05$, ** $P < 0.01$ compared to control.

treatment lead to a decline in perilipin protein level at 24 h (Fig. 2B). Conversely, 1 nM IL-6 exhibited no effect on basal fatty acid efflux (Fig. 2A). These data provide support the conclusion that the observed changes in ECAR are derived from lactate efflux rather than fatty acid efflux and that a loss of perilipin expression may contribute to the increased fatty acid efflux in the absence of lipolytic stimuli. Treatment of adipocytes with TNF α or IL-1 β for 24 h also led to a 3.5 or 2 fold increase respectively in basal glucose transport as measured by 2-deoxyglucose uptake (Fig. 2D). Interestingly the IL-1 β treatment increased glucose uptake and fatty acid efflux, without a change in ECAR. The observed metabolic changes were also accompanied by a shift in the redox status. Lower NAD⁺/NADH ratios were seen in TNF α and IL-1 β treatment at all time points and at 96 h after treatment with IL-6 (Fig. 2C).

To parallel the changes in cytokine-induced respiration to changes in the inner mitochondrial membrane potential ($\Delta\Psi_m$), we utilized TMRM staining coupled with flow cytometry analysis. Fig. 1F reveals that 24 h treatment of 3T3-L1 adipocytes with TNF α decreased TMRM staining intensity by 23% whereas treatment with IL-1 β or IL-6 had no detectable influence on the $\Delta\Psi_m$. These results are consistent with the proton leak detailed in Fig. 1B.

Fig 3. Reactive oxygen species and protein carbonylation following cytokine treatment of 3T3-L1 adipocytes. Day 6 3T3-L1 adipocytes were treated with the indicated cytokine for 24 h and mitochondrial superoxide formation (A) and protein carbonylation (B) evaluated. N=3. Protein carbonylation blot of TNF α treatment for 24-96 h was probed simultaneously with anti MnSOD (C). The break in panel (C) represents a translocation of lanes from the same image and exposure purely for illustration purposes only and does not alter the image information.

A**B****C**

Mitochondrial oxidative stress and protein carbonylation is increased by TNF α , but not by IL-1 β or IL-6. A previous report states that obesity-linked inflammation increases oxidative stress in adipose tissue (6). To assess the effect of specific cytokines on ROS synthesis, superoxide production was evaluated by accumulation of oxidized TPP-HE ($\Delta\Psi_m$ sensitive) normalized to R123 ($\Delta\Psi_m$ sensitive as well) in the mitochondria. While TNF α treatment led to a 2, 3 and 3.5 fold increase in superoxide levels in the mitochondria at 24, 48, and 96 h respectively, no significant changes were detected in IL-1 β or IL-6 treated cells (Fig. 3A).

We hypothesized that the increased superoxide would lead to increased protein carbonylation similar to that observed in adipose from diet induced obese mice (31). Using IR800 conjugated streptavidin to detect biotin hydrazide conjugated to protein carbonyls, IL-1 β or IL-6 show negligible effects on protein carbonylation when compared to control cells (Fig. 3B). In contrast, TNF α treatment increased the carbonylation of proteins at 24 h while at longer duration of treatment protein carbonylation was surprisingly decreased (Fig. 3, B and C). Further investigation revealed that the expression of the mitochondrial superoxide dismutase, SOD2, is increased by TNF α treatment at 24 h (Fig. 3C). This antioxidant response may, in part, explain the observation of a decrease in

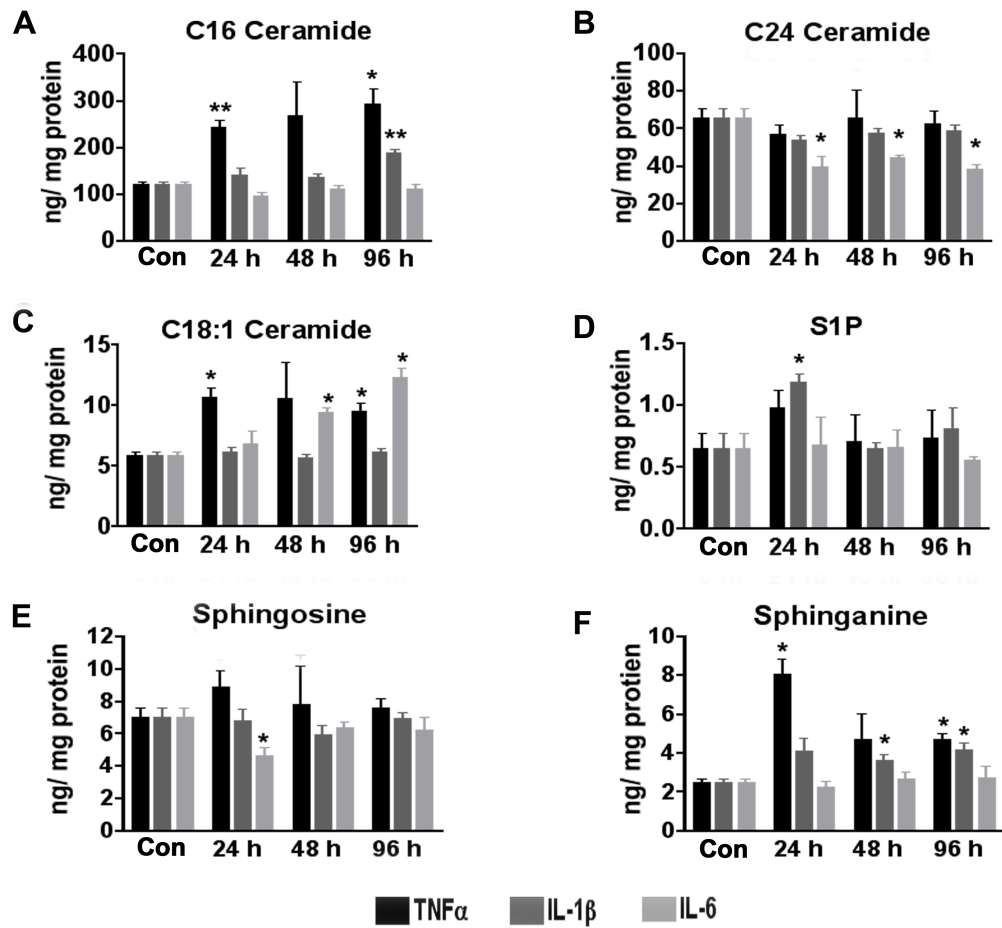


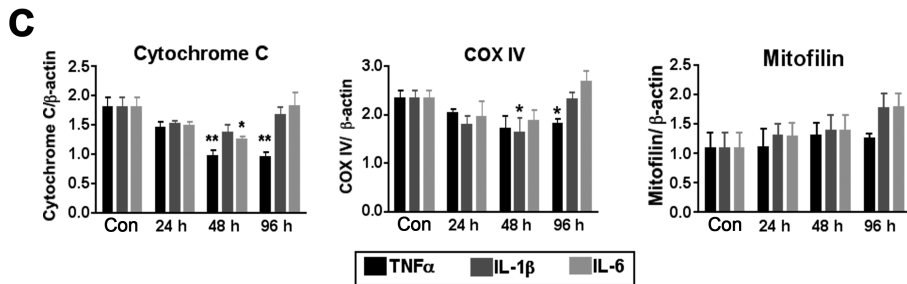
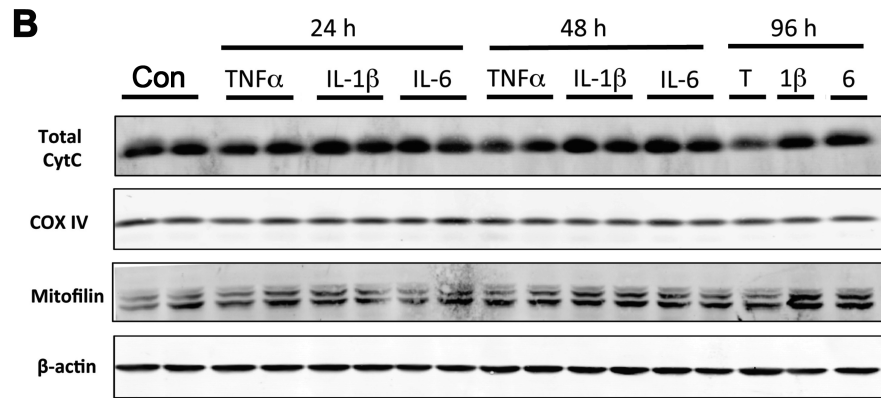
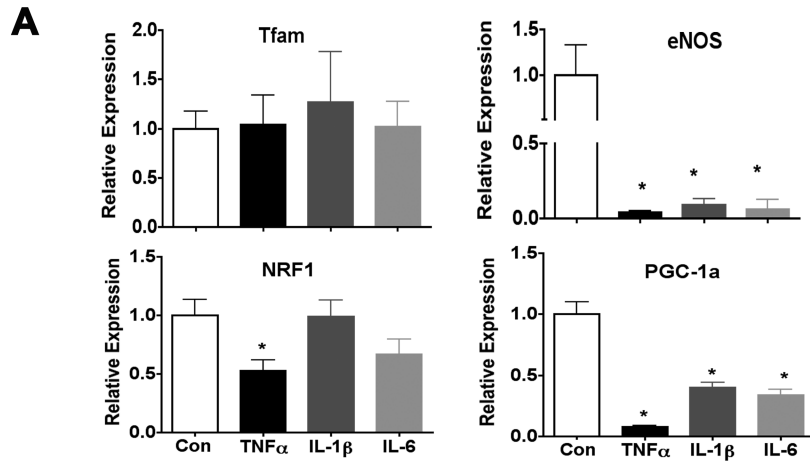
Figure 4 Sphingolipid profiles following cytokine treatment. 3T3-L1 adipocytes were treated with 1 nM of the indicated cytokine for 0-96 h. At the indicated times cellular extracts were subject to UPLC/MS/MS and the levels of sphingolipids determined. C16 ceramide (A), C24 ceramide (B), C18:1 ceramide (C), sphingosine-1 phosphate (S1P) (D), sphingosine (E) and sphinganine (F). Each bar represents the mean \pm SEM, N = 3, * $P < 0.05$ by student's t -test compared to 0 h control.

protein carbonyls found at later time points (Fig. 3C) despite an increase in superoxide (Fig. 3A).

Sphingolipid profiles are selectively altered with cytokine treatment. Compelling evidence suggests a central role for ceramides in the pathology of the metabolic syndrome (32, 33). Moreover, adipocytes robustly produce ceramides in response to high levels of palmitate or in response to pro-inflammatory stress (29). To address the effects of specific cytokines on sphingolipid synthesis, lipidomic analysis was carried out on 3T3-L1 cells treated with various cytokines. While the total cellular ceramide levels trended toward an increase with TNF α treatment, individual ceramide species showing significant increases include C16 and C18:1 (Fig. 4, A and C). C24-ceramide levels were not altered by TNF α or IL-1 β but decreased in response to IL-6 treatment (Fig. 4B). The level of sphingosine 1-phosphate (S1P), a mediator of inflammation and leukocyte trafficking (34) is transiently increased in adipocytes treated with IL-1 β , but unchanged with IL-6 (Fig. 4D). Sphinganine, the *de novo* synthetic precursor to ceramide, was increased by TNF α and IL-1 β treatment, but not altered by IL-6 (Fig. 4F).

Mitochondrial content and biogenesis markers are altered with cytokine treatment. Previous work by Curtis *et al.* has shown that TNF α treatment of 3T3-

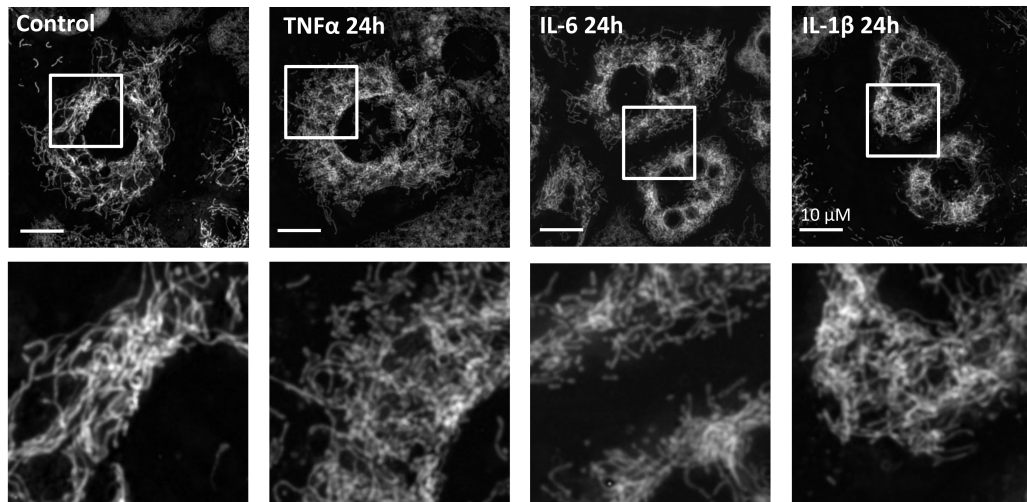
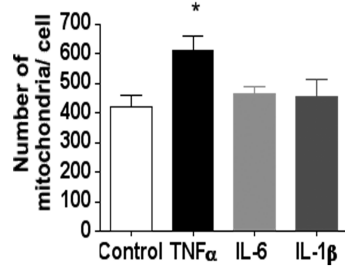
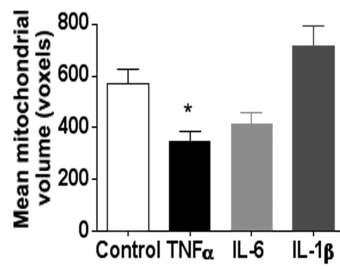
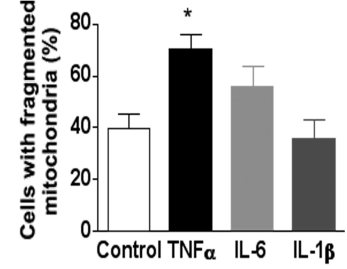
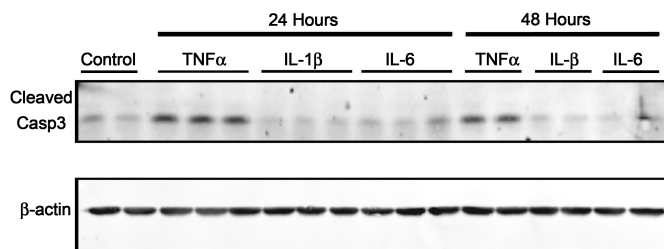
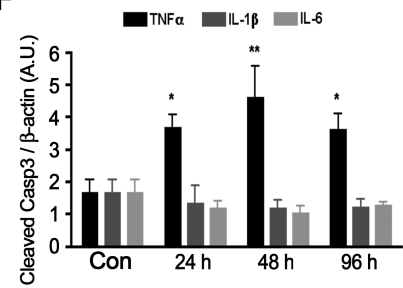
Figure 5. Expression of factors linked to mitochondrial biogenesis and function in response to cytokine treatment. 3T3-L1 adipocytes were treated with 1 nM of the indicated cytokine for 24 h and the mRNA (A) and protein (B-C) expression of factors linked to mitochondrial biogenesis and function were evaluated. Western blot analysis of adipocytes (B). Quantitation of each protein was normalized to β -actin and graphed relative to control (C) (N=6). Q-PCR results were normalized to reference mRNA transcription factor II E (TFIIE). T = $\text{TNF}\alpha$, 1 β = IL-1 β and 6 = IL-6. In panel A the graph of eNOS expression has a broken y axis so that the $\text{TNF}\alpha$ treatment group is visible.



L1 adipocytes led to decreased mRNA expression for glutathione S-transferase, a key antioxidant responsible for metabolism of much of the reactive aldehydes produced by cells (26). To evaluate the effect of cytokines on expression of genes linked to the mitochondrial biogenesis program, quantitative RT-PCR (qPCR) (Table 1) was performed on mRNA isolated from 3T3-L1 adipocytes treated with pro-inflammatory cytokines for 24 h. Interestingly, none of the cytokines (TNF α , IL-6 or IL-1 β) tested significantly altered the expression level of the transcription factor A mitochondria (Tfam). Expression of nuclear respiration factor 1 (NRF1) was selectively decreased by TNF α (Fig. 5A) and all three pro-inflammatory cytokines significantly reduced the expression of master mitochondrial biogenesis regulators, peroxisome proliferator-activated receptor gamma coactivator 1 α (PGC1 α) and endothelial nitric oxide synthase (eNOS) (Fig. 5A). Consistent with altered mitochondrial biogenesis, TNF α treatment led to a significant decrease in protein levels of nuclear-encoded cytochrome c oxidase IV (COX IV) and cytochrome c (Cyt C). However, the abundance of the inner membrane-associated protein mitofilin remained unchanged with cytokine treatment (Fig. 5B and 5C). Interleukin 1 β also decreased COXIV protein levels but this effect was only present at 48 h of treatment and returned to basal levels by 96 h. Interleukin 6 treatment caused a similar transient decrease in total Cyt C levels at 48 h (Fig. 5B and 5C).

Figure 6. Mitochondrial morphology in cytokine-treated 3T3-L1 adipocytes.

Live cell images of Mitotracker green stained 3T3-L1 adipocytes after 24 h treatment with 1 nM cytokine (A). Images of more than 15 cells were analyzed using ImageJ-3D software to determine average mitochondrial number (B) and average volume per mitochondrion (C) (N = 5-13). Each of the cells sampled was scored for mitochondrial fragmentation and the percentage of cells exhibiting fission was calculated (D) N = 6-16 for each treatment. * $P < 0.05$ compared to control. Western blot of whole cell extract detecting cleaved caspase 3 and β -actin (E). Densitometric analysis of cleaved caspase 3 Western blots, N=4-6 (F).

A**B****C****D****E****F**

Mitochondrial content and network morphology is altered by TNF α . To determine the effect of inflammatory cytokines on mitochondrial dynamics, we evaluated mitochondrial content and network morphology using fluorescence microscopy. As shown in Fig. 6, treatment of 3T3-L1 adipocytes with TNF α induced significant mitochondrial fragmentation as revealed by an increase in the number of mitochondria per cell and a decrease in mean volume per mitochondrion when compared to control cells. The number of cells exhibiting fragmented mitochondrial morphology was also increased by TNF α treatment (Fig. 6D). In contrast, IL-6 or IL-1 β treatment had no significant effect on mitochondrial morphology or fragmentation. Since apoptosis is accompanied by fission of mitochondria (22), we next investigated levels of apoptotic effector cleaved caspase 3 and found that TNF α alone induced the apoptotic program as revealed by caspase 3 cleavage (Fig. 6E). The activation of caspase 3 and induction of apoptosis has been reported in adipose from both high fat fed mice and obese humans (35).

Since mitochondrial morphology is acutely controlled through the expression, processing and localization of several key regulatory proteins (36) we analyzed the effects of cytokine treatment on the expression of fusion proteins OPA1 and MFN2, fission protein FIS1, as well as DRP1 levels and localization. Treatment

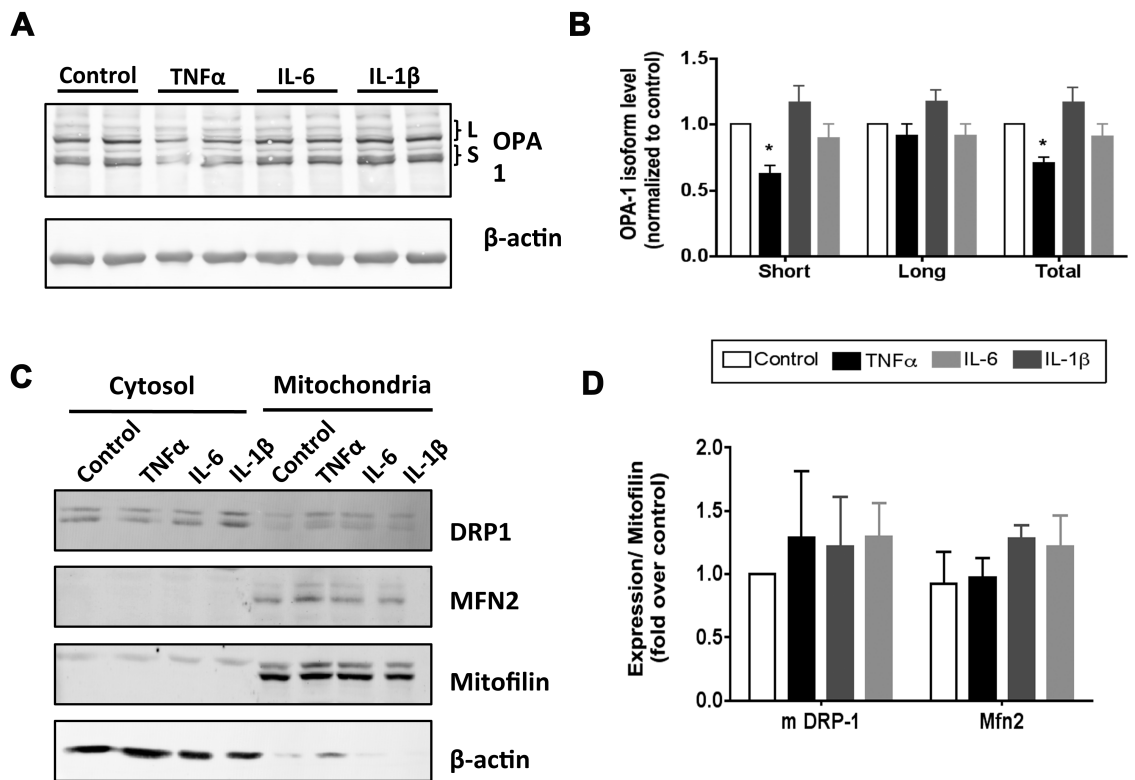


Figure 7. Expression of proteins linked to mitochondrial fission and fusion in response to cytokine treatment. Extracts from 3T3-L1 adipocytes treated for 24 h with 1 nM cytokine in complete media were immunoblotted for OPA1 or β -actin (A). Densitometric analysis of OPA1 expression from 3 independent experiments (B). Protein levels of DRP1, MFN2, mitofilin, and β -actin in cytosolic and mitochondrial cellular fractions measured by Western blot (C) and protein abundance in the mitochondrial fraction normalized to mitofilin (D).

of 3T3-L1 with $TNF\alpha$ induced a significant reduction in the level of OPA1. Closer inspection reveals a greater disappearance of the short (S) than the long (L) isoform of OPA1 when compared to controls (Fig. 7, A and B). No significant changes in OPA1 expression or processing were observed with IL-6 or IL-1 β treatment. In contrast, expression of the outer membrane fusion protein MFN2 was not altered by any of the cytokine treatments analyzed (Fig. 7, C and D). We next investigated the expression of FIS1, a mitochondrial protein thought to direct the localization of cytosolic DRP-1 to the mitochondria. Once localized at the mitochondria, DRP-1 can form a ring around the organelle facilitating constriction and fission (22). Total cellular expression of FIS1 and DRP-1 were not changed with cytokine treatment (data not shown). Likewise, the mitochondrial localization of DRP-1 did not significantly change with any of the cytokines analyzed (Fig. 7, C and D). These results suggest the decrease in expression and/or an increase in processing of OPA1 as the primary effector of increased mitochondrial fragmentation seen in $TNF\alpha$ treated adipocytes (Fig. 6).

TNF α induced respiration precedes caspase 3 activation and mitochondrial fragmentation. To determine if the altered mitochondrial function and morphology measured after $TNF\alpha$ treatment was linked to apoptosis we evaluated oxygen consumption and morphological analyses relative to caspase 3 cleavage. As shown in Fig. 8A, caspase 3 cleavage is evident as early as 2 h after $TNF\alpha$ treatment. By comparison, basal respiration is significantly increased 50% after

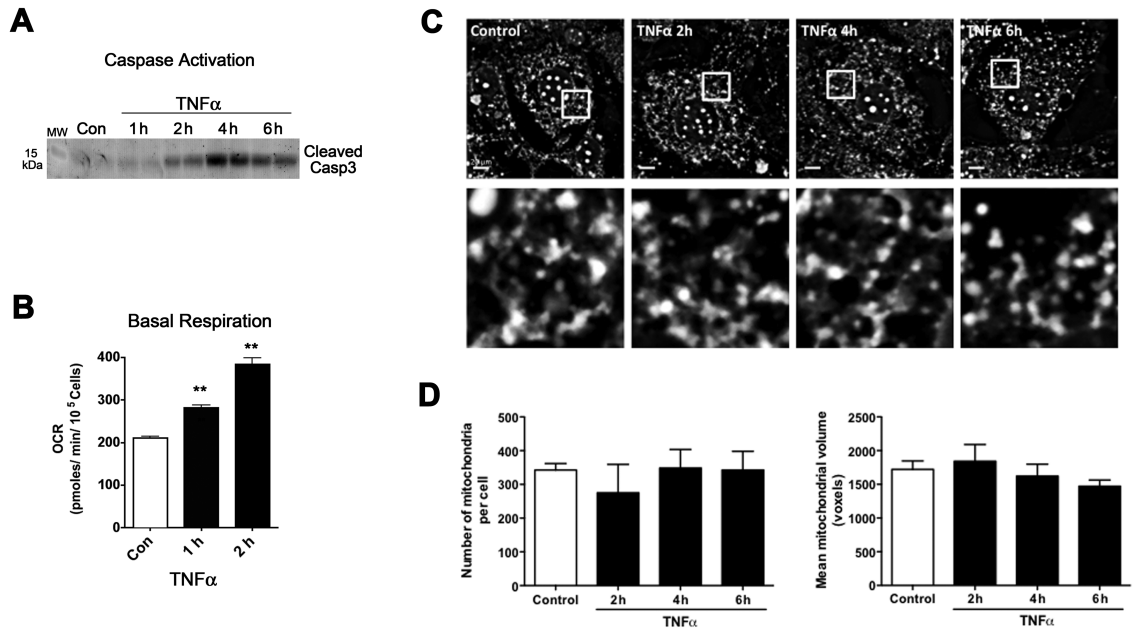


Figure 8. Acute effects of TNF α on mitochondrial fragmentation. Western blot of whole cell extract detecting cleaved caspase 3 after no treatment control or 1 nM TNF α for 1, 2, 4 and 6 h (A). Basal respiration measured by XF24 analyzer in adipocytes (Con) and after 1 nM TNF α for 1- 2 h. N=3-5, ** $P < 0.001$ (B). Fluorescent microscopy and morphometric analysis of mitotracker green stained adipocytes treated or not (Control) for 2, 4, and 6 h with 1 nM TNF α (C). Cells were scored for mitochondrial number and mean mitochondrial volume as reported in Fig. 6 (D,). N=3.

1 h of TNF α treatment (Fig. 8B). However, mitochondrial morphology was not affected by TNF α until 6 h post treatment (Fig. 8C and 8D). Taken together, these analyses reveal that TNF α first alters respiration, then activates the apoptotic pathway and eventually causes mitochondrial fragmentation (Figures 6 and 8).

Discussion

Visceral obesity is accompanied by infiltration of adipose depots with pro-inflammatory macrophages and T cells leading to the working model that immune-cell factors drive the progression from insulin sensitivity to insulin resistance (8, 9, 16, 37). In a variety of obese animal models, both nutritional and genetic, mitochondrial dysfunction has been correlated with inflammation and increased oxidative stress (6). Numerous studies aim to unravel the disease progression of type II diabetes from the lean insulin-sensitive state to obese insulin-resistant, yet it is unclear if mitochondrial dysfunction in the adipocyte will lead to obesity and tissue inflammation or if the local inflammation is causing mitochondrial dysfunction within the adipocyte. Although the initiating event remains unclear, previous studies in our laboratory show that each of the pro-inflammatory cytokines analyzed here can dramatically reduce expression of a number of antioxidants in adipocytes (38) and by-products of oxidative stress can activate macrophage to release pro-inflammatory cytokines (39) perpetuating the oxidative stress and inflammation axis in adipose. The present study was undertaken to determine the effects of three specific inflammatory cytokines that are found to be chronically elevated in obese adipose tissue on mitochondrial function in the adipocyte. Focusing on the common cytokines implicated in adipose biology, $\text{TNF}\alpha$, $\text{IL-1}\beta$ and IL-6 , we found that each cytokine leads to mitochondrial dysfunction, yet the mode of action and cellular outcome is unique for each.

Mitochondrial Respiration and Cellular Metabolism--In our studies TNF α treatment of 3T3-L1 adipocytes results in a number of dramatic cellular changes linking oxidative stress to altered mitochondrial metabolism and dynamics. There are two known receptors for TNF α (TNFR1 and TNFR2) and both are expressed in adipose tissue. While both membrane bound and soluble forms signal through TNFR1, only the membrane bound form is able to signal through TNFR2 (17). TNF α treatment of adipocytes led to a significant increase in C16 and C18:1 ceramide synthesis as well as an increase in sphinganine (Fig. 4). Ceramides, along with their derivatives, are known to interact with Bcl family members to induce mitochondrial outer membrane permeability. Increased outer membrane permeability allows the release of c (Cyt C) into the cytoplasm which can in turn initiate the apoptosis pathway through caspase activation (40). This process appears to occur selectively in TNF α treatment of adipocytes as demonstrated by increased ceramides (Fig. 4), the loss in Cyt C (Fig. 5B and 5C) and an increase in activated/cleaved caspase 3 (Fig. 6E and 6F) none of which were observed in interleukin treatments. These data suggest that TNF α exposure would lead to high levels of adipocyte apoptosis. However there are reports of several control measures in place to limit cell death (41). For example, TNFR2 is highly induced in adipose from genetic obesity models (42) (43), and since this receptor lacks the death domain, it may play a pro-survival role to combat apoptotic signaling that arises with the increased TNF α in obese adipose.

Accompanying the changes in ceramide levels, TNF α treatment leads to a shift in the cellular redox status shown by the decreased NAD⁺/ NADH ratio (Fig. 2C). Cellular respiration was increased at 24 h followed by a decrease by 96 h (Fig. 1). TNF α increased proton leak and diminished $\Delta\Psi_m$ while causing a significant decrease in ATP-coupled respiration at 48 and 96 h. Although increased proton leak could be sufficient to decrease $\Delta\Psi_m$ (24) we cannot rule out other effects such as increased permeability to explain $\Delta\Psi_m$ loss. These actions could be mediated by TNF α directly or by other intermediates such as ceramides. Interestingly, the synthetic ceramide analog C2-ceramide was described to have similar effects on cardiomyocytes to that of TNF α in the adipocyte. In the cardiomyocyte study, C2-ceramide stimulated Cyt c release from the mitochondria, was accompanied by $\Delta\Psi_m$ and decreased ATP levels prior to cell death (44) TNF α treatment also increased basal glucose uptake (Fig. 2) and basal ECAR (Fig. 1). All these data are consistent with TNF α -dependent uncoupling of oxygen consumption and ATP synthesis. This uncoupling leads to a compensatory increase in aerobic glycolysis without complete oxidation, similar to the Warburg effect seen in cancer biology (45, 46). Moreover, Chen et al (47) reported similar results in 3T3-L1 adipocytes treated with TNF α . They found decreased intracellular ATP levels and decreased $\Delta\Psi_m$, further supporting our mitochondrial dysfunction data. TNF α also resulted in a significant time dependent loss of perilipin (Fig. 2B) that was accompanied by increased fatty

acid release as measured by elevated NEFA efflux at 24 h (Fig. 2A). *In vivo*, constitutive up regulation of lipolysis leads to increased circulating FFAs in the fed state, perhaps contributing to lipotoxicity in obese subjects (11).

In contrast to the effects mediated by $\text{TNF}\alpha$, $\text{IL}1\beta$ had less metabolic impact on mitochondrial function. $\text{IL}1\beta$ signals to activate transcription through c-Jun, NF- κB as well as increase cellular cAMP levels (48). In this study $\text{IL}1\beta$ had little impact on basal respiration, ATP coupled respiration, and proton leak until the latest 96 h time point, where it decreased these parameters (Fig. 1). $\text{IL}1\beta$ does cause mitochondria dysfunction by reducing the maximum respiratory capacity at all time points measured (Fig. 1D). The source of the reduced respiratory capacity remains unknown, but it is not likely a reduction in mitochondrial mass since no differences were detected by microscopy or mitochondrial protein level. The pattern of mitochondrial dysfunction resulting from $\text{IL}1\beta$ exposure is distinct from that seen with $\text{TNF}\alpha$ treatment, highlighting the unique characteristics of each signaling pathway as the primary effectors of these alterations. Similar to $\text{TNF}\alpha$ treatment, $\text{IL}1\beta$ treated cells did exhibit lower NAD^+/NADH ratios as well as increased glucose uptake, but unlike $\text{TNF}\alpha$ showed no change in ECAR or $\Delta\Psi_m$ (Fig. 1E-F and 2D). After 24 h treatment with $\text{IL}1\beta$, 3T3-L1 adipocytes did exhibit diminished levels of perilipin proteins (Fig. 2B) and increase basal fatty acid efflux (Fig. 2A), however the decrease in perilipin level was transient and was actually significantly increased by 96 h.

Of the cytokines analyzed in this study, IL-6 is divergent from the others in that it does not directly activate transcription factors NF- κ B or c-jun (21, 47). IL-6 is also controversial in what role it has as an inducer of obesity-linked insulin resistance. While the expression is highly correlated to adiposity and up to 30% of circulating IL-6 is estimated to be adipose derived in healthy individuals, there are reports of IL-6 having anti-inflammatory roles as well (49, 50). In this study, IL-6 treatment of adipocytes did result in mitochondrial dysfunction at all time points analyzed as indicated by the reduced mitochondrial respiratory capacity (Fig. 1D). However the cytokine had little effect on other respiratory parameters until the late 96 h time point, when IL-6 treated cells exhibited increased basal, proton leak-induced and coupled respiration (Fig. 1A-C). The delayed response to IL-6 of basal respiration and proton leak point to a secondary effector, perhaps a target gene of JAK/ STAT pathway. Unlike TNF α or IL-1 β , treatment with IL-6 is able to increase ATP turnover (Fig. 1C) suggesting an increased energy demand following exposure. IL-6 also reduced the NAD⁺/ NADH ratio, but again this was only observed after 96 h of treatment suggesting an indirect effector downstream of the IL-6 signal. IL-6 did not alter adipocyte basal glucose transport, perilipin expression, or lipolysis (Fig. 2). Our results suggest that exposure of adipocytes to 1nM (20 pg/ mL) IL-6 has very little direct effect on adipose metabolism. More focused studies are needed to determine if IL-6 signaling or a secondary mediator is responsible for changes in mitochondrial function after 96 h. Other

studies have demonstrated that infusion with recombinant IL-6 stimulates lipolysis and fat oxidation selectively in the muscle without metabolic effects in the adipose tissue in humans (51). This work is in agreement with our findings.

Oxidative Stress--TNF α treatment led to a biphasic change in the oxidative stress program. At shorter times (24 h) TNF α increased superoxide anion levels and protein carbonylation while at longer time points there was an increase in mitochondrial superoxide, yet reduced protein carbonylation was observed (Fig. 3). Since elevated $\Delta\Psi_m$ and electron transport are reported to be a major source of superoxide production in the mitochondria (19, 52), it was surprising to detect a sharp rise in mitochondrial superoxide in conjunction with reduced $\Delta\Psi_m$ (Fig.s 3A and 3F). However, our data is consistent with the work of Chen et al. (47) who found evidence of decreased $\Delta\Psi_m$ and increased cellular ROS levels using H2-DCFDA staining coupled with flow cytometer or microscopic analyses after chronic TNF α in 3T3-L1 adipocytes. Moreover, one report concludes that dihydrolipoamide dehydrogenase, the E3 shared by alpha-ketoglutarate dehydrogenase and pyruvate dehydrogenase, is a source of ROS (superoxide and hydrogen peroxide) in the presence of substrate but absence of NAD $^+$ (18). Since TNF α leads to a reduction in NAD $^+$ levels (Fig. 2C), dihydrolipoamide dehydrogenase offers one possible source for the observed increase in mitochondrial superoxide (Fig. 3A). NADPH oxidase is also known to be activated by TNF α treatment (53) and many report increased cellular ROS after

TNF α treatment of adipocytes (47, 54), our work demonstrates that there is also an increase in superoxide production within the mitochondria with this potent ROS inducer.

IL-1 β elicited no significant alteration of mitochondrial superoxide production or protein carbonylation (Fig. 3) indicating a state of normal oxidative homeostasis with this cytokine. IL-1 β did slightly increase C16 ceramide levels at 96 h, S1P at 24 h and sphinganine at 48-96 h (Fig. 4). However, these increased sphingolipid species were not accompanied by a loss in Cyt C or increase in caspase 3 activation as was measured with TNF α (Fig. 5B). In fact, IL-1 β did not alter any of the mitochondrial protein levels measured, but did significantly reduce the expression of eNOS and PGC-1 α mRNA (Fig. 5A). Importantly, despite the decrease of eNOS and PGC-1 α mRNA levels, we find no significant change in mitochondrial mass or morphology (54, 55). These results caution the exclusive use of mRNA profiling as a means to interpret cellular metabolism.

There was also no change observed in mitochondrial superoxide production or protein carbonylation (Fig. 3) after IL-6 treatment. Analysis of sphingolipids after IL-6 treatment did present a varied pattern depending on the lipid species. While sphinganine, S1P, and C16 all remained constant, C24 ceramide was significantly reduced after 24-96 h and C18:1 was elevated after 48 h of IL-6 treatment (Fig. 4). With regard to ceramide-mediated decrease in $\Delta\Psi_m$, there

was a transient loss of Cyt C seen at 48 h (Fig. 5C), but no change mitochondrial morphology or in caspase 3 activation (Fig. 6).

Mitochondrial Dynamics--Inflammatory cytokine treatment had a major effect on both mitochondrial biogenesis and dynamics. Mitochondria are very dynamic and through fusion and fission form vast networks and fragment or divide respectively. In our studies, mRNA expression of mitochondrial biogenesis factors such as PGC-1 α and NRF-1 were decreased with TNF α treatment as were the protein levels of some components of electron transport, Cyt C and COXIV (Fig. 5C). However, mRNA expression of Tfam and the protein levels of mitofilin are stable after TNF α treatment (Fig. 5). Despite relatively little change in mitofilin level, mitochondria were significantly more fragmented after TNF α treatment, most likely due to the lower levels of the inner membrane fusion protein OPA1, notably a loss of the short isoform (Fig. 7). Recently, the protein OPA1, usually related to mitochondrial fusion, was described in the adipocyte as a regulator of hormone-stimulated lipolysis by acting as an A-kinase anchoring protein on the surface of the lipid droplets. Interestingly, OPA1 was found to interact with perilipin promoting its stability as evidenced by perilipin down regulation upon OPA1 gene silencing (56). The role for OPA1 in basal lipolysis was not evaluated in this paper, but it is tempting to speculate that a decrease in OPA1 could down regulate perilipin, thus altering lipid droplet protein coating and disrupting lipolysis regulation. While this could provide a novel explanation for

our basal lipolysis increase with TNF α , it does not explain the increased fatty acid efflux and transient perilipin reduction in IL- β treated cells.

Since mitochondrial morphology results from the equilibrium of the fusion and fission rates (21) either an increase in the rate of fission or a decrease in the rate of fusion can cause a fragmented mitochondrial appearance. OPA1 is processed in response to a variety of stress conditions and loss of mtDNA, dissipation of $\Delta\Psi_m$, or a decrease of mitochondrial ATP levels all can initiate OPA1 processing by OMA1 (57), among other proteases. Clearly treatment of 3T3-L1 adipocytes with TNF α creates conditions that are favorable for OPA1 cleavage, but the cause of the diminished short isoform remains undetermined. OPA1 processing is necessary for its function but an imbalance in the ratio of long to short isoforms can affect its function as mitochondrial fusion protein (58). Thus, this imbalance in OPA1 isoforms could be sufficient to explain the fragmented mitochondria phenotype observed. Although Chen et al. (47) reported increased levels of the fission protein DRP1 by TNF α treatment, we did not observed similar results. This discrepancy could be due to differences in the antibodies used for immunodetection of DRP1, or the dose (17 ng/mL vs 4 ng/mL) and duration (24 h vs 96 h) of treatment. Since the distribution of DRP1 is more important than its level of expression when assessing its function as a fission protein (29) and we did not observe any signs of translocation of DRP1 to the mitochondria, we believe that OPA1 decrease is sufficient to explain the mitochondrial fragmentation observed in our conditions. In contrast to TNF α , but consistent

with stable fission and fusion protein levels, we were not able to detect any impact of IL-1 β or IL-6 on mitochondrial morphology or dynamics (Fig. 6).

Overall, the results reported herein indicate that inflammatory cytokines have unique and distinct influences on mitochondrial respiration, oxidative stress and dynamics. TNF α most dramatically alters 3T3-L1 adipocyte functions whereas IL-1 β and IL-6 have more modest effects. These results are consistent with findings using TNF α receptor null mice that exhibit attenuated obesity-linked metabolic dysfunction (59). Moreover, since IL-6 can induce low levels of TNF α synthesis by 3T3-L1 adipocytes it is not unreasonable to consider that some of the chronic effects of interleukins are mediated by TNF α production and signaling. As such, while each of the cytokines is considered pro-inflammatory, TNF α exhibits the most profound influences on mitochondrial function in the 3T3-L1 adipocyte.

Acknowledgements

We thank the Minnesota Supercomputing Institute for software support in primer design, Kazutoshi Aoyama for technical assistance in flow cytometry as well as Duncan Clarke the use of the Olympus Deltavision microscope. We also appreciate X. Mai Persson at the CTSA Metabolomics Core at Mayo Clinic for providing technical expertise in mass spectrometry of sphingolipid analyses. A special thanks is extended to Marissa Lee for expert technical support with cell culture.

Grants

This work was supported by NIH RO1 DK084669 (to DAB) and NIH P30DK050456, the Minnesota Obesity Center. MDJ was supported by UL1 TR000135 from the National Center for Advancing Translational Sciences (NCATS). JK was supported by a doctoral scholarship from CONICYT-CHILE. SL was supported by FONDAP 15130011, ACT1111 and FONDECYT 1120212 from CONICYT, Chile. MAD was supported by NIH training grant T32DK007203 and R01AG020866.

Author Contributions

W.H. and D.B. contributed to the conception and design of the research; W.H., J.K., J.B., M.D. and R.F. performed the experiments, analyzed data and generated figures; W.H, J.K., S.L. and D.B. interpreted the results of the experiments; W.H. drafted the manuscript; W.H., D.B., J.K., S.L., M.D., M.J. E.A. edited and revised the manuscript.

References

1. Jo, J., Shreif, Z., and Periwal, V. (2012) Quantitative dynamics of adipose cells. *Adipocyte*. **1**, 80–88
2. Carmean, C. M., Cohen, R. N., and Brady, M. J. (2014) Systemic regulation of adipose metabolism. *Biochim. Biophys. Acta*. **1842**, 424–430
3. Varela, L., and Horvath, T. L. (2012) Leptin and insulin pathways in POMC and AgRP neurons that modulate energy balance and glucose homeostasis. *EMBO Rep*. **13**, 1079–1086
4. Byerly, M. S., Swanson, R., Wei, Z., Seldin, M. M., McCulloh, P. S., and Wong, G. W. (2013) A central role for C1q/TNF-related protein 13 (CTRP13) in modulating food intake and body weight. *PLoS ONE*. **8**, e62862
5. Galic, S., Oakhill, J. S., and Steinberg, G. R. (2010) Adipose tissue as an endocrine organ. *Mol. Cell. Endocrinol*. **316**, 129–139
6. Fernández-Sánchez, A., Madrigal-Santillán, E., Bautista, M., Esquivel-Soto, J., Morales-González, A., Esquivel-Chirino, C., Durante-Montiel, I., Sánchez-Rivera, G., Valadez-Vega, C., and Morales-González, J. A. (2011) Inflammation, oxidative stress, and obesity. *Int J Mol Sci*. **12**, 3117–3132
7. van den Borst, B., Schols, A. M. W. J., de Theije, C., Boots, A. W., Köhler, S. E., Goossens, G. H., and Gosker, H. R. (2013) Characterization of the inflammatory and metabolic profile of adipose tissue in a mouse model of chronic hypoxia. *J. Appl. Physiol*. **114**, 1619–1628
8. Cildir, G., Akıncılar, S. C., and Tergaonkar, V. (2013) Chronic adipose tissue inflammation: all immune cells on the stage. *Trends in Molecular Medicine*. **19**, 487–500
9. Gregor, M. F., and Hotamisligil, G. S. (2011) Inflammatory mechanisms in obesity. *Annu. Rev. Immunol*. **29**, 415–445
10. Langin, D., Dicker, A., Tavernier, G., Hoffstedt, J., Mairal, A., Rydén, M., Arner, E., Sicard, A., Jenkins, C. M., Viguier, N., van Harmelen, V., Gross, R. W., Holm, C., and Arner, P. (2005) Adipocyte lipases and defect of lipolysis in human obesity. *Diabetes*. **54**, 3190–3197
11. Gaidhu, M. P., Anthony, N. M., Patel, P., Hawke, T. J., and Ceddia, R. B. (2010) Dysregulation of lipolysis and lipid metabolism in visceral and subcutaneous adipocytes by high-fat diet: role of ATGL, HSL, and AMPK. *Am. J. Physiol., Cell Physiol*. **298**, C961–71
12. Bremer, A. A., and Jialal, I. (2013) Adipose tissue dysfunction in nascent metabolic syndrome. *J. Obes*. **2013**, 393192–8
13. Deng, Y., and Scherer, P. E. (2010) Adipokines as novel biomarkers and regulators of the metabolic syndrome. *Ann. N. Y. Acad. Sci*. **1212**, E1–E19
14. Weisberg, S. P., McCann, D., Desai, M., Rosenbaum, M., Leibel, R. L., and Ferrante, A. W. (2003) Obesity is associated with macrophage accumulation in adipose tissue. *J. Clin. Invest*. **112**, 1796–1808

15. Kotsias, F., Hoffmann, E., Amigorena, S., and Savina, A. (2013) Reactive oxygen species production in the phagosome: impact on antigen presentation in dendritic cells. *Antioxid. Redox Signal.* **18**, 714–729
16. Lee, B.-C., and Lee, J. (2014) Cellular and molecular players in adipose tissue inflammation in the development of obesity-induced insulin resistance. *Biochim. Biophys. Acta.* **1842**, 446–462
17. Cabal-Hierro, L., and Lazo, P. S. (2012) Signal transduction by tumor necrosis factor receptors. *Cell. Signal.* **24**, 1297–1305
18. Tretter, L., and Adam-Vizi, V. (2005) Alpha-ketoglutarate dehydrogenase: a target and generator of oxidative stress. *Philos. Trans. R. Soc. Lond., B, Biol. Sci.* **360**, 2335–2345
19. Adam-Vizi, V. (2005) Production of reactive oxygen species in brain mitochondria: contribution by electron transport chain and non-electron transport chain sources. *Antioxid. Redox Signal.* **7**, 1140–1149
20. Miller, A.-F. (2012) Superoxide dismutases: ancient enzymes and new insights. *FEBS Letters.* **586**, 585–595
21. Kuzmicic, J., Del Campo, A., López-Crisosto, C., Morales, P. E., Pennanen, C., Bravo-Sagua, R., Hechenleitner, J., Zepeda, R., Castro, P. F., Verdejo, H. E., Parra, V., Chiong, M., and Lavandero, S. (2011) [Mitochondrial dynamics: a potential new therapeutic target for heart failure]. *Rev Esp Cardiol.* **64**, 916–923
22. Youle, R. J., and van der Blik, A. M. (2012) Mitochondrial fission, fusion, and stress. *Science.* **337**, 1062–1065
23. van der Blik, A. M., Shen, Q., and Kawajiri, S. (2013) Mechanisms of mitochondrial fission and fusion. *Cold Spring Harb Perspect Biol.* **5**, a011072–a011072
24. Brand, M. D., and Nicholls, D. G. (2011) Assessing mitochondrial dysfunction in cells. *Biochem. J.* **435**, 297–312
25. Xu, X., and Arriaga, E. A. (2010) Chemical cytometry quantitates superoxide levels in the mitochondrial matrix of single myoblasts. *Anal. Chem.* **82**, 6745–6750
26. Curtis, J. M., Grimsrud, P. A., Wright, W. S., Xu, X., Foncea, R. E., Graham, D. W., Brestoff, J. R., Wiczer, B. M., Ilkayeva, O., Cianflone, K., Muoio, D. E., Arriaga, E. A., and Bernlohr, D. A. (2010) Downregulation of adipose glutathione S-transferase A4 leads to increased protein carbonylation, oxidative stress, and mitochondrial dysfunction. **59**, 1132–1142
27. Frohnert, B. I., Sinaiko, A. R., Serrot, F. J., Foncea, R. E., Moran, A., Ikramuddin, S., Choudry, U., and Bernlohr, D. A. (2011) Increased adipose protein carbonylation in human obesity. *Obesity.* **19**, 1735–1741
28. Blachnio-Zabielska, A. U., Persson, X.-M. T., Koutsari, C., Zabielski, P., and Jensen, M. D. (2012) A liquid chromatography/tandem mass spectrometry method for measuring the in vivo incorporation of plasma free fatty acids into intramyocellular ceramides in humans. *Rapid Commun.*

- Mass Spectrom.* **26**, 1134–1140
29. Blachnio-Zabielska, A. U., Koutsari, C., Tchkonja, T., and Jensen, M. D. (2012) Sphingolipid content of human adipose tissue: relationship to adiponectin and insulin resistance. *Obesity (Silver Spring)*. **20**, 2341–2347
 30. Parra, V., Eisner, V., Chiong, M., Criollo, A., Moraga, F., Garcia, A., Härtel, S., Jaimovich, E., Zorzano, A., Hidalgo, C., and Lavandro, S. (2008) Changes in mitochondrial dynamics during ceramide-induced cardiomyocyte early apoptosis. *Cardiovasc. Res.* **77**, 387–397
 31. Grimsrud, P. A., Picklo, M. J., Griffin, T. J., and Bernlohr, D. A. (2007) Carbonylation of adipose proteins in obesity and insulin resistance: identification of adipocyte fatty acid-binding protein as a cellular target of 4-hydroxynonenal. *Molecular & Cellular Proteomics*. **6**, 624–637
 32. Holland, W. L., Brozinick, J. T., Wang, L.-P., Hawkins, E. D., Sargent, K. M., Liu, Y., Narra, K., Hoehn, K. L., Knotts, T. A., Siesky, A., Nelson, D. H., Karathanasis, S. K., Fontenot, G. K., Birnbaum, M. J., and Summers, S. A. (2007) Inhibition of ceramide synthesis ameliorates glucocorticoid-, saturated-fat-, and obesity-induced insulin resistance. *Cell Metab.* **5**, 167–179
 33. Yang, G., Badeanlou, L., Bielawski, J., Roberts, A. J., Hannun, Y. A., and Samad, F. (2009) Central role of ceramide biosynthesis in body weight regulation, energy metabolism, and the metabolic syndrome. *Am. J. Physiol. Endocrinol. Metab.* **297**, E211–24
 34. Chi, H., and Flavell, R. A. (2005) Cutting edge: regulation of T cell trafficking and primary immune responses by sphingosine 1-phosphate receptor 1. *J. Immunol.* **174**, 2485–2488
 35. Alkhouri, N., Gornicka, A., Berk, M. P., Thapaliya, S., Dixon, L. J., Kashyap, S., Schauer, P. R., and Feldstein, A. E. (2010) Adipocyte apoptosis, a link between obesity, insulin resistance, and hepatic steatosis. *J. Biol. Chem.* **285**, 3428–3438
 36. Parra, V., Verdejo, H., Del Campo, A., Pennanen, C., Kuzmicic, J., Iglewski, M., Hill, J. A., Rothermel, B. A., and Lavandro, S. (2011) The complex interplay between mitochondrial dynamics and cardiac metabolism. *J. Bioenerg. Biomembr.* **43**, 47–51
 37. Roth Flach, R. J., Matevossian, A., Akie, T. E., Negrin, K. A., Paul, M. T., and Czech, M. P. (2013) β 3-Adrenergic receptor stimulation induces E-selectin-mediated adipose tissue inflammation. *J. Biol. Chem.* **288**, 2882–2892
 38. Long, E. K., Olson, D. M., and Bernlohr, D. A. (2013) High-fat diet induces changes in adipose tissue trans-4-oxo-2-nonenal and trans-4-hydroxy-2-nonenal levels in a depot-specific manner. *Free Radical Biology and Medicine*. **63**, 390–398
 39. Frohnert, B. I., Long, E. K., Hahn, W. S., and Bernlohr, D. A. (2013) Glutathionylated Lipid Aldehydes are Products of Adipocyte Oxidative Stress and Activators of Macrophage Inflammation. 10.2337/db13-0777

40. Ganesan, V., Perera, M. N., Colombini, D., Datskovskiy, D., Chadha, K., and Colombini, M. (2010) Ceramide and activated Bax act synergistically to permeabilize the mitochondrial outer membrane. *Apoptosis*. **15**, 553–562
41. Herold, C., Rennekampff, H. O., and Engeli, S. (2013) Apoptotic pathways in adipose tissue. *Apoptosis*. **18**, 911–916
42. Hofmann, C., Lorenz, K., Braithwaite, S. S., Colca, J. R., Palazuk, B. J., Hotamisligil, G. S., and Spiegelman, B. M. (1994) Altered gene expression for tumor necrosis factor-alpha and its receptors during drug and dietary modulation of insulin resistance. *Endocrinology*. **134**, 264–270
43. Keller, M. P., Choi, Y., Wang, P., Davis, D. B., Rabaglia, M. E., Oler, A. T., Stapleton, D. S., Argmann, C., Schueler, K. L., Edwards, S., Steinberg, H. A., Chaibub Neto, E., Kleinhanz, R., Turner, S., Hellerstein, M. K., Schadt, E. E., Yandell, B. S., Kendziorski, C., and Attie, A. D. (2008) A gene expression network model of type 2 diabetes links cell cycle regulation in islets with diabetes susceptibility. *Genome Res*. **18**, 706–716
44. Parra, V., Moraga, F., Kuzmicic, J., López-Crisosto, C., Troncoso, R., Torrealba, N., Criollo, A., Díaz-Elizondo, J., Rothermel, B. A., Quest, A. F. G., and Lavandero, S. (2013) Calcium and mitochondrial metabolism in ceramide-induced cardiomyocyte death. *Biochim. Biophys. Acta*. **1832**, 1334–1344
45. Upadhyay, M., Samal, J., Kandpal, M., Singh, O. V., and Vivekanandan, P. (2013) The Warburg effect: insights from the past decade. *Pharmacol. Ther.* **137**, 318–330
46. WARBURG, O. (1956) On the origin of cancer cells. *Science*. **123**, 309–314
47. Chen, X.-H., Zhao, Y.-P., Xue, M., Ji, C.-B., Gao, C.-L., Zhu, J.-G., Qin, D.-N., Kou, C.-Z., Qin, X.-H., Tong, M.-L., and Guo, X.-R. (2010) TNF-alpha induces mitochondrial dysfunction in 3T3-L1 adipocytes. *Mol. Cell. Endocrinol.* **328**, 63–69
48. O'Neill, L. A. J. (2008) The interleukin-1 receptor/Toll-like receptor superfamily: 10 years of progress. *Immunol. Rev.* **226**, 10–18
49. Mizuhara, H., O'Neill, E., Seki, N., Ogawa, T., Kusunoki, C., Otsuka, K., Satoh, S., Niwa, M., Senoh, H., and Fujiwara, H. (1994) T cell activation-associated hepatic injury: mediation by tumor necrosis factors and protection by interleukin 6. *J. Exp. Med.* **179**, 1529–1537
50. Brandt, C., Jakobsen, A. H., Adser, H., Olesen, J., Iversen, N., Kristensen, J. M., Hojman, P., Wojtaszewski, J. F. P., Hidalgo, J., and Pilegaard, H. (2012) IL-6 regulates exercise and training-induced adaptations in subcutaneous adipose tissue in mice. *Acta Physiol (Oxf)*. **205**, 224–235
51. Wolsk, E., Mygind, H., Grøndahl, T. S., Pedersen, B. K., and van Hall, G. (2010) IL-6 selectively stimulates fat metabolism in human skeletal muscle. *Am. J. Physiol. Endocrinol. Metab.* **299**, E832–40
52. Murphy, M. P. (2009) How mitochondria produce reactive oxygen species. *Biochem. J.* **417**, 1–13

53. Yang, B., and Rizzo, V. (2007) TNF-alpha potentiates protein-tyrosine nitration through activation of NADPH oxidase and eNOS localized in membrane rafts and caveolae of bovine aortic endothelial cells. *Am. J. Physiol. Heart Circ. Physiol.* **292**, H954–62
54. Houstis, N., Rosen, E. D., and Lander, E. S. (2006) Reactive oxygen species have a causal role in multiple forms of insulin resistance. *Nature.* **440**, 944–948
55. Valerio, A., Cardile, A., Cozzi, V., Bracale, R., Tedesco, L., Pisconti, A., Palomba, L., Cantoni, O., Clementi, E., Moncada, S., Carruba, M. O., and Nisoli, E. (2006) TNF-alpha downregulates eNOS expression and mitochondrial biogenesis in fat and muscle of obese rodents. *J. Clin. Invest.* **116**, 2791–2798
56. Pidoux, G., Witczak, O., Jarnæss, E., Myrvold, L., Urlaub, H., Stokka, A. J., Küntziger, T., and Taskén, K. (2011) Optic atrophy 1 is an A-kinase anchoring protein on lipid droplets that mediates adrenergic control of lipolysis. *EMBO J.* **30**, 4371–4386
57. Baricault, L., Ségui, B., Guégand, L., Olichon, A., Valette, A., Larminat, F., and Lenaers, G. (2007) OPA1 cleavage depends on decreased mitochondrial ATP level and bivalent metals. *Exp. Cell Res.* **313**, 3800–3808
58. Griparic, L., Kanazawa, T., and van der Bliek, A. M. (2007) Regulation of the mitochondrial dynamin-like protein Opa1 by proteolytic cleavage. *J. Cell Biol.* **178**, 757–764
59. Steinberg, G. R., Michell, B. J., van Denderen, B. J. W., Watt, M. J., Carey, A. L., Fam, B. C., Andrikopoulos, S., Proietto, J., Gorgun, C. Z., Carling, D., Hotamisligil, G. S., Febbraio, M. A., Kay, T. W., and Kemp, B. E. (2006) Tumor necrosis factor alpha-induced skeletal muscle insulin resistance involves suppression of AMP-kinase signaling. *Cell Metab.* **4**, 465–474

CHAPTER THREE

Inflammation and ER Stress Regulate Branched-Chain Amino Acid Uptake and Metabolism in Adipocytes

Burrill, J.S., Long, E.K., Reilly, B., Deng, Y., Armitage, I.M., Scherer, P.E.,
Bernlohr, D.A. (2015) *Molecular Endocrinology* 29(3):411-420.

This chapter contains an original research article previously published.
Reproduced with permission from *Molecular Endocrinology*, Copyright 2015.

Joel Burrill performed experiments in their entirety from figures 1 - 4 and 6A,
prepared samples for experimental collaborations in figure 5, and performed
experiments on samples prepared by collaborators in figures 6B-D.

Summary

Inflammation plays a critical role in the pathology of obesity-linked insulin resistance and is mechanistically linked to the effects of macrophage-derived cytokines on adipocyte energy metabolism, particularly that of the mitochondrial branched chain amino acid (BCAA) and tricarboxylic acid (TCA) pathways. To address the role of inflammation on energy metabolism in adipocytes we utilized high fat fed C57Bl/6J mice and lean controls and measured down regulation of genes linked to BCAA and TCA cycle metabolism selectively in visceral but not in subcutaneous adipose tissue, brown fat, liver or muscle. Using 3T3-L1 cells, TNF α and other pro-inflammatory cytokine treatments reduced the expression of genes linked to BCAA transport and oxidation. Consistent with this, [14 C]-leucine uptake and conversion to triglycerides was markedly attenuated in TNF α -treated adipocytes whereas conversion to protein was relatively unaffected. Since inflammatory cytokines lead to induction of ER stress, we evaluated the effects of tunicamycin or thapsigargin treatment of 3T3-L1 cells and measured a similar down regulation in the BCAA/TCA cycle pathway. Moreover, transgenic mice overexpressing XBP1s in adipocytes similarly down regulated genes of BCAA and TCA metabolism in vivo. These results indicate that inflammation and ER stress attenuate lipogenesis in visceral adipose depots by down regulating the BCAA/TCA metabolism pathway and are consistent with a model whereby the accumulation of serum BCAA in the obese insulin-resistant state is linked to adipose inflammation.

Introduction

Obesity-linked type 2 diabetes (T2D) and its associated health complications are major health care concerns worldwide and at the molecular level are linked to increased abundance and activity of classically activated macrophages and other immune cells in adipose tissue (1-3). Increased immune cells produce a chronic low-grade inflammatory state exemplified by elevated adipose $\text{TNF}\alpha$, IL-6, IL-1 β and IFN γ primarily in visceral, and to a lesser extent, subcutaneous depots (4).

The positive inflammatory poise of adipose tissue leads to the down regulation of adipocyte genes linked to the anti-inflammatory response system and an increase in mitochondrial reactive oxygen species (ROS), increased ER stress and loss of electron transport activity (3, 5). Although the exact molecular mechanisms that tie ROS to insulin resistance are complex, the ROS-dependent activation of the unfolded protein response and the NF- κ B / JNK signaling pathways have been implicated by a variety of *in situ* and *in vivo* models (6-8).

Recent work has identified adipose tissue and adipocytes as a major contributor to whole body branched chain amino acid catabolism (9). The branched chain amino acids leucine, isoleucine and valine are transported into adipocytes and metabolized in the mitochondria to form the anapleurotic intermediates acetyl-CoA and succinyl-CoA thereby enabling maximal pyruvate metabolism to citrate and subsequent lipogenesis (10). Work by Herman et al (9) have shown that adipocytes readily metabolize BCAA to lipogenic precursors and that maximal

lipogenic rate requires replenishment of the BCAA pathway. Recently, metabolomics studies of human obesity and metabolic dysfunction have revealed a connection between circulating BCAAs and insulin resistance and a variety of analyses have demonstrated that the accumulation of serum BCAA is a molecular biomarker of the insulin resistant state (11-17). Moreover, Bcat2 knockout mice that are insulin resistant have elevated circulating BCAAs (18). In addition, elevated serum BCAA in the setting of a high fat diet may activate the mTOR-dependent serine phosphorylation of IRS-1 (19, 20). While a variety of rodent and human studies have shown the branched chain keto-acid dehydrogenase (BCKD) complex plays a pivotal role in BCAA metabolism, there is much still unknown about adipose tissue regulation of the BCAA pathway and the role of depot-specific functions (17). Herein we report a role of inflammation in controlling the BCAA/TCA metabolism pathway suggesting that accumulation of leucine, isoleucine and valine in the serum is at least in part, a result of decreased BCAA and TCA cycle metabolism selectively in inflamed visceral adipose tissue.

Research Design and Methods

Animals: Male C57Bl/6J mice were placed on a normal chow (~4% fat by weight) or a high-fat (~35% fat by weight, Bio-Serv F3282, Frenchtown NJ) diet at weaning (21). At 12-15 weeks of age, mice were killed by cervical dislocation, and tissues were harvested, frozen in liquid nitrogen and stored at -80° C until further processing. The University of Minnesota Institutional Animal Care and Use Committee approved all experiments. The male TRE-Xbp1s and adipocyte-specific adiponectinP-rtTA transgenic mice (referred to as FIXs mice) were generated by the transgenic core facility at UTSW and described in (22, 23). Mice were maintained on a 12-hour dark/12-hour light cycle from 6 a.m. to 6 p.m. and housed in groups of no more than 5 with unlimited access to water and chow (2916, Teklad, Indianapolis IN) or Dox-containing (600mg/kg) chow diets (Bio-Serv, Frenchtown NJ) and induced with Dox for 48h.

Chemical reagents: Recombinant mouse TNF α , IL-6, IL-1 β and IFN γ were purchased from R&D Systems (Minneapolis, MN). Antibodies were obtained from commercial sources: β -actin (Sigma, St. Louis MO); Bcat2, Sdha, Bckdha, Atp5a (Abcam, Cambridge MA). Isotopes of leucine were purchased from Perkin-Elmer (Waltham, MA). Bay11-7085 was purchased from Cayman Chemical (Ann Arbor, MI).

Quantitative RT-PCR: Expression of mRNA was measured by quantitative RT-PCR. Briefly, total RNA was isolated from tissue or 3T3-L1 adipocytes using Trizol reagent (Invitrogen Corp., Grand Island NY) according to manufacturer's protocol. RNA was treated with DNase I and cDNA was synthesized using iScript cDNA synthesis kit (BioRad, Hercules CA). Amplification was monitored with iQ SYBR Green Supermix and the MyiQ detection system (BioRad, Hercules CA). Data was analyzed using the $-\Delta\Delta CT$ method and normalized to TFIIE expression. Supplemental table 1 contains the gene names, symbols, accession numbers and primer sequences used to amplify and detect target transcripts.

Cell culture: 3T3-L1 fibroblasts were maintained and differentiated into adipocytes as described previously (24). Differentiation was induced by addition of DMEM containing 10% fetal bovine serum (FBS), 0.5 mM methylisobutylxanthine, 0.25 μ M dexamethasone and 170 μ M insulin. The methylisobutylxanthine and dexamethasone were removed after two days and the insulin was removed after four days. Differentiated 3T3-L1 cells were maintained in DMEM with 10% FBS and used in experiments six to twelve days after induction.

mRNA	Accession Number	Forward (F) and Reverse (R) primers
TFIIE	NM_026584	F: CAAGGCTTTAGGGGACCAGATAC R: CATCCATTGACTCCACAGTGACAC
SLC1A5	NM_009201	F: GGTGGTCTTCGCTATCGTCTTTG R: GCAGGACGACAGAATGATTTG
BCAT2	NM_001243053	F: TTCCCAGAGACTCAAGAGAAGTGC R: GGAGATAGAGAAGAAGCCAAGGTTTC
BCKDHA	NM_007533	F: AAGCCTCCTCTTCTCCGATGTG R: GCAAAAGTCACCTGGAATGC
BCKDHB	NM_199195	F: GTGCCCTGGATAACTCATTAGCC R: CAAACTGGATTTCCGCAATAGC
DBT	NM_010022	F: GGAAAAGCAGACAGGAGCCATAC R: TCTCATCACAATCCCGAAGTGG
DLD	NM_007861	F: AAGTCTTACCAGGCGTTCAGC R: GGCAGATTTGATGGCAGCAAC
IVD	NM_019826	F: CATCAGTGGTGGATTCATCGGAG R: CAAATCTGTCTTGGCATAACAGAC
MCCC1	NM_023644	F: GGAGATGAACACCAGGCTACAAGTG R: AGAGAGATGAACCAACGGTCCAG
MCCC2	NM_030026	F: CGGCACACATCCAGAGAAAAC R: CCTTTGACGGTGGCATCGTTAG
ECHS1	NM_053119	F: CCAAGCACTGGAGACCTTTGAG R: CACCAAGAGCATAACCATTGACAG
HADH	NM_178878	F: GAAAAACCTAAGGCTGGAGATGAG R: TGGTGGTGGCATTGGCTATG
HIBCH	NM_146108	F: GGACATCAAAGCACTCTCAGAAGC R: CTCCACCCACATCAGGAAATAGTC
ACAT1	NM_144784	F: TGGTGGGGTAAAACCTGAAGACC R: ATGGGAGTAATCTCACTGGCAAAC
PCCA	NM_144844	F: GCCAAGAGAGCAAAGTCAACAC R: GAAAACTAAAGCCATCCCTGGTC
PCCB	NM_025835	F: TGGAGTCATCCCGCAGATTTTC R: CACAGAGCATCAACATCATTGTCG
MUT	NM_008650	F: CCGTTCTCATTTCCTTTGGG R: GTCCTCTGGGTTTTGCCTTTC
SLC3A2	NM_001161413	F: TGAGTCCAGCATCTTTCACATCC R: AGTTGAGCACCCACAGGTAACG
SLC7A5	NM_011404	F: CTACTTCTTTGGTGTCTGGTGGAA R: GAGGTACCACCTGCATCAACTTC
PCx	NM_001162946	F: TGGTGGCCTGTACCAAAGG R: CGTCGGAGTTGCCAGACTTC
CS	NM_026444	F: GGACAATTTTCCAACCAATCTGC R: TCGGTTCAATCCCTCTGCATA
ACO2	NM_080633	F: GCAAGGACATAAACCCAGGAAGTG R: TGACATCCACAGCATCAGC
IDH2	NM_173011	F: AAAACATCCCCCGCCTTGTC R: AAGCCCGAAATGGACTCGTC
OGDH	NM_001252282	F: ACAGTAGGAGGTTCTATGG R: CAGGGGTCTCAAACCTCTG
SDHA	NM_023281	F: GGAACACTCCAAAACAGACC R: AAACCCTGCCTCAGAAAAGG
SDHB	NM_023374	F: CAGACAAGACTGGAGATAAACCC R: GAAGAGGGTAGATTTTGGAGAC
SDHD	NM_025848	F: AGGGGGATGAAGGATAAG R: ATGGTGGTCAAAGGCAAC
FH1	NM_010209	F: GTTAGGAGGTGAACCTGGC R: AGTAAGAGGGACAGCATCC
FATP1	NM_011977	F: CGCTTTCTGCGTATCGTCTGCAAG R: AAGATGCACGGGATCGTGTCT
LPL	NM_008509	F: AGGGCTCTGCCTGAGTTGTA R: AGAAATTTGGAAGCCTGGT
CD36	NM_007643	F: TGGAGCTGTTATTGGTGCAG R: TGGGTTTTGCACATCAAAGA
BCAT1	NM_07532	F: CAACTATGGAGAATGGTCTAAGCT R: TGTCCAGTCGCTCTTCTCTTC
PREF1	NM_010052	F: GACCCACCCTGTGACCCC R: CAGGCAGCTCGTGACCCC

Supplemental Table 1 – Primers used for quantitative PCR to measure gene expression.

Leucine uptake and fractionation: Briefly, day 8 differentiated adipocytes were treated with 1nM TNF α for 24h, serum starved for 2 hours in DMEM and radioactive leucine added for 5-180 minutes. Total cellular uptake was measured using [^3H (3,4)]-leucine while incorporation into lipid and protein pools were measured using [^{14}C (U)]-leucine. Fractionation of incorporated ^{14}C -leucine was accomplished using a hexane:isopropanol:water (3:2:1) extraction where lipids partitioned into the organic phase while radioactive protein was collected into the precipitate.

Metabolite extraction and analysis: Polar metabolites were extracted from cells or mouse serum using a chloroform:methanol extraction procedure. Serum was added to a 1.5 mL centrifuge tube containing 500 μL chloroform, 250 μL methanol, and 150 μL 0.9% sodium chloride. The mixture was vortexed and centrifuged at 13000g for 10 minutes. The upper aqueous/methanol layer was removed to a new tube and the chloroform layer was washed with 1:1 0.9% sodium chloride:methanol. 3 mL of methanol was added to the aqueous phase to facilitate drying under nitrogen. The dried samples were stored at -80°C until NMR analysis. Immediately prior to NMR analysis, the dried powder/film was resuspended in 100 μL 100 mM sodium phosphate in D_2O , pH 7.4 containing 20 μM trimethylsilyl propionic-2,2,3,3- d_4 acid as calibration standard.

NMR metabolite analysis: NMR experiments were performed at 25°C on a Bruker Avance III 700 MHz spectrometer with a 1.7mm CryoProbe. One-dimensional

noesy spectra were acquired with 128 transients using 65,536 data points under fully relaxed conditions. Assignments were made using Chenomx 7.5 (Edmonton, Canada). Spectra were exponentially line broadened by 1Hz, Fourier transformed, phase and baseline corrected. Spectra were calibrated to an internal 20 μ M Trimethylsilyl-tetradeuterosodium propionate (TSP) standard to establish metabolite concentrations and as a chemical shift reference. Metabolite assignments were made according to the chemical shifts and pattern of coupling constants using the Chenomx compound library (Chenomx, Edmonton, Canada).

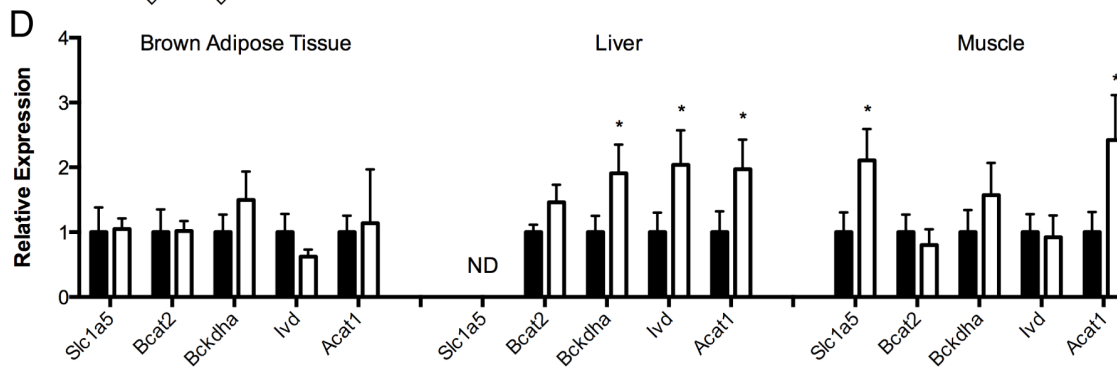
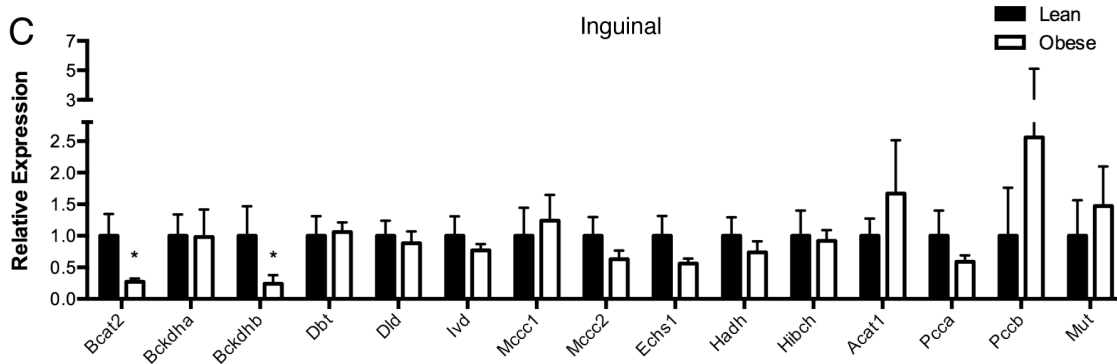
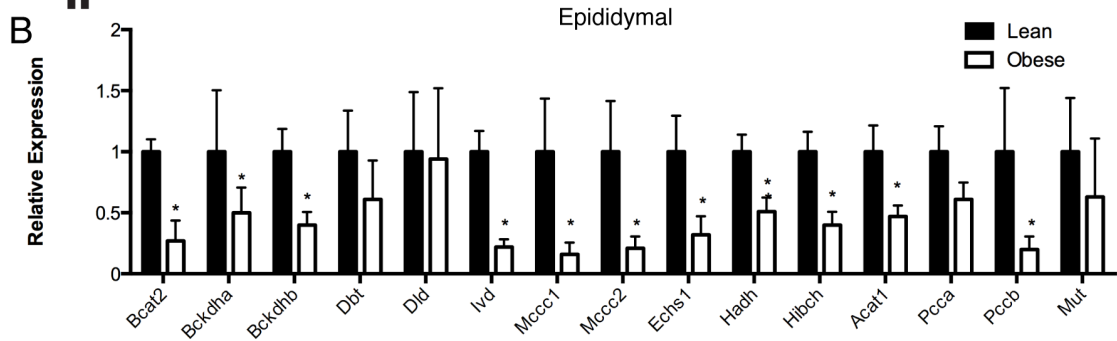
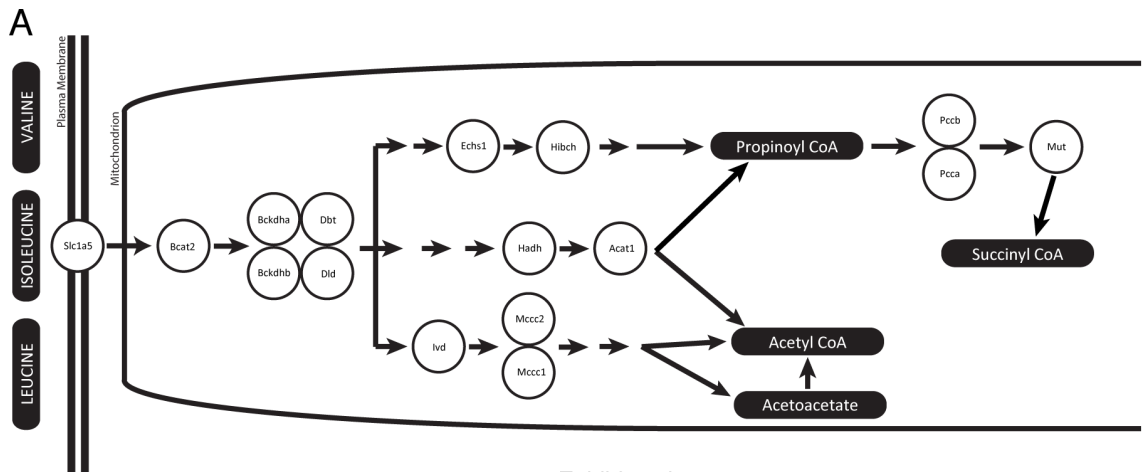
Immunoblot analysis: 3T3-L1 adipocytes treated with and without TNF α were homogenized using a glass-teflon homogenizer in homogenization buffer (20 mM Tris-HCl, 220 mM Mannitol, 70 mM Sucrose, 1 mM EDTA, 0.1 mM EGTA pH 7.4) supplemented with protease inhibitors (Calbiochem, Darmstadt Germany). For Bcat2 analysis, homogenates were centrifuged at 700g to remove nuclei, unbroken cells and the lipid cake and mitochondria recovered by further centrifugation at 12,000g. Equal amounts of protein were separated by SDS-PAGE, transferred to PVDF immobilon-FL (Millipore, Billerica MA) membranes and blocked in Odyssey® Blocking Buffer (LI-COR Biosciences, Lincoln NE). Membranes were incubated with infrared-conjugated secondary antibodies and visualized using Odyssey® Infrared Imager (LI-COR Biosciences, Lincoln NE).

Statistical analysis: All values are expressed as mean \pm SEM. Statistical significance was determined using the two-tailed Student *t* test assuming unequal variances, or where appropriate, a two-way ANOVA with Bonferroni post hoc analysis. *P* values < 0.05 are considered significant (*) with an increased significance of *p* value < 0.01 indicated (**).

Results

Obesity and inflammation down-regulate expression of genes linked to BCAA metabolism selectively in adipose tissue and cultured adipocytes. Our laboratory has recently demonstrated that macrophage-derived inflammatory factors down regulate the expression of genes linked to antioxidant biology in adipocytes and lead to mitochondrial dysfunction (25). Moreover, in mouse models, oxidative stress is strongly biased towards the visceral relative to the subcutaneous depot where inflammation is the greatest, antioxidant genes are down regulated, reactive aldehydes accumulate and protein carbonylation is increased (26). During the course of our studies we also evaluated the expression of genes linked to BCAA metabolism in adipose tissue of high fat fed C57Bl/6J mice and compared it to lean littermates. Figure 1A shows schematic representation of the proteins involved in BCAA uptake and mitochondrial metabolism. Figures 1B and 1C show that relative to lean controls the mRNA level of essentially every BCAA metabolism pathway protein was down regulated in epididymal adipose tissue of high fat fed mice but not in subcutaneous fat. To assess if down-regulation of BCAA pathway gene expression was adipose specific, a panel of enzymes was profiled in brown fat, muscle and liver and expression was found to not be affected and in the case of liver, was increased (Figure 1D). These results demonstrate pathway specific down regulation of the BCAA metabolism enzymes in visceral adipose tissue.

Figure 1 – Obesity down regulates the expression of genes of BCAA metabolism. A) Schematic diagram of cellular BCAA metabolism, B) Expression of BCAA metabolism genes in epididymal or C) inguinal white adipose tissue in C57Bl/6J mice maintained on a low fat (filled bars) or high fat (open bars) diet. D) Expression of BCAA metabolism genes in brown adipose tissue, liver and gastrocnemius skeletal muscle tissue. Error bars represent standard error of the mean and * representing $p < 0.05$ and n equals 6-12 per group.

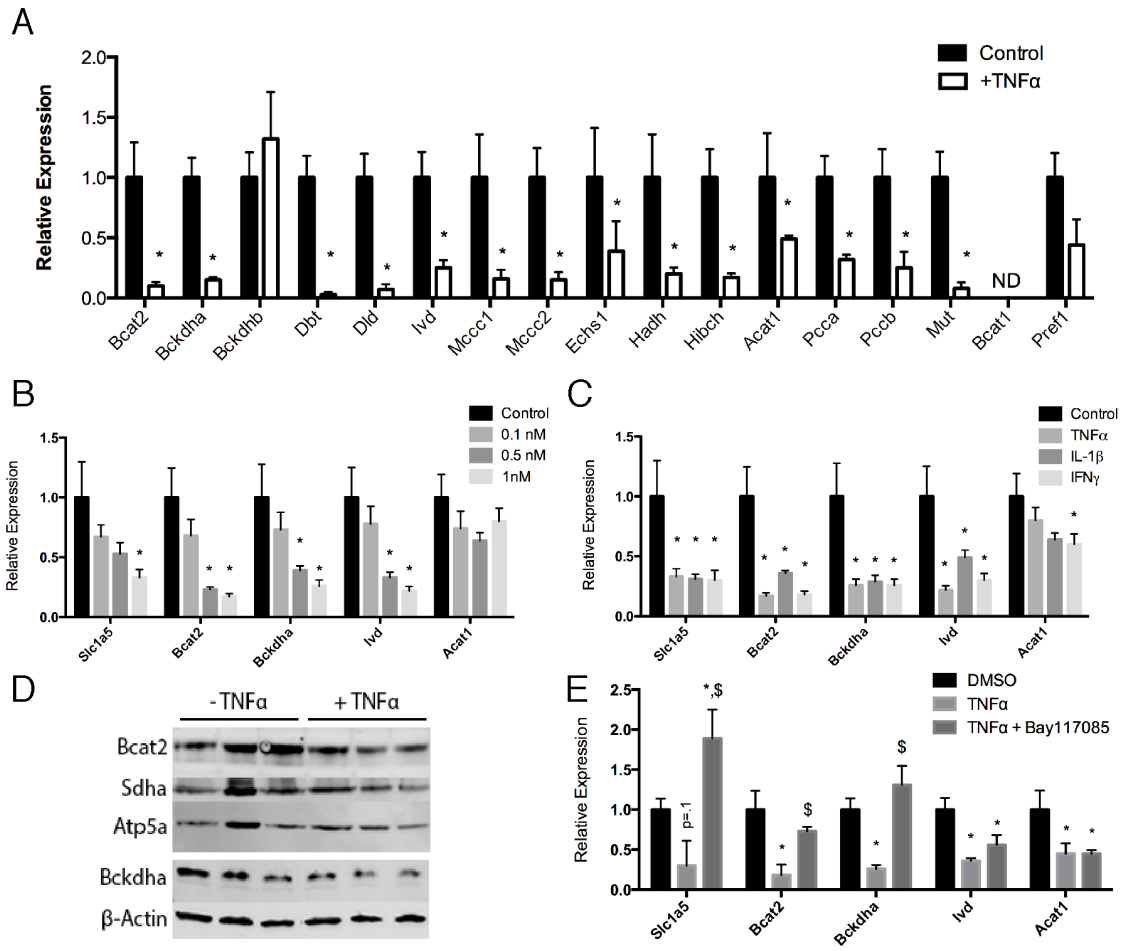


Immune cell-derived inflammatory factors have been shown to down regulate many metabolic genes and in order to determine the cytokines on BCAA metabolism we treated 3T3-L1 adipocytes with TNF α and measured the mRNA levels of genes linked to BCAA metabolism. Figure 2A shows that essentially the entire BCAA pathway is coordinately down regulation in response to TNF α . In addition, markers of pre-adipocytes, branched chain amino-acid transaminase 1 (Bcat1) and preadipocyte factor 1 (Pref1), were not increased by TNF α treatment indicating de-differentiation is not occurring (Figure 2A). We also observed a dose-dependent down regulation with varying concentrations of TNF α (Figure 2B) and that other inflammatory factors (interleukin-6 (IL-6), interleukin 1 β (IL-1 β) and interferon γ (IFN γ) similarly down regulated BCAA gene expression (Figure 2C). Furthermore, the expression of branched chain amino-acid transaminase 2 (Bcat2), the enzyme responsible for the conversion of the BCAAs to their respective α -ketoacids, and the branched chain keto-acid dehydrogenase α subunit, were also reduced similarly at the protein level in response to TNF α (Figure 2D). It is important to note that TNF α did not lead to de-differentiation of 3T3-L1 adipocytes, cytokine addition did not increase the expression of Pref1 or Bcat1 (results not shown). Since TNF α activates the canonical NF- κ B pathway we evaluated if pharmacologic inhibition of the NF- κ B pathway, by inhibiting I κ B α phosphorylation with Bay11-7085, would affect expression of BCAA genes in response to TNF α . Figure 2E shows that for Slc1a5, Bcat2 and Bckdha, treatment of day 8 3T3-L1 adipocytes with Bay11-7085 attenuated the TNF α -

driven down regulation suggesting that NF- κ B plays a role in the decreased expression of BCAA genes.

Since BCAA metabolism serves as a source of anaplerotic replenishment for the TCA cycle, as leucine is metabolized to acetyl-CoA, isoleucine to acetyl-CoA and succinyl-CoA and valine to succinyl-CoA, we characterized the mRNA expression of enzymes linked to the TCA cycle enzymes in TNF α treated 3T3-L1 adipocytes and similarly found nearly the entire pathway down-regulated in response to cytokine treatment (Figure 3A). Importantly, pyruvate carboxylase (Pcx), the primary source of anaplerotic oxaloacetate, was similarly down-regulated. Similarly, succinate dehydrogenase α -subunit (Sdha) protein levels were also decreased after TNF α treatment (Figure 2D). Furthermore, we investigated the expression of the same panel of TCA enzymes in inguinal (Figure 3B) and epididymal (Figure 3C) white adipose tissue from chow and high fat fed mice and again found epididymal fat to have reduced levels of expression while subcutaneous fat remained largely unaffected, if not increased. These results support the general consideration that inflammation drives the expansion of the subcutaneous depot while limiting the visceral depot through targeted regulation of the BCAA and TCA cycle pathways.

Figure 2 – Inflammatory factors down regulate the expression of genes of BCAA metabolism. A) Expression of BCAA metabolism genes in 3T3-L1 adipocytes treated on day 8 post differentiation for 24 h with 1nM TNF α . B) Expression of BCAA metabolism genes in 3T3-L1 adipocytes treated on day 8 post differentiation for 24 h with varying concentrations of TNF α . C) Expression of BCAA metabolism genes in 3T3-L1 adipocytes treated on day 8 post differentiation for 24 h with 1nM of the indicated cytokine. D) Expression of Bcat2, Sdha, Bckdha, Atp5a and β -actin in 3T3-L1 adipocytes treated for 24h on day 8 post differentiation with 1nM TNF α . E) Expression of BCAA metabolism genes in 3T3-L1s treated on day 8 post differentiation for 24h with 1nM TNF α and 10 μ M Bay11-7085 (\$ represents p<0.05 compared to TNF α treatment). ND represents not detectable, error bars represent standard error of the mean and * representing p<0.05 compared to control and n equals 6 per treatment group.



Transport of BCAAs and the metabolic effect of enzyme down-regulation. To parallel the analysis of gene expression in the BCAA pathway with metabolic processes we evaluated BCAA transport. Two systems facilitate BCAA uptake into adipocytes. Slc1a5 mediates direct BCAA transport of leucine, isoleucine and valine whereas Slc3a2 and Slc7a5 form a heterodimeric plasma membrane complex exchanging internal glutamine and asparagine for external BCAA (27-30). As shown in Figure 4A, TNF α treatment of 3T3-L1 adipocytes down regulated the expression of Slc1a5 but did not affect the expression of either Slc3a2 or Slc7a5. Furthermore, expression of Slc1a5 was selectively down regulated in the epididymal, but not subcutaneous depot of high fat fed mice (Figure 4B). To parallel the down regulation of Slc1a5 with transport, we evaluated [³H]-leucine uptake in response to TNF α treatment using the 3T3-L1 adipocyte system. Figure 3C shows that influx was diminished ~50% in TNF α treated adipocytes. To further investigate the fate of the internalized leucine, we extracted the metabolites and monitored the metabolism of [¹⁴C]-leucine into protein and lipid. Consistent with down regulation of the entire BCAA pathway, conversion of the leucine into triglyceride was markedly attenuated (Figure 4D) whereas conversion of internalized leucine into protein was largely unaffected (Figure 4E).

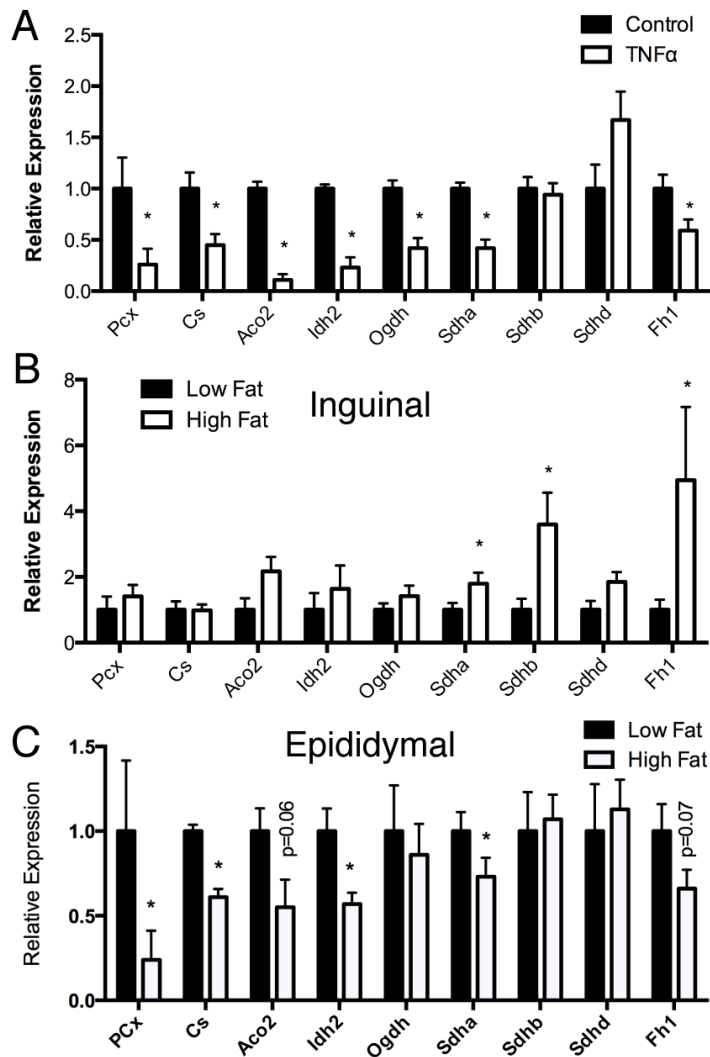


Figure 3 – Obesity and inflammation down regulate TCA cycle and anaplerotic reaction enzyme gene expression. A) Expression of TCA cycle metabolism genes in 3T3-L1 adipocytes treated with or without 1nM TNFα for 24h. Expression of TCA cycle genes in B) inguinal white adipose tissue and C) epididymal white adipose tissue from low fat or high fat fed C57Bl/6J mice. Error bars represent standard error of the mean and * representing $p < 0.05$ and n equals 6-12 per group.

Intracellular metabolomics of TNF α treated 3T3-L1 adipocytes. Since the metabolism of [^{14}C]-leucine to lipid, but not protein, was markedly attenuated, we analyzed the steady-state level of intracellular metabolites as a mechanism towards understanding BCAA and TCA cycle metabolism. As shown in Figure 5A we measured an accumulation of intracellular BCAAs in TNF α treated 3T3-L1s compared to controls. Furthermore, intracellular glutamine and asparagine levels were reduced following TNF α treatment (Figure 5B), suggesting exchange of glutamine/asparagine for BCAAs through the Slc7a5/Slc3a2 transport system may be compensating for reduced transport through Slc1a5. Furthermore a reduction asparagine synthetase, which is observed in adipose tissue of *ob/ob* mice, could explain the reduction in asparagine in TNF α treated 3T3-L1 cells (31). In addition we evaluated organic acid intermediates and measured an increase of 2-oxoglutarate, a decrease in fumarate and pyruvate and increased lactate levels (Figure 5C) consistent with decreased activity of the TCA cycle.

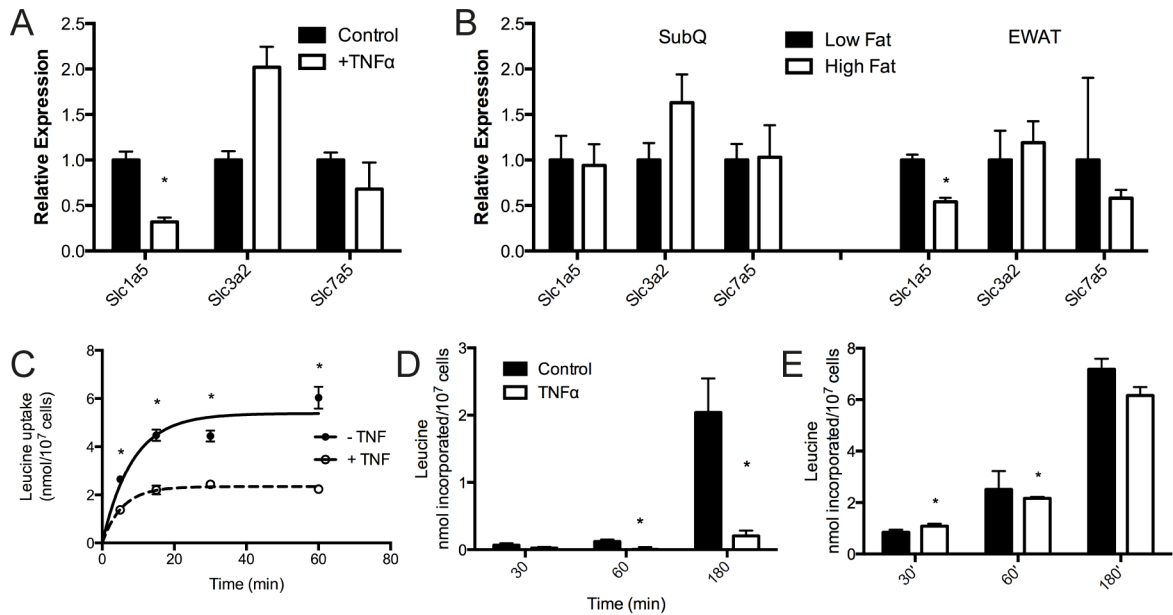


Figure 4 – Leucine transport and metabolism in 3T3-L1 adipocytes. A) Expression of leucine transport proteins in 3T3-L1 adipocytes treated for 24h with 1nM TNF α . B) Expression of leucine transport proteins in inguinal and epididymal white adipose tissue from mice maintained on chow (black bars) or high fat diet (white bars) for 12 weeks. C) Total [³H]-leucine uptake in 3T3-L1 adipocytes treated with 1nM TNF α . D) [¹⁴C]-leucine fractionated into lipid or E) protein after 24h TNF α treatment. Error bars represent standard error of the mean and * representing p<0.05 and n equals 6 per group.

ER Stress and the BCAA pathway. Since inflammatory cytokines induce ER stress *in vivo* and TNF α treatment of 3T3-L1 adipocytes similarly induces the unfolded protein response and activation of Jnk (32, 33), we evaluated the effect of ER stress on the BCAA pathway. Two experimental systems were utilized to probe the role of ER stress on the BCAA pathway. Firstly, 3T3-L1 cells were treated with either tunicamycin or thapsigargin to induce accumulation of non-glycosylated and therefore unfolded proteins or inhibit the calcium re-uptake pump SERCA, respectively. As shown in Figure 6A, treatment with either tunicamycin or thapsigargin led to the down regulation of genes linked to the BCAA pathway. This result suggested that increased ER stress, or the ER stress response pathway, affects gene expression of targets linked to mitochondrial BCAA metabolism. Extending these observations, tunicamycin or thapsigargin also down regulated several key antioxidant genes including Prdx3 and Gsta4 as well as the key mitochondrial transcriptional co-activator PGC1 α and mitochondrial biogenesis signal regulator eNOS (data not shown). These results imply that ER stress reprograms mitochondrial systems broadly at the level of both mitochondrial biogenesis and metabolism. However, both tunicamycin and thapsigargin treatment may lead to secondary effects unrelated to ER stress and as such we utilized a molecular genetic method specific to ER stress-the selective expression of spliced XBP1 in adipose tissue.

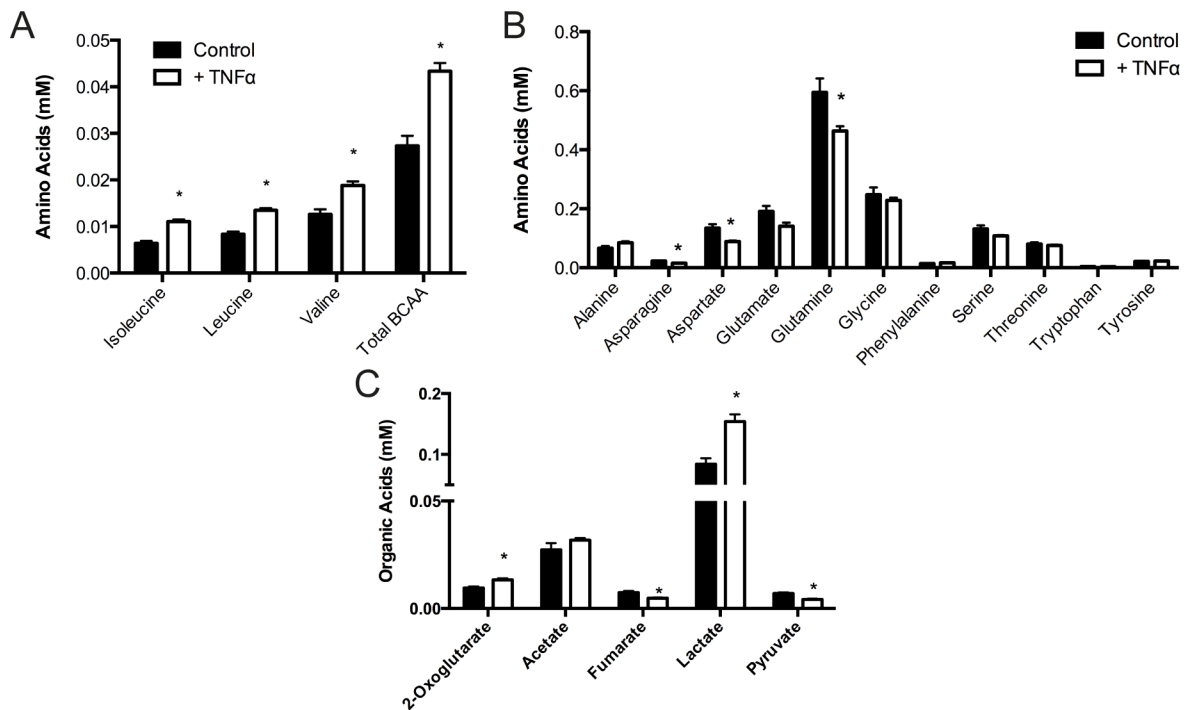


Figure 5 – Metabolomics analysis of 3T3-L1 cells. 3T3-L1 adipocytes were treated for 24h with 1nM TNF α and the intracellular levels of branched chain amino acids (A), amino acids (B) and organic acids (C) analyzed. Error bars represent standard error of the mean and * representing $p < 0.05$ and n equals 6 per group.

Utilizing transgenic mice expressing Xbp1s inducibly driven by the adiponectin promoter (referred to as FIXs mice), we evaluated subcutaneous and visceral adipose tissue from low fat fed FIXs and wild type C57Bl/6J mice for the regulation of genes linked to the BCAA pathway. Since adiponectin is expressed to high levels in subcutaneous adipose tissue as well as visceral depot we assessed the expression of spliced and total Xbp1 in the two locales. As shown in Figure 6B, Xbp1s was expressed in both depots but to highest levels in the subcutaneous site. Possibly with high level of Xbp1s mRNA in the subcutaneous depot, the expression of genes linked to the BCAA pathway was markedly decreased in subcutaneous fat (Figure 6C) while only moderately decreased in the visceral depot (Figure 6D). Similar to the results with tunicamycin and thapsigargin, the expression of key antioxidants Prdx3 and Gsta4 were markedly down regulated in subcutaneous fat from the FIXs mouse as were the mitochondrial biogenesis regulators eNOS and PGC1 α (data not shown). These results suggest that even under conditions of low fat feeding where ER stress is not developed that transgenic expression of Xbp1s drives the down regulation of the BCAA pathway. These results suggest that ER stress can lead to BCAA pathway down regulation but does not demonstrate that ER stress is required for BCAA pathway control.

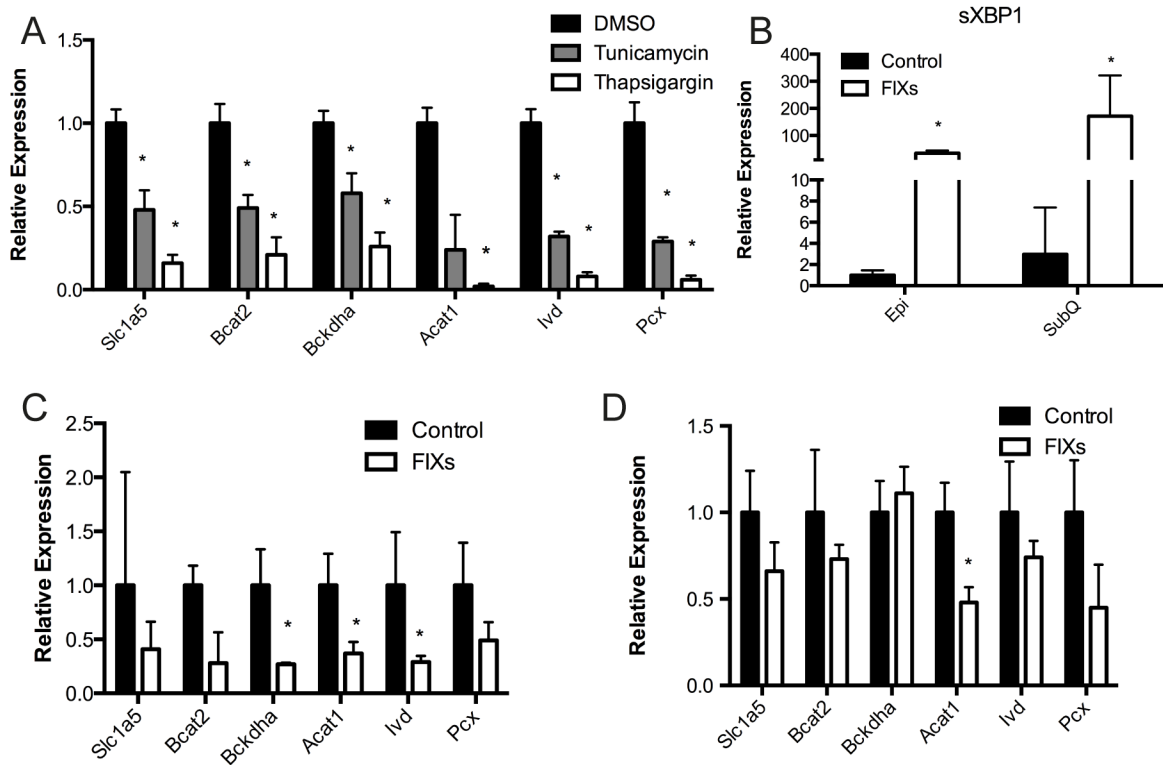


Figure 6 – ER stress down regulates BCAA metabolism genes. A) 3T3-L1 adipocytes were treated for 24h with 5µM tunicamycin, 1µM thapsigargin or DMSO and the expression of BCAA/TCA genes analyzed. B) Expression of spliced XBP1 in epididymal and subcutaneous fat of wild type and FIXs mice. Expression of BCAA/TCA metabolism genes in wild type and transgenic mice over expressing spliced XBP1 (FIXs) maintained on a chow diet in the C) inguinal or D) epididymal depot. Error bars represent standard error of the mean and * representing $p < 0.05$ and n equals 4-8 per group.

Discussion

The work described here profiles a previously unappreciated regulatory system controlling the branched chain amino acid metabolism pathway and a potential explanation for the observation of elevated circulating BCAAs in insulin resistance and type 2-diabetes. It has been previously shown that elevated circulating BCAAs are one of the best predictive biomarkers for development of type 2 diabetes but it has been unclear as to the mechanistic basis of this observation (9, 13, 14). Previous work from Herman et al (ref 9) has shown that reduced uptake of BCAA by adipose tissue may be sufficient to elevate circulating BCAA. However, it is not likely that mitochondrial dysfunction per se leads to insulin resistance for in many cases, mitochondrial dysfunction is compensated for by increased glycolysis and substrate-level phosphorylation that in turn reduces the serum glucose level (34).

To investigate the effect of inflammation on the BCAA pathway we first assessed the expression of BCAA metabolism enzymes in adipose tissue from lean and obese mice. The expression of BCAA genes in the epididymal depots of mice maintained on a high fat diets were significantly down regulated relative to lean control mice whereas those in the inguinal depot were largely unaffected (Figures 1B, 1C). The subcutaneous depot exhibited a trend towards down regulation of BCAA genes but clearly not to the same extent as does visceral fat. Similarly, 3T3-L1 adipocytes treated with the pro-inflammatory cytokine, TNF α and

demonstrated a coordinate down-regulation of essentially the entire pathway (Figure 2A) and the down regulation was measured in response to other inflammatory factors suggesting that inflammation broadly affects BCAA metabolism (Figure 2C). This effect was largely abated when 3T3-L1s were co-treated with TNF α and Bay11-7085 suggesting the observed down-regulation is at least in part dependent on the NF- κ B pathway (Figure 2E). Interestingly, IFN γ that is made by T cells also down regulated adipocyte BCAA metabolism genes indicating that cells other than inflammatory macrophages may play a role in affecting adipocyte lipid metabolism (Figure 2C). Functional analysis of BCAA metabolism using [14 C]-leucine incorporation into lipid pools corroborated the loss of BCAA metabolism with essentially no effect on amino acid incorporation into protein (Figures 4D, 4E). [3 H]-leucine uptake is reduced \sim 50% due to down regulation of Slc1a5 but even when the data are normalized to uptake, conversion of leucine to lipid is dramatically reduced (Figure 4C). Moreover, since increased oxidative stress leads to potentiated carbonylation of BCAA pathway enzymes (34), the mechanism of decreased BCAA metabolism is likely a combination of both reduced expression and carbonylation of pathway enzymes. Consistent with reduced BCAA uptake but essentially no BCAA metabolism, the intracellular pool of BCAA was increased in TNF α treated adipocytes.

The TNF α -mediated down regulation of mitochondrial metabolism was not restricted to the BCAA pathway. Indeed, our metabolomic analysis of TNF α treated 3T3-L1 adipocytes also revealed changes in the TCA cycle intermediates (Figure 5C). Moreover, the expression of several TCA cycle enzymes was down regulated at the mRNA level following TNF α treatment (Figure 3A) and each of the TCA cycle enzymes is carbonylated under conditions of increased oxidative stress (34). The same pattern of TCA cycle enzymes being down regulated was evident in visceral adipose tissue. It should also be stressed that the key enzyme controlling mitochondrial oxaloacetate, pyruvate carboxylase, is significantly down regulated in epididymal fat and TNF α treated adipocytes. Since pyruvate carboxylase is a key lipogenic enzyme mediating metabolism of glucose-derived pyruvate, the results are also consistent with decreased flux of glucose into triglyceride in response to inflammation. However, TCA cycle enzyme gene expression is increased in subcutaneous adipose tissue (Figure 3B) implying that inflammation biases nutrient uptake and metabolism away from the visceral depot and towards the subcutaneous depot due to attenuation of de novo lipogenesis.

In many systems mitochondrial dysfunction is correlated with an increase in endoplasmic reticulum (ER) stress (35, 36). To determine if ER stress could influence mitochondrial dysfunction, specifically BCAA metabolism, via regulation of the BCAA metabolism pathway we used both pharmacologic and molecular

genetic methods to induce ER stress. Figure 6 shows that pharmacologic activation of ER stress either via inducing the unfolded protein response (tunicamycin) or by inhibition of calcium reuptake (thapsagargin) resulted in down regulation of BCAA metabolism genes in the 3T3-L1 cell culture system. Extending this analysis in vivo, adipose specific overexpression of spliced XBP1 (FIXs) resulted in down regulation of BCAA genes largely in subcutaneous adipose depots where XBP1s is expressed at the mRNA level to the greatest extent (Figure 6B). Interestingly, such mice also exhibit increased plasma leucine levels (Deng and Scherer, in preparation), suggesting that ER stress is sufficient to cause adipose mitochondrial dysfunction as well as decreased BCAA metabolism.

In sum, our results suggest that inflammation regulates BCAA metabolism and lipogenesis in visceral adipose tissue. Furthermore, the results presented suggest that within the context of adult fat pad expansion, inflammation limits visceral adipose tissue while allowing for continued expansion of the subcutaneous depot via depot specific regulation of mitochondrial metabolism.

Acknowledgements

We thank the members of the Bernlohr research group who provided helpful suggestions regarding this work as well as the Minnesota Supercomputing Institute (MSI) for support in data analysis. We would also like to thank Todd Rappe and the Minnesota NMR Center for assistance with data collection and metabolomic analyses. We also thank Drs. Fredric Kraemer (Stanford University) and Christopher Lynch (Penn State University) for helpful discussions.

References

1. Ogden, C. L., Carroll, M. D., Kit, B. K., and Flegal, K. M. (2012) Prevalence of Obesity and Trends in Body Mass Index Among US Children and Adolescents, 1999-2010. *JAMA*. **307**, 483–490
2. Matsuzawa, Y. (2006) The metabolic syndrome and adipocytokines. *FEBS Letters*. **580**, 2917–2921
3. Schipper, H. S., Prakken, B., Kalkhoven, E., and Boes, M. (2012) Adipose tissue-resident immune cells: key players in immunometabolism. *Trends Endocrinol Metab*. **23**, 407–415
4. Maury, E., and Brichard, S. M. (2010) Adipokine dysregulation, adipose tissue inflammation and metabolic syndrome. *Mol. Cell. Endocrinol*. **314**, 1–16
5. Guilherme, A., Virbasius, J. V., Puri, V., and Czech, M. P. (2008) Adipocyte dysfunctions linking obesity to insulin resistance and type 2 diabetes. *Nat. Rev. Mol. Cell Biol*. **9**, 367–377
6. Houstis, N., Rosen, E. D., and Lander, E. S. (2006) Reactive oxygen species have a causal role in multiple forms of insulin resistance. *Nature*. **440**, 944–948
7. Furukawa, S., Fujita, T., Shimabukuro, M., Iwaki, M., Yamada, Y., Nakajima, Y., Nakayama, O., Makishima, M., Matsuda, M., and Shimomura, I. (2004) Increased oxidative stress in obesity and its impact on metabolic syndrome. *J. Clin. Invest*. **114**, 1752–1761
8. Anderson, E. J., Lustig, M. E., Boyle, K. E., Woodlief, T. L., Kane, D. A., Lin, C.-T., Price, J. W., Kang, L., Rabinovitch, P. S., Szeto, H. H., Houmard, J. A., Cortright, R. N., Wasserman, D. H., and Neuffer, P. D. (2009) Mitochondrial H₂O₂ emission and cellular redox state link excess fat intake to insulin resistance in both rodents and humans. *J. Clin. Invest*. **119**, 573–581
9. Herman, M. A., She, P., Peroni, O. D., Lynch, C. J., and Kahn, B. B. (2010) Adipose tissue branched chain amino acid (BCAA) metabolism modulates circulating BCAA levels. *J. Biol. Chem*. **285**, 11348–11356
10. Newgard, C. B. (2012) Interplay between Lipids and Branched-Chain Amino Acids in Development of Insulin Resistance. *Cell Metab*. **15**, 606–614
11. Batch, B. C., Shah, S. H., Newgard, C. B., Turer, C. B., Haynes, C., Bain, J. R., Muehlbauer, M., Patel, M. J., Stevens, R. D., Appel, L. J., Newby, L. K., and Svetkey, L. P. (2013) Branched chain amino acids are novel biomarkers for discrimination of metabolic wellness. *Metab. Clin. Exp*. **62**, 961–969
12. Sears, D. D., Hsiao, G., Hsiao, A., Yu, J. G., Courtney, C. H., Ofrecio, J. M., Chapman, J., and Subramaniam, S. (2009) Mechanisms of human insulin resistance and thiazolidinedione-mediated insulin sensitization. *Proc. Natl. Acad. Sci. U.S.A*. **106**, 18745–18750

13. Newgard, C. B., An, J., Bain, J. R., Muehlbauer, M. J., Stevens, R. D., Lien, L. F., Haqq, A. M., Shah, S. H., Arlotto, M., Slentz, C. A., Rochon, J., Gallup, D., Ilkayeva, O., Wenner, B. R., Yancy, W. S., Eisenson, H., Musante, G., Surwit, R. S., Millington, D. S., Butler, M. D., and Svetkey, L. P. (2009) A branched-chain amino acid-related metabolic signature that differentiates obese and lean humans and contributes to insulin resistance. *Cell Metab.* **9**, 311–326
14. Wang, T. J., Larson, M. G., Vasan, R. S., Cheng, S., Rhee, E. P., McCabe, E., Lewis, G. D., Fox, C. S., Jacques, P. F., Fernandez, C., O'Donnell, C. J., Carr, S. A., Mootha, V. K., Florez, J. C., Souza, A., Melander, O., Clish, C. B., and Gerszten, R. E. (2011) Metabolite profiles and the risk of developing diabetes. *Nat. Med.* **17**, 448–453
15. Magkos, F., Bradley, D., Schweitzer, G. G., Finck, B. N., Eagon, J. C., Ilkayeva, O., Newgard, C. B., and Klein, S. (2013) Effect of Roux-en-Y gastric bypass and laparoscopic adjustable gastric banding on branched-chain amino acid metabolism. **62**, 2757–2761
16. McCormack, S. E., Shaham, O., McCarthy, M. A., Deik, A. A., Wang, T. J., Gerszten, R. E., Clish, C. B., Mootha, V. K., Grinspoon, S. K., and Fleischman, A. (2012) Circulating branched-chain amino acid concentrations are associated with obesity and future insulin resistance in children and adolescents. *Pediatr Obes.* 10.1111/j.2047-6310.2012.00087.x
17. Lackey, D. E., Lynch, C. J., Olson, K. C., Mostaedi, R., Ali, M., Smith, W. H., Karpe, F., Humphreys, S., Bedinger, D. H., Dunn, T. N., Thomas, A. P., Oort, P. J., Kieffer, D. A., Amin, R., Bettaieb, A., Haj, F. G., Permana, P., Anthony, T. G., and Adams, S. H. (2013) Regulation of adipose branched-chain amino acid catabolism enzyme expression and cross-adipose amino acid flux in human obesity. *Am. J. Physiol. Endocrinol. Metab.* **304**, E1175–87
18. Zhou, Y., Jetton, T. L., Goshorn, S., Lynch, C. J., and She, P. (2010) Transamination is required for {alpha}-ketoisocaproate but not leucine to stimulate insulin secretion. *J. Biol. Chem.* **285**, 33718–33726
19. She, P., Zhou, Y., Zhang, Z., Griffin, K., Gowda, K., and Lynch, C. J. (2010) Disruption of BCAA metabolism in mice impairs exercise metabolism and endurance. *J. Appl. Physiol.* **108**, 941–949
20. She, P., Reid, T. M., Bronson, S. K., Vary, T. C., Hajnal, A., Lynch, C. J., and Hutson, S. M. (2007) Disruption of BCATm in mice leads to increased energy expenditure associated with the activation of a futile protein turnover cycle. *Cell Metab.* **6**, 181–194
21. Surwit, R. S., Kuhn, C. M., Cochrane, C., McCubbin, J. A., and Feinglos, M. N. (1988) **Diet-Induced Type II Diabetes in C57BL/6J Mice.** **37**, 1163
22. Sun, K., Wernstedt Asterholm, I., Kusminski, C. M., Bueno, A. C., Wang, Z. V., Pollard, J. W., Brekken, R. A., and Scherer, P. E. (2012) Dichotomous effects of VEGF-A on adipose tissue dysfunction. *Proc. Natl. Acad. Sci.*

- U.S.A. **109**, 5874–5879
23. Deng, Y., Wang, Z. V., Tao, C., Gao, N., Holland, W. L., Ferdous, A., Repa, J. J., Liang, G., Ye, J., Lehrman, M. A., Hill, J. A., Horton, J. D., and Scherer, P. E. (2012) The Xbp1s/GalE axis links ER stress to postprandial hepatic metabolism. *J. Clin. Invest.* **123**, 455–468
 24. Student, A. K., Hsu, R. Y., and Lane, M. D. (1980) Induction of fatty acid synthetase synthesis in differentiating 3T3-L1 preadipocytes. *J. Biol. Chem.* **255**, 4745
 25. Hahn, W. S., Kuzmicic, J., Burrill, J. S., Donoghue, M. A., Foncea, R., Jensen, M. D., Lavandero, S., Arriaga, E. A., and Bernlohr, D. A. (2014) Proinflammatory cytokines differentially regulate adipocyte mitochondrial metabolism, oxidative stress, and dynamics. *Am. J. Physiol. Endocrinol. Metab.* **306**, E1033–45
 26. Long, E. K., Olson, D. M., and Bernlohr, D. A. (2013) High-fat diet induces changes in adipose tissue trans-4-oxo-2-nonenal and trans-4-hydroxy-2-nonenal levels in a depot-specific manner. *Free Radical Biology and Medicine.* **63**, 390–398
 27. Segawa, H., Fukasawa, Y., Miyamoto, K., Takeda, E., Endou, H., and Kanai, Y. (1999) Identification and functional characterization of a Na⁺-independent neutral amino acid transporter with broad substrate selectivity. *Journal of Biological Chemistry.* **274**, 19745–19751
 28. Utsunomiya-Tate, N., Endou, H., and Kanai, Y. (1996) Cloning and functional characterization of a system ASC-like Na⁺-dependent neutral amino acid transporter. *J. Biol. Chem.* **271**, 14883–14890
 29. Kanai, Y., Segawa, H., Miyamoto, K. I., Uchino, H., Takeda, E., and Endou, H. (1998) Expression cloning and characterization of a transporter for large neutral amino acids activated by the heavy chain of 4F2 antigen (CD98). *J. Biol. Chem.* **273**, 23629–23632
 30. Fuchs, B. C., and Bode, B. P. (2005) Amino acid transporters ASCT2 and LAT1 in cancer: partners in crime? *Semin. Cancer Biol.* **15**, 254–266
 31. Keller, M. P., Choi, Y., Wang, P., Davis, D. B., Rabaglia, M. E., Oler, A. T., Stapleton, D. S., Argmann, C., Schueler, K. L., Edwards, S., Steinberg, H. A., Chaibub Neto, E., Kleinhanz, R., Turner, S., Hellerstein, M. K., Schadt, E. E., Yandell, B. S., Kendzioriski, C., and Attie, A. D. (2008) A gene expression network model of type 2 diabetes links cell cycle regulation in islets with diabetes susceptibility. *Genome Res.* **18**, 706–716
 32. Xue, X., Piao, J.-H., Nakajima, A., Sakon-Komazawa, S., Kojima, Y., Mori, K., Yagita, H., Okumura, K., Harding, H., and Nakano, H. (2005) Tumor necrosis factor alpha (TNFalpha) induces the unfolded protein response (UPR) in a reactive oxygen species (ROS)-dependent fashion, and the UPR counteracts ROS accumulation by TNFalpha. *J. Biol. Chem.* **280**, 33917–33925
 33. Baregamian, N., Song, J., Bailey, C. E., Papaconstantinou, J., Evers, B. M., and Chung, D. H. (2009) Tumor Necrosis Factor- α and Apoptosis

- Signal-Regulating Kinase 1 Control Reactive Oxygen Species Release, Mitochondrial Autophagy and C-Jun N-Terminal Kinase/P38 Phosphorylation During Necrotizing Enterocolitis. *Oxid Med Cell Longev.* **2**, 297–306
34. Curtis, J. M., Hahn, W. S., Stone, M. D., Inda, J. J., Drouillard, D. J., Kuzmicic, J. P., Donoghue, M. A., Long, E. K., Armien, A. G., Lavandero, S., Arriaga, E., Griffin, T. J., and Bernlohr, D. A. (2012) Protein carbonylation and adipocyte mitochondrial function. *J. Biol. Chem.* **287**, 32967–32980
 35. Yuzefovych, L. V., Musiyenko, S. I., Wilson, G. L., and Rachek, L. I. (2013) Mitochondrial DNA Damage and Dysfunction, and Oxidative Stress Are Associated with Endoplasmic Reticulum Stress, Protein Degradation and Apoptosis in High Fat Diet-Induced Insulin Resistance Mice. *PLoS ONE.* **8**, e54059
 36. Lim, J. H., Lee, H. J., Ho Jung, M., and Song, J. (2009) Coupling mitochondrial dysfunction to endoplasmic reticulum stress response: a molecular mechanism leading to hepatic insulin resistance. *Cell. Signal.* **21**, 169–177

CHAPTER FOUR

Rictor Oxidation and Disruption of the Mammalian Target of Rapamycin Complex 2 (mTORC2) Links Mitochondrial Oxidative Stress to Insulin Resistance in Adipocytes

Olson, D.H., Burrill, J.S., Bernlohr, D.A. (2015) *In preparation*

This chapter contains an original research article in preparation for submission.

Joel Burrill performed the experiments in Figure 3C and D, confirmed results in Figure 1A, 1D and 3B and helped write and edit this chapter.

Summary

Oxidative stress has been implicated in the development of obesity-induced insulin resistance and is correlated with down-regulated expression of Peroxiredoxin-3 (Prdx3), a primary mitochondrial antioxidant responsible for converting mitochondrial hydrogen peroxide to water and oxygen. Silencing of Prdx3 (Prdx3KD) in 3T3-L1 adipocytes provides mechanistic insight into the role of adipose mitochondrial oxidative stress and insulin resistance. Prdx3KD cells showed a two-fold increase in H₂O₂, decreased insulin signaling, reduced insulin-stimulated glucose transport, attenuated phosphorylation of the mTORC2 substrate S473AKT, as well as increased protein side chain oxidation. The decrease in glucose uptake can be rescued by pre-treatment with N-acetylcysteine (NAC). These changes in insulin sensitivity occur independently from ER stress as revealed by no detectable changes in BIP, phospho-eIF2 α or phospho-JNK protein. Cysteine oxidation analysis indicates that rictor is highly oxidized in Prdx3KD cells and co-immunoprecipitation analysis reveal decreased association with mTOR implying reduced activation of the mTORC2. NAC treatment of Prdx3KD adipocytes rescued rictor-mTOR complex formation. Taken together, these data suggest a novel mechanism whereby increased mitochondrial oxidative stress leads to cysteine oxidation of rictor and decreased association with mTOR, effectively inhibiting signaling capabilities of mTORC2, thus driving insulin resistance.

Introduction

It is well accepted that within obese, insulin resistant, adipose tissue exists a low-grade, chronic inflammation (1-4). Release of pro-inflammatory cytokines such as Tumor necrosis factor alpha (TNF α) from resident macrophages acting on adipocytes is known to be a major driver of adipose tissue insulin resistance (5). Although cytokines are able to activate several pathways within the cell, the induction of mitochondrial dysfunction is a hallmark feature of adipocyte cytokine treatment (5-7).

Importantly, mitochondrial dysfunction has been linked to insulin resistance in adipose tissue as well as liver and muscle (8-13). Classic markers of mitochondrial dysfunction include decreased oxidative phosphorylation capacity as well as increased oxidative stress (10). Although the term oxidative stress encompasses many forms of reactive oxidants, the production and signaling mechanisms of reactive oxygen species (ROS) are the best characterized. Additionally, while cells are capable of producing ROS at many sites, mitochondria are thought to be a major contributor (14).

During the process of oxidative phosphorylation electrons are passed between complexes of the electron transport chain with the final electron acceptor being molecular oxygen, resulting in the formation of water. Under basal conditions a

small fraction of electrons, if mishandled, can react with molecular oxygen to form superoxide anion.

Within the mitochondria, superoxide anion is quickly metabolized to hydrogen peroxide (H_2O_2) by superoxide dismutase 2 (SOD2). Hydrogen peroxide, a relatively stable molecule, if not metabolized to water and molecular oxygen by antioxidants, is able to diffuse out of the mitochondria where it can modify redox sensitive proteins outside of its immediate environment (2, 15, 16). Hydrogen peroxide, even at low levels can modify sulfur atoms of methionine and cysteine containing proteins (2). Because cysteine residues are typically found within the active site of proteins, their oxidation often renders proteins inactive (17, 18).

Results from our lab suggest that in visceral adipose tissue of obese, insulin resistant mice, oxidative stress results from a selective down regulation of several key mitochondrial antioxidant enzymes responsible for metabolizing H_2O_2 (19). One antioxidant that is consistently down-regulated *in vivo* is peroxiredoxin-3 (Prdx3) (19). The peroxiredoxin family of enzymes is made up of six isoforms and is one of the most ancient and abundant families of antioxidants in existence (20). Peroxiredoxins are capable of reducing peroxynitrite, lipid peroxides as well as H_2O_2 through the oxidation of specific cysteine residues found on each isoform (21, 22). PRDX3 is unique in that it is the only antioxidant found to localize solely to the mitochondria (23). Whole body knockout of Prdx3 in mice

results in increased white adipose tissue accumulation, increased oxidative stress, adipokine dysregulation and whole body insulin resistance (24).

Furthermore, transgenic mice over expressing Prdx3 are protected from high fat diet induced insulin resistance highlighting the critical role oxidative stress plays in preserving insulin sensitivity (24). Moreover, in the adipose tissue of obese, insulin resistant humans, Prdx3 is known to be transcriptionally down-regulated (26). Although it is clear that Prdx3 plays an important role in maintaining metabolic homeostasis, the underlying pathways driving insulin resistance within adipose tissue have not been well investigated. Moreover, while inflammation induced oxidative stress can result in insulin resistance, it is not known if mitochondrial oxidative stress *alone* is sufficient to induce insulin resistance in adipocytes.

By knocking down Prdx3 in 3T3-L1 cells we have generated an adipocyte model where mitochondrial dysfunction results in insulin resistance *independent* of inflammation and endoplasmic reticulum stress. Instead, the major driver appears to be oxidation and disassociation of the mammalian target of rapamycin complex 2 (mTORC2) leading to decreased phosphorylation of S473-AKT, decreased glucose uptake and insulin resistance. Importantly, insulin sensitivity as well as mTORC2 formation can be restored with pretreatment of NAC, a potent antioxidant, pointing to oxidative stress as the major trigger for insulin resistance in this model.

Methods

Differentiation of 3T3-L1 adipocytes and insulin stimulation

3T3-L1 fibroblasts were grown to confluence and differentiated using the standard dexamethasone, methylisobutylxanthine, and insulin protocol.

Differentiation was assessed by triglyceride accumulation and the expression of adipocyte marker proteins such as the adipocyte fatty acid-binding protein and the peroxisome proliferator-activated receptor gamma. Cells were harvested between days 8-10 for assaying. Insulin stimulated cells were serum starved in KRH buffer containing 5% BSA for 2 hours on Day 8 post differentiation. Cells were stimulated with 100nM insulin was added and incubated for 30 minutes at 37°C. All wells were harvested in hypotonic buffer containing 0.1% SDS.

Samples were spun at 100,000g for 1 hour and supernatant collected for protein determination.

Quantitative real-time PCR (qRT-PCR)

Total RNA was extracted from 3T3-L1 cells and tissue using TRIzol reagent according to the manufacturer's protocol (Invitrogen, Grand Island, NY, USA).

Real-time amplification was performed using a Bio-Rad CFX96 machine using iQ SYBR Green Supermix and the recommended thermocycler parameters (Bio-Rad, Hercules, CA, USA). Gene expression assays were performed for glutathione peroxidase 4 (Gpx4), peroxiredoxin 3 (Prdx3), manganese superoxide dismutase (SOD2), Glutathione-S-Transferase 4 (GSTA4). Relative gene

expression comparisons were carried out using the $-\Delta\Delta\text{CT}$ method and normalized to transcription factor 2E (TFIIIE) as an endogenous control.

H₂O₂ measurements

On day 8 of differentiation 3T3-L1 cells were harvested, sonicated and spun at 10,000g for 10 minutes in 150ul of 0.25M sodium phosphate buffer containing 0.1% Triton-X. Supernatant was removed and assay was performed as recommended by the Amplex Red Hydrogen Peroxide/Peroxidase Assay Kit (Invitrogen, Grand Island, NY, USA).

Cellular and mitochondrial respiration

Cellular respiration and proton efflux were analyzed using the XF24 Analyzer and system software (Seahorse Bioscience, Billerica, MA). 3T3-L1 fibroblasts were grown and differentiated in XF24 V7 culture dishes coated with 0.2% gelatin (Sigma). On day 8 of differentiation, cells were washed with and switched to serum-free modified, no-bicarbonate, low-phosphate DMEM (D5030) supplemented with 1× glutamax (Invitrogen), 1 mM sodium pyruvate, 25 mM glucose, and 0–1 nM cytokine and allowed to equilibrate for 1 h in a non-CO₂ 37°C incubator. After cartridge calibration, cells were placed in the XF24 analyzer, where cellular oxygen consumption and extracellular acidification rate were measured four times under basal conditions and then three times after the addition of 2 μM oligomycin through port A, three times after 0.4 μM FCCP

addition through port B, and twice after 2 μ M antimycin A addition through port C. Measurement protocol for each condition was as follows: mix for 2 min, wait for 2 min, and measure for 2 min. Oxygen consumption rate (μ mol/min) and extracellular acidification rate (ECAR; mpH/min) data obtained from the Seahorse XF24 Software were normalized to the eGFP control cell line.

2-Deoxyglucose uptake assay.

Cellular uptake of 2-deoxyglucose was assessed in 3T3-L1 adipocytes under basal conditions. On day 8, cells were washed in PBS and incubated for 2 h in serum-free KRH buffer (10 mM HEPES, 10 μ M NaCl, 1.2 mM KH₂PO₄, 1.2 mM MgSO₄, 2 mM Sodium Pyruvate, 4.7 mM KCl, 2.2 mM CaCl₂, and 0.5% fatty acid free BSA, pH 7.4). Cells were then stimulated with 100 nM insulin and incubated at 37°C and 5% CO₂ for 15 minutes. Uptake assay was initiated by adding 2-deoxyglucose to a final concentration of 100 μ M at 0.5 μ Ci 2-[³H]deoxyglucose/ml. Cells were incubated for 5 min at 37°C and 5% CO₂. Uptake was terminated by washing three times with ice-cold PBS. Cells were lysed in 1% Triton X-100, and lysate was subjected to scintillation counting. Intracellular 2-[³H]deoxyglucose was determined by linear regression of a standard curve of known concentrations.

Hemocytometer

On day 8 of differentiation cells were trypsinized in 0.5ml Trypsin. Once lifted 1ml of complete medium was added to each well. 200uL were transferred to a new tube containing 500uL of PBS and 300uL of 0.4% Trypan blue. 20uL of this sample were then loaded into a hemocytometer and counted. All quadrants were counted 2 times for each sample.

Generation of peroxidoredoxin 3-silenced adipocytes.

The 3T3-L1 fibroblasts were transduced with lentivirus carrying short hairpin RNA (shRNA) as described previously. The shRNA clone directed toward Prdx3 (TRCN0000120672) and eGFP control mRNA were purchased from the University of Minnesota Genomic Center. The full hairpin sequence used for the Prdx3 shRNA:

CCGGCCACAGGCTTTGTAATTCTAACTCGAGTTAGAATTACAAAGCCTGTGG
TTTTTG.

Aldehyde measurement

As described previously, cells were homogenized in 50mM sodium acetate buffer containing 5mM amino-oxyacetic acid with 250µM BHT and 500µM DTPA at pH 5.0, spiked with deuterated internal standards and incubated for 1h on ice. Samples were vortexed, centrifuged, run over Strata-X-AW columns before analysis by liquid chromatography-tandem mass spectrometry (LC-MS/MS) on

an AB/Sciex API 4000Qtrap mass spectrometer. Stable-isotope dilution was used for quantitation of aldehydes (19).

Glutathione measurements

Cells were grown in six-well plates as described previously. Cells were washed twice in ice-cold PBS, scraped, sonicated and centrifuged prior to the assay. The supernatant was collected, deprotonated and assayed for oxidized and total glutathione by the Glutathione Assay Kit according to manufacturer's instructions (Cayman Chemical, Ann Arbor, MI). The glutathione levels were normalized to protein content determined by bicinchoninic acid assay (Sigma Aldrich, St. Louis, MO).

Biotin-switch method for detecting oxidized cysteines

Mitochondria were isolated from cells by differential centrifugation as described previously (25). Oxidized cysteines were labeled using a modified protocol from what was described previously (26). Briefly, proteins were precipitated with 20% TCA, resuspended, free thiols blocked with n-ethylmaleimide (Sigma Aldrich, St. Louis, MO), reduced with sodium arsenite, labeled with biotin-maleimide (Sigma Aldrich, St. Louis, MO), separated by SDS-PAGE and detected using IR-conjugated streptavidin (Li-Cor Biosciences, Lincoln, NE).

Results

Obesity induced insulin resistance results in decreased mitochondrial antioxidant transcript levels. Studies in our lab have shown that adipose tissue from multiple mouse models of obesity induced insulin resistance show a selective transcriptional down regulation of the mitochondrial antioxidants. Mitochondrial antioxidants Glutathione S-transferase alpha 4 (Gsta4), Prdx3, Glutathione peroxidase 4 (Gpx4) and Aldehyde dehydrogenase 2 (Aldh2) were all down regulated in visceral adipose tissue of both high fat fed C57Bl/6J mice as well as ob/ob mice (Fig. 1A and 1B). On the other hand, cytoplasmic isoforms of these antioxidants showed little to no change in expression levels (data not shown). Additionally, treatment of 3T3-L1 adipocytes with either dexamethasone (DEX) or TNF α , two commonly used methods to induce insulin resistance in adipocytes, revealed a similar transcriptional down-regulation.

DEX treatment resulted in significant down regulation of Sod2, Gpx4 and Gsta4 (Fig. 1C) while TNF α induced down-regulation of Prdx3, Gpx4, Aldh2 and Gsta4 as well as an increase in Sod2 (Fig. 1D). Together the animal and cellular data suggest that under insulin resistant conditions the mitochondria may be generating a significant pool of reactive oxygen species (ROS) due to depletion of antioxidant capacity. Furthermore, the increased expression of Sod2 coupled to decreased expression of Prdx3, Gpx4, Aldh2 and Gsta4 suggests that H₂O₂ could be the ROS accumulating in highest concentration. Hypothesizing that

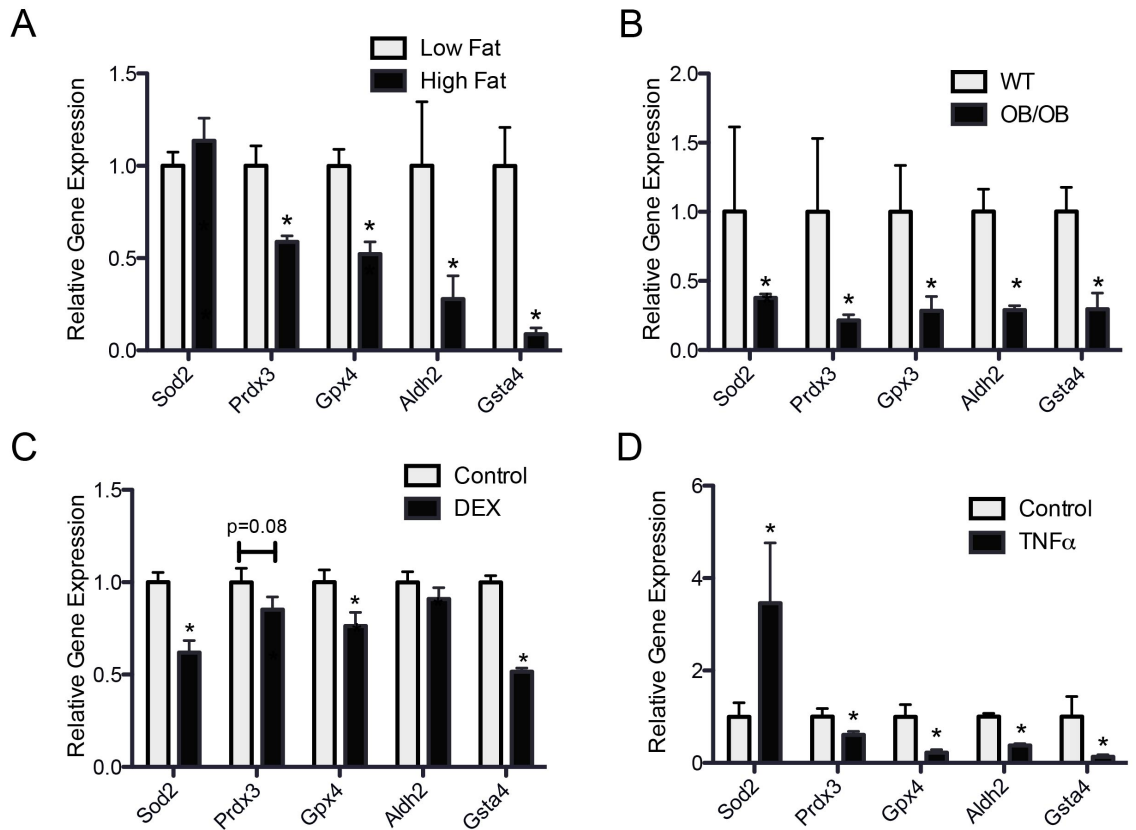


Figure 1 – Obesity and inflammation down-regulate the expression of mitochondrial antioxidants. Expression of mitochondrial antioxidants in A) epididymal white adipose tissue from 12 week mice fed a high fat diet for 8 weeks, B) epididymal white adipose tissue from *ob/ob* mice, 3T3-L1s treated with C) dexamethasone or D) TNF α

mitochondrially derived ROS could drive insulin resistance independent of inflammation, we developed a knockdown cell line of Prdx3, the primary mitochondrial antioxidant responsible for metabolizing upwards of 90% of mitochondrially derived H₂O₂.

Prdx3KD cells differentiate normally, show an increase in cell number with decreased diameter. Prdx3 silenced 3T3-L1 adipocytes show a significant decrease in both transcript and protein levels of Prdx3 compared to their controls (Fig. 2A). Additionally, Prdx3KD differentiate normally showing similar protein levels of both peroxisome proliferator-activated receptor gamma (PPAR- γ) and adipocyte fatty acid binding protein (AFABP) between cell lines (Fig. 2B). Oil-red-O staining of intracellular lipids show similar accumulation of triglyceride within the adipocytes (Fig. 2C). It is known that adipocyte differentiation and cell division is modulated by increases in oxidative stress. Interestingly, Prdx3KD cells showed an increase in cell number as well as a decrease in adipocyte diameter on day 8 of differentiation. Using two independent methods to quantify cell number, a hemocytometer and a cellometer, both confirm an increase in cell number in Prdx3KD cells compared to control (Fig. 2D). Moreover, cell diameter measurements taken by the cellometer reveal a decrease in cell size in the Prdx3KD cells (Fig. 2E).

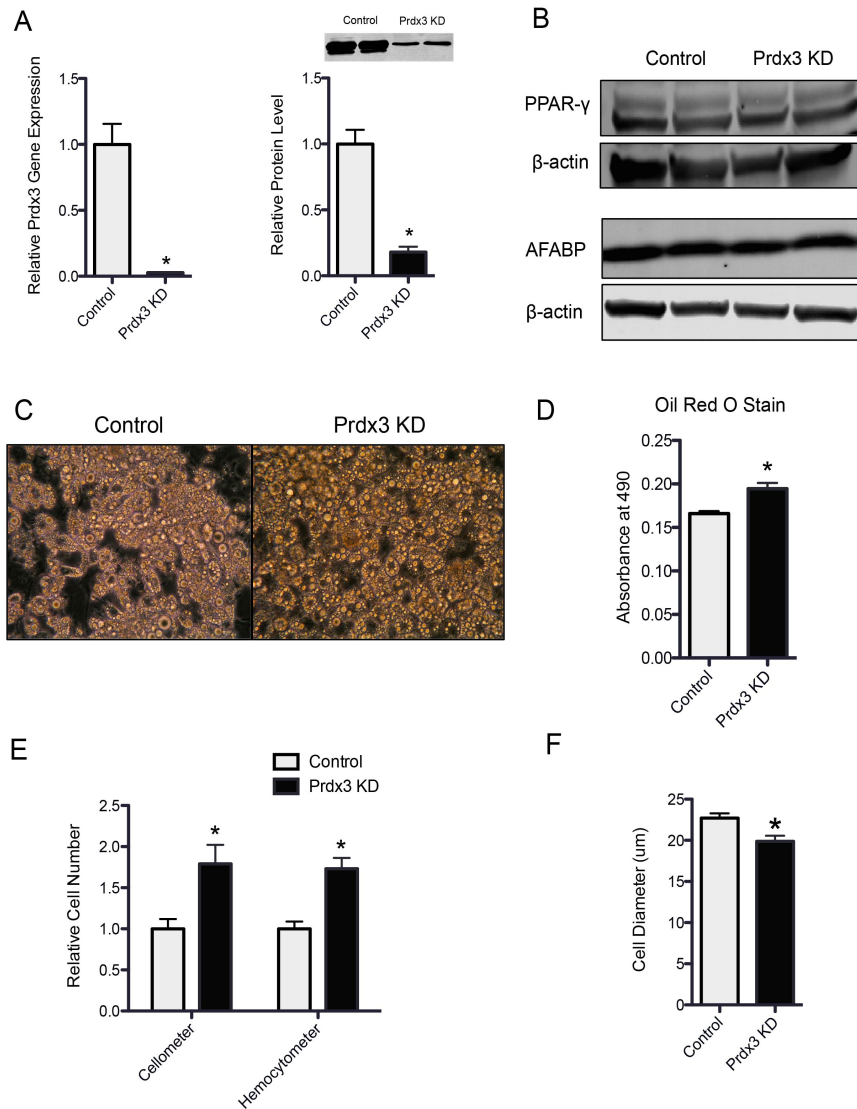


Figure 2 – Prdx3 KD 3T3-L1 characterization. Expression of Prdx3 at a A) mRNA and B) protein level post knockdown with shRNA. B) Adipocyte differentiation controls on day 8 post differentiation. C) Morphology of Prdx3 KD cells on day 8 post differentiation. D) Lipid accumulation measured by Oil Red O staining. E) Cell number and F) size of differentiated Prdx3 KD 3T3-L1 cells

Prdx3KD adipocytes display increased oxidative stress. Prdx3 is the primary and most potent antioxidant responsible for metabolizing H₂O₂ within the mitochondria. Therefore, as expected, silencing Prdx3 in 3T3-L1 adipocytes results in increased H₂O₂ levels detected using Amplex Red (Fig. 3A).

Differentiated Prdx3KD adipocytes display an approximately two-fold increase in H₂O₂ concentration present in whole cell lysate compared to control cells.

Importantly, knockdown of Prdx3 did not change the antioxidant expression of Sod2, Gpx4 or Gsta4 (Fig. 3B). Additionally, Prdx3KD cells also displayed an increase in oxidized glutathione, a common marker of oxidative stress (Fig. 3C).

Because H₂O₂ was increased we hypothesized that other downstream reactive species would be increased as well. It has been well established in our lab that H₂O₂ in the presence of ferrous iron can react to form the hydroxyl radical.

Oxidation of lipids by the hydroxyl radical can ultimately form a family of reactive α,β -unsaturated aldehydes capable of covalently modifying proteins through a process termed protein carbonylation. Indeed, Prdx3KD cells showed an increase in free aldehyde levels compared to control. Using mass spectrometry we detected increased free levels of the highly reactive aldehyde, 4-hydroxy-hexanal (4-HHE) in Prdx3KD cells (Fig. 3D). Although free 4-HHE levels were significantly elevated in the Prdx3KD cells, free levels of 4-hydroxy-nonanal (4-HNE) were not changing nor could we detect changes in protein carbonylation using an antibody against 4-HNE (Fig. 3E).

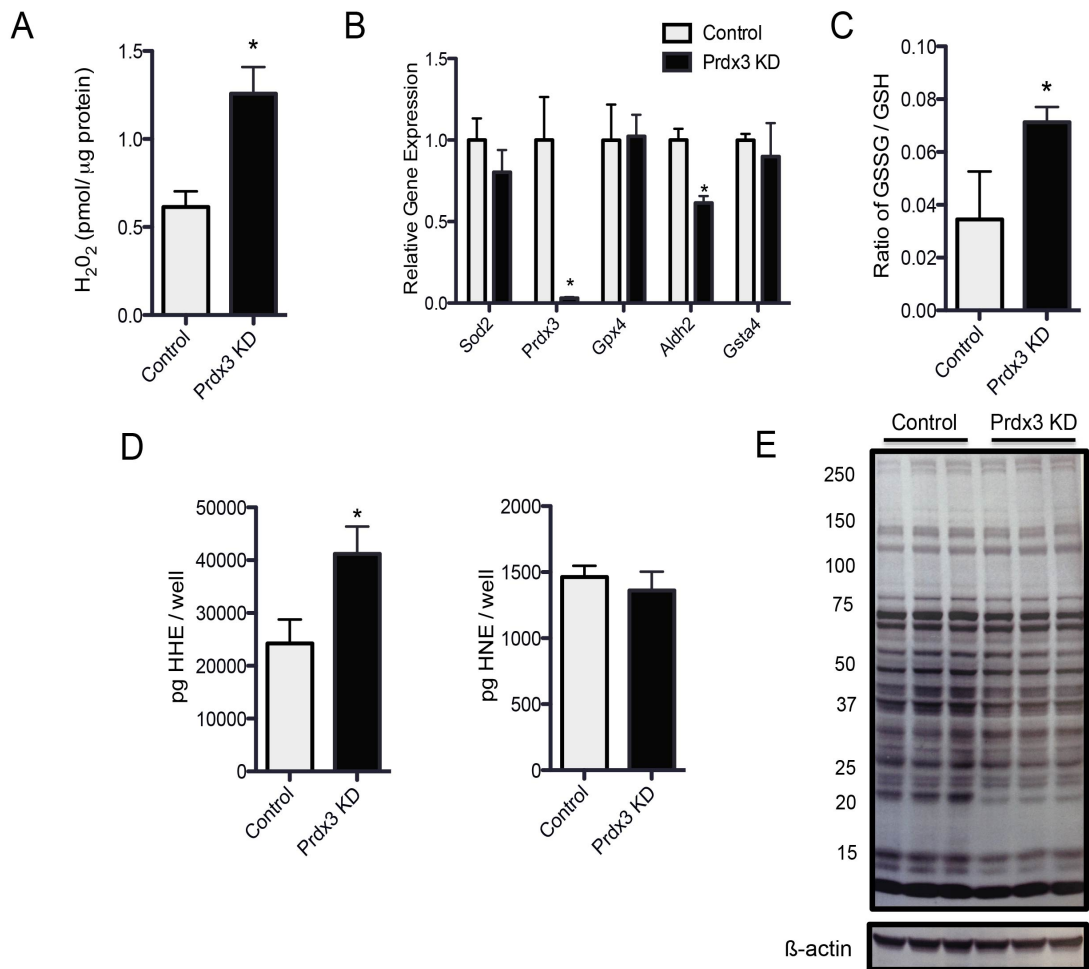


Figure 3 – Oxidative stress in Prdx3 KD adipocytes. A) H_2O_2 levels in Prdx3 KD adipocytes. B) Expression of mitochondrial antioxidants in Prdx3 KD adipocytes. C) Ratio of oxidized and reduced glutathione levels in Prdx3 KD adipocytes. D) Free α,β -unsaturated aldehyde levels and E) carbonylated proteins in Prdx3 KD adipocytes

Prdx3KD results in mitochondrial dysfunction. It is now well accepted that oxidative stress is a precipitating factor contributing to mitochondrial dysfunction. Prdx3 cells exhibit many common defining features of mitochondrial dysfunction. Mitochondrial respiration was assessed in intact, differentiated adipocytes using Seahorse and XF Analyzer. Real time measurements of OCR revealed deficiencies in both maximal respiration and coupled respiration in intact Prdx3KD cells compared to control (Fig. 4A and 4B).

In addition to decreases in coupled and maximal respiration, Prdx3KD cells display an increase in membrane potential as measured using the membrane potential dependent dye tetramethylrodamine methyl ester (TMRM). Accumulation of TMRM in the mitochondria is associated with decreased mitochondrial function and respiration (Fig. 4C). Prdx3KD cells also display an approximately seven-fold increase in lactate secretion into the media compared to control cells. GLUT1 up-regulation is another typical characteristic of cell exposure to oxidative stress. Consistent with this, Prdx3KD cells show a modest increase in intracellular GLUT1 protein expression compared to control cells (Fig. 4E).

Silencing of Prdx3 results in insulin resistance that can be rescued with NAC.

Loss of Prdx3 in 3T3-L1 adipocytes resulted in decreased propagation of the insulin signaling cascade. Western blotting analysis revealed deficiencies in the

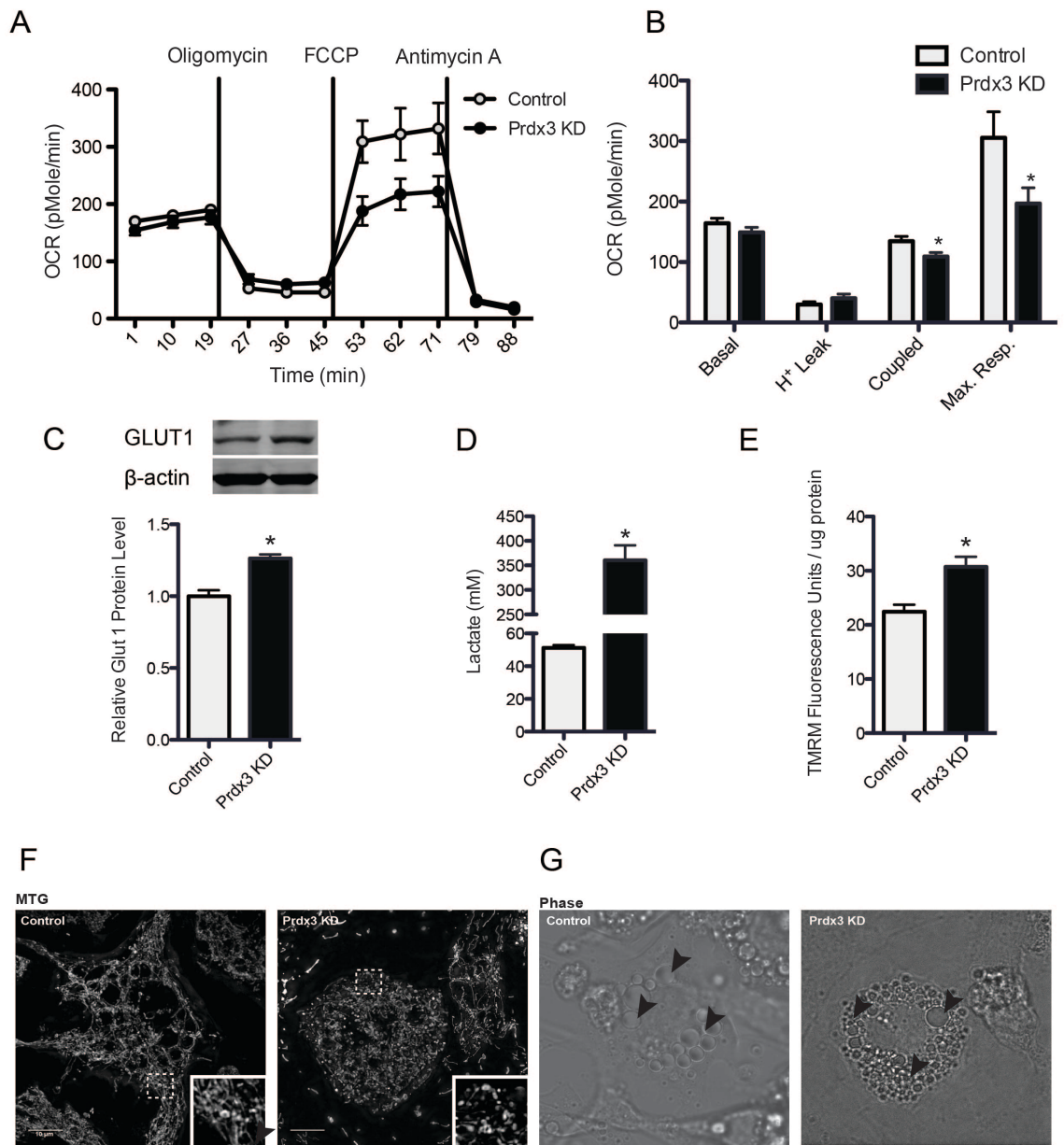


Figure 4 – Mitochondrial function and morphology in Prdx3 KD adipocytes.

A, B) Mitochondrial respiration of control and Prdx3 KD adipocytes as measured by a Seahorse XF24 Analyzer. C) GLUT1 protein expression and D) lactate production in Prdx3 KD adipocytes. E) Mitochondrial membrane potential, F) mitochondrial morphology and G) structure in Prdx3 KD and control adipocytes.

phosphorylation of S473-AKT (Fig 5A and 5C) as well as increased basal and stimulated phosphorylation of S307-IRS1 (Fig 5A and 5B). Prdx3KD cells exhibited a significant decrease in total protein levels of IRS1 under basal and stimulated conditions (Fig 5B). Previous work has shown that phosphorylation of S307-IRS1 can occur as a result of increases in oxidative stress (27). Additionally, because S307-IRS1 targets it for degradation, decreases in total protein levels of IRS1 is expected (27). No significant changes in basal or stimulated T308-AKT phosphorylation were observed. Furthermore, visceral WAT from mice fed a high-fat diet displayed decreased phosphorylation on both S473-AKT and T308-AKT in the basal and insulin stimulated conditions (Fig 5D).

Additionally, insulin stimulated glucose uptake in Prdx3KD cells was also impaired. Prdx3KD cells show impairments in glucose uptake following insulin stimulation (Fig 5F). No changes in basal glucose uptake were seen between cell lines although increases in both Glut1 expression and protein were seen in Prdx3KD cells (Fig 4C). Excitingly, twenty-four hour pretreatment with NAC, a commonly used antioxidant capable of metabolizing oxidants as well as replenishing glutathione pools, showed complete rescue of the glucose uptake in Prdx3KD cells (Fig 5F).

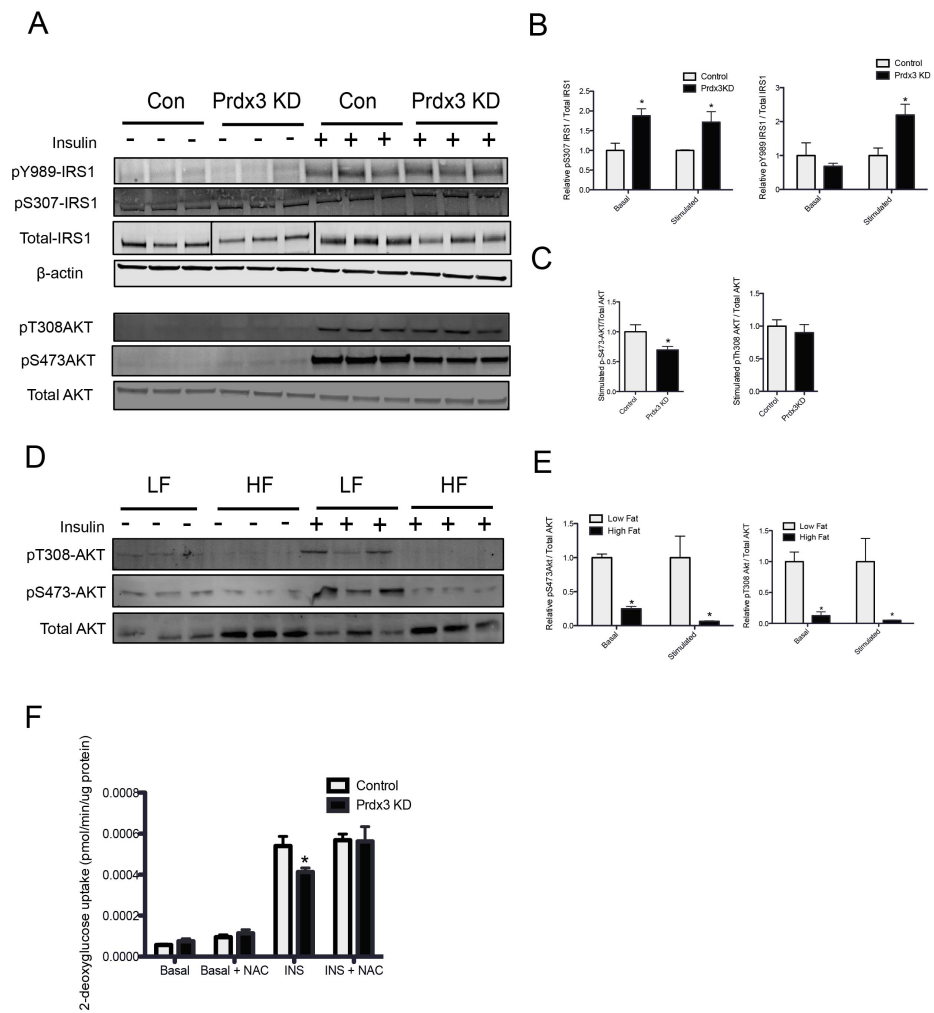


Figure 5 – Decreased insulin signaling in Prdx3 KD adipocytes A) Insulin signaling as measured by IRS and AKT phosphorylation and B) quantitation of western blots in Prdx3 KD and control adipocytes. D) Insulin signaling in epididymal adipose tissue from mice fed a chow or high fat diet with and without insulin stimulation and E) quantitation. F) Insulin stimulated glucose uptake in Prdx3 KD and control adipocytes.

Insulin resistance is not a result of endoplasmic reticulum stress (ER-stress) or the mitochondrial unfolded protein response (mito-UPR). It is well established that mitochondrial dysfunction and ER-stress are two major drivers of insulin resistance in many cell types. Interestingly, although Prdx3KD cells are insulin resistant and display mitochondrial dysfunction, they are occurring independent of ER-stress activation. No changes in the canonical ER-stress markers binding immunoglobulin protein (BIP), phospho-eukaryotic translation factor 2A (eIF2 α), phospho-c-Jun N-terminal kinase (JNK) or adiponectin secretion were noted in KD cells lines compared to control (Fig 6A). Moreover, Prdx3KD cells show no transcriptional activation of activating transcription factor 6 (ATF6), Activating transcription factor 4 (ATF4) and spliced X-box protein 1 (sXBP1), common downstream markers of ER-stress (Fig 6B).

Additionally, although Prdx3KD cells exhibit mitochondrial dysfunction it is not sufficient to induce the mitochondrial unfolded protein response (mito-UPR). Two markers of the mito-UPR, CLP protease (CLPP) and LON protease (LONP) showed no difference in protein levels in KD cells compared to control (Fig 6C and 6D). Together these data suggest that the insulin resistance induced by Prdx3KD is not a result of activation of either ER-stress or the mito-UPR.

Insulin resistance is driven by decreased mTORC2 formation and activity.

Prdx3KD cells show no difference in T308-AKT phosphorylation between cells

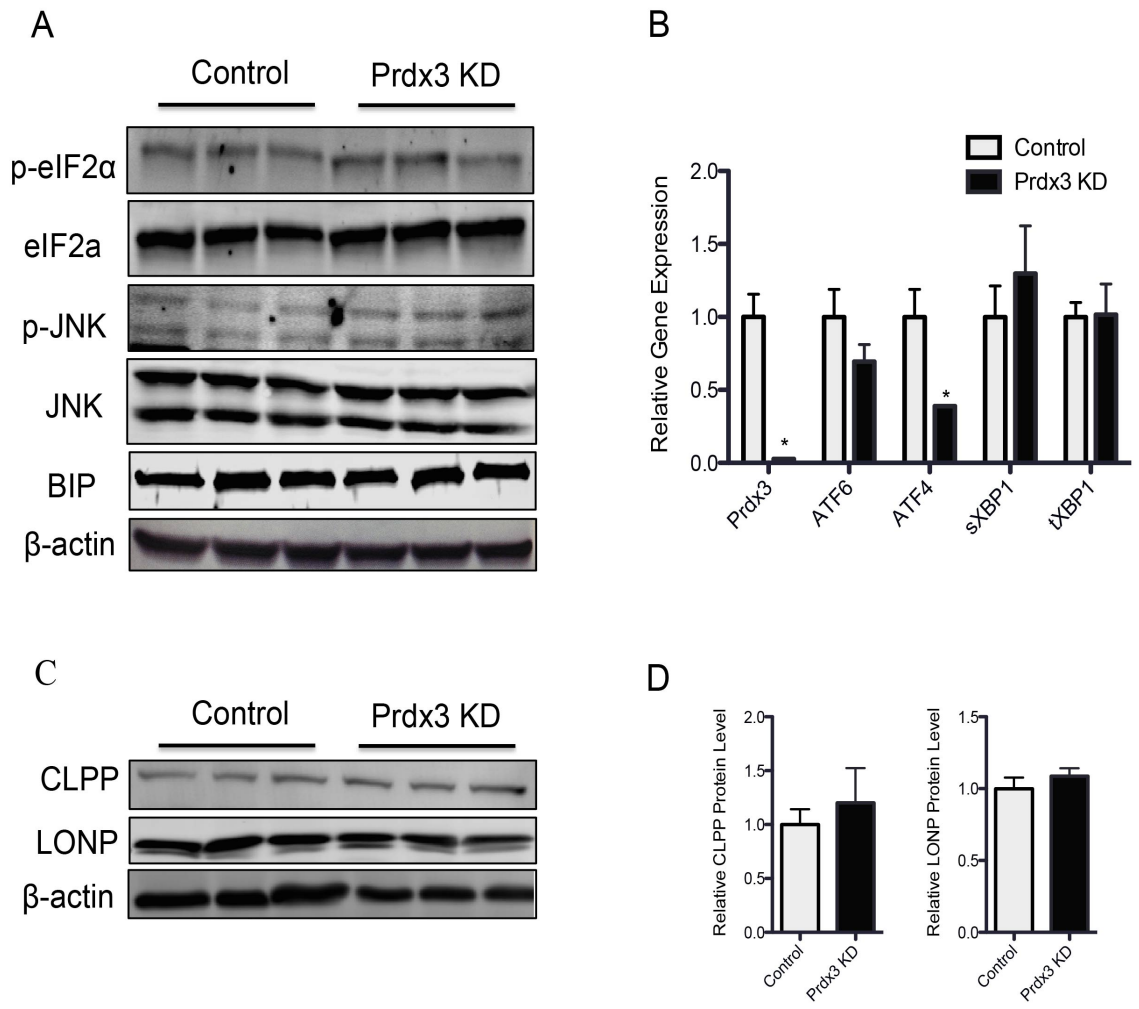


Figure 6 – Prdx3 KD adipocytes do not exhibit ER stress or mtUPR. A) Protein and B) mRNA expression of markers of ER stress in Prdx3 KD and control adipocytes. C) Western blot and D) quantification of protein markers of mtUPR in Prdx3 KD and control adipocytes.

lines, however Prdx3KD cells do show decreases phosphorylation at S473 similar to what is seen in obese, insulin resistant mice. mTORC2 is responsible for phosphorylating AKT at S473. Therefore decreased S473-AKT suggests impaired mTORC2 activity. Previous work performed in liver suggests that mTORC2 stability and complex formation may be sensitive to hydrogen peroxide. Co-immunoprecipitation assays revealed decreased association between two major components of the mTORC2, Rictor and mTOR in both Prdx3KD cells (Fig 7A) as well as in high-fat fed animals (Fig 7C) compared to their respective control. Importantly we found that twenty-four hour pretreatment with NAC was able to rescue complex formation in the Prdx3KD cell lines (Fig 7B) suggesting that increases in ROS was driving insulin resistance by destabilizing mTORC2 formation.

Oxidation of Rictor results in dissociation of mTORC2. Because Prdx3KD cells exhibit increased oxidative stress, we hypothesized that protein oxidation could be one mechanism by which insulin resistance was being induced. Two independent methods to evaluate cysteine oxidation, biotin-switch and dimedone labeling were both used to identify cysteine residues on proteins that have been oxidized to sulfenic acids. Both methods were capable of identifying increases in protein oxidation within the Prdx3KD cell line. Western blotting with an antibody against oxidized proteins labeled with biotin (biotin-switch) revealed an increase in oxidized proteins within the mitochondria in Prdx3KD cells (Fig 7D).

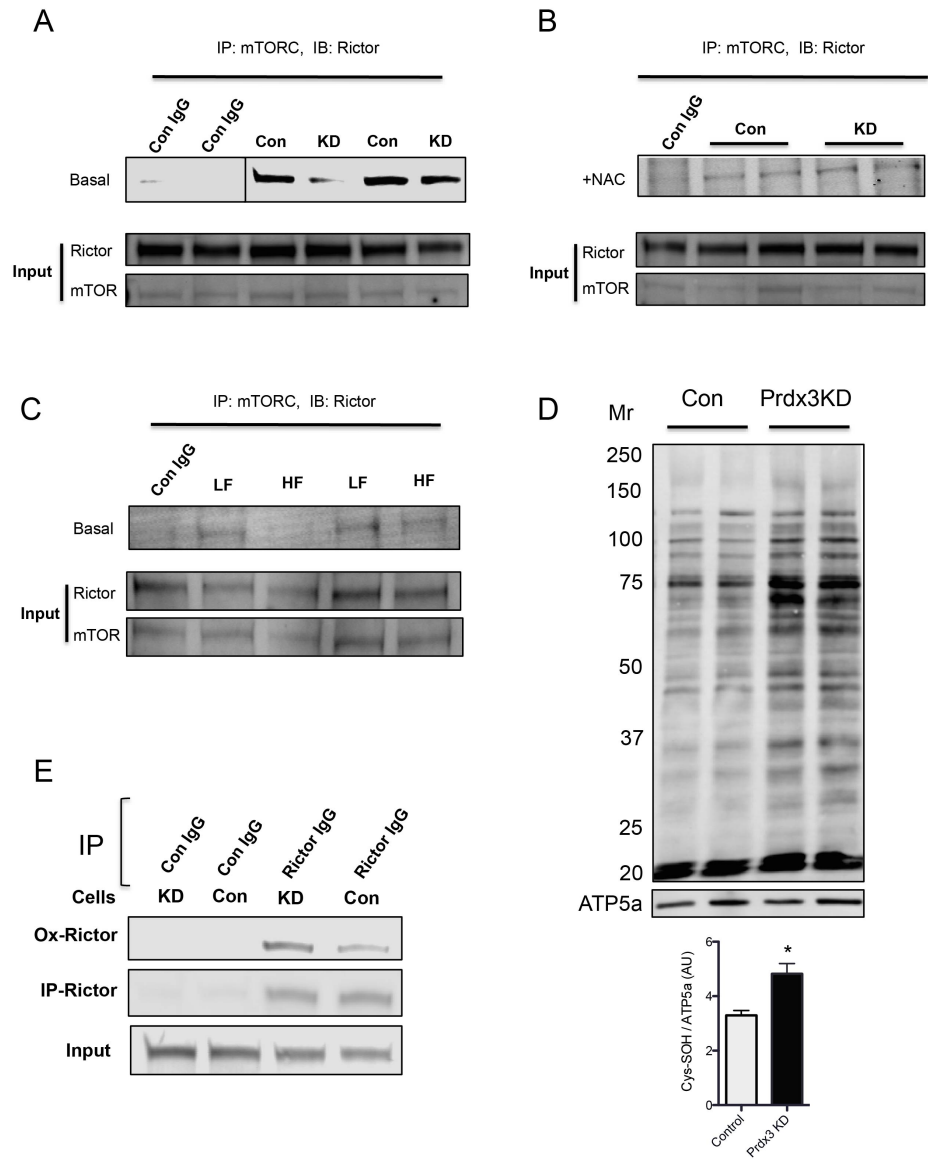


Figure 7 – Prdx3 KD induces protein oxidation and mTORC2 disruption. A) Co-immunoprecipitation of mTOR and Rictor in Prdx3 KD and control adipocytes basally or B) with NAC treatment and C) from mice fed a chow or high-fat diet. D) Mitochondrial cysteine oxidation as measured by biotin-switch in Prdx3 KD and control adipocytes. E) Rictor oxidation in Prdx3 KD and control adipocytes.

Furthermore, detection of oxidized proteins labeled with dimedone in whole cell lysates also confirm an increase in protein oxidation as well in the Prdx3KD cells (data not shown).

Because we hypothesize that oxidation of mTORC2 is responsible for the decrease in complex formation we investigated the oxidation status of rictor, a major subunit, and one thought to be critical in complex formation in mTORC2. Immunoprecipitation of dimidone labeled rictor revealed increased oxidation of rictor in Prdx3KD cells compared to control (Fig 7E). Together these data support the hypothesis that oxidation of rictor results in dissociation and activity of mTORC2 ultimately leading to insulin resistance in Prdx3KD cells.

Discussion

The aim of this work was to evaluate the role of oxidative stress and its contribution to insulin resistance in within adipocytes. Previously, and more comprehensively here, it has been shown that obesity induced insulin resistance results in a mitochondrial specific antioxidant down-regulation (19). More specifically, both high-fat fed mice as well as ob/ob mice, two well-characterized models of obesity induced insulin resistance show a mitochondrial specific, antioxidant, transcriptional down-regulation. Additionally, treatment with either TNF α or DEX, two different cell culture models of insulin resistance in 3T3-L1 adipocytes, mimicked similar down-regulation in mitochondrial antioxidants (Figure 1). One antioxidant that is consistently downregulated in multiple models of insulin resistance in adipocytes is Prdx3 (19). Whole body knockout of Prdx3 results in insulin resistance characterized by decreased glucose tolerance and insulin sensitivity (30). On the other hand, transgenic mice overexpressing Prdx3 are protected from high-fat diet induced decreases in glucose tolerance and insulin sensitivity (24). Importantly, these data not only point to the mitochondria as an important generator of ROS, but also highlight the importance of Prdx3 and its contribution to whole body insulin sensitivity

Because oxidative stress is a hallmark feature of obese, insulin resistant adipose tissue, we were interested in identifying important metabolic pathways that are regulated by oxidative stress, independent of inflammation, within the adipocyte

itself. Knockdown of Prdx3 in adipocytes provides a tool to mechanistically study the effects of mitochondrially generated oxidative stress on adipocyte insulin sensitivity. Importantly our results show that silencing Prdx3 in adipocytes results in increased oxidative stress and insulin resistance mediated by decreased mTORC2 activity and subsequent decreases in S473-AKT phosphorylation.

Differentiated 3T3-L1 adipocytes from Prdx3KD cells have a two-fold increase in intracellular H₂O₂ level (Fig 3A). Additionally, Prdx3KD cells exhibit increased oxidized-to-reduced glutathione levels and increased levels of the basal glucose transporter, GLUT1 (Fig 4C). GLUT1 up-regulation is a hallmark characteristic of exposure to oxidative stress (28, 29). It is known that H₂O₂ is capable of activating transcription factors that function to up-regulate the transcription of stress sensitive genes like GLUT1 (29). Moreover, Prdx3KD cells exhibit deficiencies in mitochondrial function. Whole cell measurements of oxygen consumption revealed deficits in maximal respiration and ATP turnover, two common features of mitochondrial dysfunction (Fig 4A). Together these data provide evidence that Prdx3KD is sufficient to induce oxidative stress and mitochondrial dysfunction within adipocytes that is similar to what is seen in other obesity induced, insulin resistant models.

In addition to mitochondrial dysfunction knockdown of Prdx3 also leads to decreased insulin stimulated glucose uptake as well as impairments in the insulin

signaling cascade (Figure 5). Interestingly, because mitochondrial dysfunction, ER-stress and insulin resistance occur simultaneously in many models of insulin resistance, we hypothesized that Prdx3KD would result in activation of ER-stress as well (30-32). However, we were unable to detect any activation of the canonical ER-stress markers at a transcript or protein level (Figure 6). In addition, we do not see increased cleavage of caspase-3, a commonly used marker of apoptosis (data not shown) nor changes in adiponectin secretion, a marker of both ER-fitness as well as adipocyte function. Together these data suggest that the ER is functioning properly, is not accumulating misfolded proteins and therefore is not eliciting an unfolded protein response. These data also point away from ER-stress and towards aberrations in alternative pathways that could be explain the deficiencies in insulin stimulated glucose uptake seen in the Prdx3KD cells.

Insulin signaling within muscle, adipose and liver has been studied for decades. It is well known that following insulin stimulation, AKT becomes phosphorylated at two distinct sites S473 and T308 (33, 34). PDK1, the kinase responsible for phosphorylating AKT at the T308 site has been extensively studied (35, 36). However, the kinase responsible for phosphorylation at S473 was only recently identified (34). In their landmark paper, Sarbassov *et al.* identified mTORC2 as the complex responsible for phosphorylating AKT at S473.

mTORC2 is a large, cytoplasmic protein complex made up of mTOR, rictor and SIN1 (37). mTOR belongs to a family of protein kinases termed Phosphatidylinositol-3-kinase-related kinases (PIKK) which function by phosphorylating proteins on serine and threonine residues (38). Additionally, rictor and SIN1 both play important roles in maintaining mTORC2 stability and activity (39-41). Although whole body knockouts of rictor, SIN1 or mTOR are embryonic lethal, adipose specific deletion, as well as muscle specific deletion, of rictor is characterized by insulin resistance, hyper-insulinemia, decreased S473-AKT phosphorylation, GLUT4 translocation and glucose uptake (39, 40, 42-46). Together these data point to rictor as a major regulator of mTORC2 activity and ultimately insulin sensitivity itself. Because phosphorylation at S473-AKT, a site required for full activation of AKT and glucose uptake, is decreased in the Prdx3KD cells we hypothesized that mTORC2 activity within these cells was decreased.

Complex formation of mTORC2 plays an important role in maintaining the kinase activity required to phosphorylate S473-AKT. Previous experiments suggest that deletion of either rictor or SIN1 results in decreased mTORC2 activity as a result of decreased complex association (41, 47). Co-immunoprecipitation experiments in Prdx3KD cells revealed decreased association between mTOR and rictor suggesting impaired complex formation (Fig 7A). Importantly, mTORC2 formation can be rescued following a twenty-four hour pretreatment with NAC. NAC is an

antioxidant that is known to decrease oxidative stress by directly metabolizing reactive oxygen species as well as replenishing glutathione levels. Moreover, in Prdx3KD cells NAC is also able to rescue the deficit seen in insulin stimulated glucose uptake (Fig 7B). Rescue of both mTORC2 formation and insulin stimulated glucose uptake in the Prdx3KD cells provides evidence in support of the hypothesis that oxidative stress is driving insulin resistance, at least in part, through decreased mTORC2 formation.

Importantly work from Wang *et al.* reveal similar results showing that hepatic Sirt1 deficiency in mice resulted in increased oxidative stress, insulin resistance and decreased association of mTORC2 within the liver (48). This paper was the first to suggest that increases in ROS production could result in disruption of mTORC2, inhibiting its ability to phosphorylate AKT, thus driving insulin resistance (48). One mechanism by which ROS could lead to disruption of mTORC2 formation is through cysteine oxidation.

Within proteins, cysteine residues make up approximately 2% of amino acid residues (49). Although underrepresented, cysteine residues are many times found within active sites of proteins and their oxidation can render proteins inactive (50). Additionally, it is estimated that 10% of cysteine residues are redox sensitive (2).

Two different methods for detecting cysteine sulfenic acids, biotin-switch and dimedone labeling, revealed increases in protein oxidation within whole cell lysates as well as isolated mitochondria in Prdx3KD cells compared to control (Fig 7D). Both dimedone labeling as well as the biotin-switch method are used to identify cysteine residues on proteins that have been oxidized to sulfenic acids (51-53). Although we can detect changes in protein oxidation by western blot, these methods do not allow for assessment of what specific proteins are being oxidized. Because rictor is known to modulate complex formation of mTORC2 we investigated the possibility that rictor oxidation could be destabilizing mTORC2, decreasing complex formation and its ability to phosphorylate AKT at S473.

Compared to mTOR and SIN1, rictor, with 37 cysteines, contains the highest percentage of cysteine residues, 2.1% compared to 1.4% and 1.7% respectively. Interestingly, amino-acid alignment of rictor between humans and mice revealed that all 37 cysteines are conserved, suggesting evolutionary importance. In 2002, TOR2 components, were identified in budding yeast (54). The TORC2 found in yeast contains proteins, Tor, the mTOR orthologue, Avo1, the SIN1 orthologue, as well as Avo3, the rictor orthologue (54). Sequence analysis within conserved domains of rictor revealed one conserved cysteine residue, C728, between yeast and humans. Although interesting, further experimentation is needed to speculate on the importance of this conserved residue. In the future it will be interesting to determine the cysteine residues on rictor that are oxidized in the

Prdx3KD cells. Additionally, future site directed mutagenesis experiments could potentially reveal important cysteine residues required for either protein-protein interaction or catalytic function of mTORC2.

In summary, our results highlight the importance of Prdx3 in regulating the oxidative stress environment in adipocytes. These data together support a mechanism where increased H₂O₂ levels can drive insulin resistance through destabilization of mTORC2 ultimately resulting in decreased glucose uptake. Furthermore, our studies have identified rictor, a critical component of mTORC2, as one protein that becomes selectively oxidized in the Prdx3KD cells. Although it is unclear at this point, which residues are being oxidized, this observation provides insight into potentially novel molecular mechanism contributing to insulin action.

References

1. Grimsrud, P. A., Picklo, M. J., Griffin, T. J., and Bernlohr, D. A. (2007) Carbonylation of adipose proteins in obesity and insulin resistance: identification of adipocyte fatty acid-binding protein as a cellular target of 4-hydroxynonenal. *Molecular & Cellular Proteomics*. **6**, 624–637
2. Fisher-Wellman, K. H., and Neuffer, P. D. (2012) Linking mitochondrial bioenergetics to insulin resistance via redox biology. *Trends Endocrinol Metab*. **23**, 142–153
3. Xu, H., Barnes, G. T., Yang, Q., Tan, G., Yang, D., Chou, C. J., Sole, J., Nichols, A., Ross, J. S., Tartaglia, L. A., and Chen, H. (2003) Chronic inflammation in fat plays a crucial role in the development of obesity-related insulin resistance. *J. Clin. Invest*. **112**, 1821–1830
4. Monteiro, R., and Azevedo, I. (2010) Chronic inflammation in obesity and the metabolic syndrome. *Mediators of Inflammation*. **2010**, 1–10
5. Peraldi, P., and Spiegelman, B. (1998) TNF-alpha and insulin resistance: summary and future prospects. *Mol. Cell. Biochem*. **182**, 169–175
6. Chen, X.-H., Zhao, Y.-P., Xue, M., Ji, C.-B., Gao, C.-L., Zhu, J.-G., Qin, D.-N., Kou, C.-Z., Qin, X.-H., Tong, M.-L., and Guo, X.-R. (2010) TNF-alpha induces mitochondrial dysfunction in 3T3-L1 adipocytes. *Mol. Cell. Endocrinol*. **328**, 63–69
7. Hahn, W. S., Kuzmicic, J., Burrill, J. S., Donoghue, M. A., Foncea, R., Jensen, M. D., Lavandero, S., Arriaga, E. A., and Bernlohr, D. A. (2014) Proinflammatory cytokines differentially regulate adipocyte mitochondrial metabolism, oxidative stress, and dynamics. *Am. J. Physiol. Endocrinol. Metab*. **306**, E1033–45
8. Petersen, K. F., Befroy, D., Dufour, S., Dziura, J., Ariyan, C., Rothman, D. L., DiPietro, L., Cline, G. W., and Shulman, G. I. (2003) Mitochondrial dysfunction in the elderly: possible role in insulin resistance. *Science*. **300**, 1140–1142
9. Lowell, B. B., and Shulman, G. I. (2005) Mitochondrial dysfunction and type 2 diabetes. *Science*. **307**, 384–387
10. Kusminski, C. M., and Scherer, P. E. (2012) Mitochondrial dysfunction in white adipose tissue. **23**, 435–443
11. Hu, F., and Liu, F. (2011) Mitochondrial stress: A bridge between mitochondrial dysfunction and metabolic diseases? *Cell. Signal*. **23**, 1528–1533
12. Curtis, J. M., Grimsrud, P. A., Wright, W. S., Xu, X., Foncea, R. E., Graham, D. W., Brestoff, J. R., Wiczer, B. M., Ilkayeva, O., Cianflone, K., Muoio, D. E., Arriaga, E. A., and Bernlohr, D. A. (2010) Downregulation of adipose glutathione S-transferase A4 leads to increased protein carbonylation, oxidative stress, and mitochondrial dysfunction. **59**, 1132–1142
13. Raza, H., John, A., and Howarth, F. C. (2015) Increased oxidative stress

- and mitochondrial dysfunction in zucker diabetic rat liver and brain. *Cell. Physiol. Biochem.* **35**, 1241–1251
14. Sena, L. A., and Chandel, N. S. (2012) Physiological roles of mitochondrial reactive oxygen species. *Mol. Cell.* **48**, 158–167
 15. Hertog, den, J., Groen, A., and van der Wijk, T. (2005) Redox regulation of protein-tyrosine phosphatases. *Arch. Biochem. Biophys.* **434**, 11–15
 16. Loh, K., Deng, H., Fukushima, A., Cai, X., Boivin, B., Galic, S., Bruce, C., Shields, B. J., Skiba, B., Ooms, L. M., Stepto, N., Wu, B., Mitchell, C. A., Tonks, N. K., Watt, M. J., Febbraio, M. A., Crack, P. J., Andrikopoulos, S., and Tiganis, T. (2009) Reactive oxygen species enhance insulin sensitivity. *Cell Metab.* **10**, 260–272
 17. Denu, J. M., and Tanner, K. G. (1998) Specific and reversible inactivation of protein tyrosine phosphatases by hydrogen peroxide: evidence for a sulfenic acid intermediate and implications for redox regulation. *Biochemistry.* **37**, 5633–5642
 18. Flint, D. H., Tuminello, J. F., and Emptage, M. H. (1993) The inactivation of Fe-S cluster containing hydro-lyases by superoxide. *Journal of Biological Chemistry.* **268**, 22369–22376
 19. Long, E. K., Olson, D. M., and Bernlohr, D. A. (2013) High-fat diet induces changes in adipose tissue trans-4-oxo-2-nonenal and trans-4-hydroxy-2-nonenal levels in a depot-specific manner. *Free Radical Biology and Medicine.* **63**, 390–398
 20. Knoop, B., Loumaye, E., and Van Der Eecken, V. (2007) Evolution of the peroxiredoxins. *Subcell. Biochem.* **44**, 27–40
 21. Chae, H. Z., Kim, H.-J., Kang, S. W., and Rhee, S. G. (1999) Characterization of three isoforms of mammalian peroxiredoxin that reduce peroxides in the presence of thioredoxin. *Diabetes Res. Clin. Pract.* **45**, 101–112
 22. Bryk, R., Griffin, P., and Nathan, C. (2000) Peroxynitrite reductase activity of bacterial peroxiredoxins. *Nature.* **407**, 211–215
 23. Araki, M., Nanri, H., Ejima, K., Murasato, Y., Fujiwara, T., Nakashima, Y., and Ikeda, M. (1999) Antioxidant Function of the Mitochondrial Protein SP-22 in the Cardiovascular System. *Journal of Biological Chemistry.* **274**, 2271–2278
 24. Chen, L., Na, R., Gu, M., Salmon, A. B., Liu, Y., Liang, H., Qi, W., Van Remmen, H., Richardson, A., and Ran, Q. (2008) Reduction of mitochondrial H₂O₂ by overexpressing peroxiredoxin 3 improves glucose tolerance in mice. *Aging Cell.* **7**, 866–878
 25. Frezza, C., Cipolat, S., and Scorrano, L. (2007) Organelle isolation: functional mitochondria from mouse liver, muscle and cultured fibroblasts. *Nat Protoc.* **2**, 287–295
 26. García-Santamarina, S., Boronat, S., Domènech, A., Ayté, J., Molina, H., and Hidalgo, E. (2014) Monitoring in vivo reversible cysteine oxidation in proteins using ICAT and mass spectrometry. *Nat Protoc.* **9**, 1131–1145

27. Potashnik, R., Bloch-Damti, A., Bashan, N., and Rudich, A. (2003) IRS1 degradation and increased serine phosphorylation cannot predict the degree of metabolic insulin resistance induced by oxidative stress. *Diabetologia*. **46**, 639–48
28. Kozlovsky, N., Rudich, A., Potashnik, R., Ebina, Y., Murakami, T., and Bashan, N. (1997) Transcriptional Activation of the Glut1 Gene in Response to Oxidative Stress in L6 Myotubes. *Journal of Biological Chemistry*. **272**, 33367–33372
29. Emerling, B. M., Platanias, L. C., Black, E., Nebreda, A. R., Davis, R. J., and Chandel, N. S. (2005) Mitochondrial reactive oxygen species activation of p38 mitogen-activated protein kinase is required for hypoxia signaling. *Mol. Cell. Biol.* **25**, 4853–4862
30. Ozcan, U., Cao, Q., Yilmaz, E., Lee, A.-H., Iwakoshi, N. N., Ozdelen, E., Tuncman, G., Görgün, C., Glimcher, L. H., and Hotamisligil, G. S. (2004) Endoplasmic reticulum stress links obesity, insulin action, and type 2 diabetes. *Science*. **306**, 457–461
31. Nakatani, Y., Kaneto, H., Kawamori, D., Yoshiuchi, K., Hatazaki, M., Matsuoka, T. A., Ozawa, K., Ogawa, S., Hori, M., Yamasaki, Y., and Matsuhisa, M. (2004) Involvement of Endoplasmic Reticulum Stress in Insulin Resistance and Diabetes. *Journal of Biological Chemistry*. **280**, 847–851
32. Boden, G., Duan, X., Homko, C., Molina, E. J., Song, W., Perez, O., Cheung, P., and Merali, S. (2008) Increase in endoplasmic reticulum stress-related proteins and genes in adipose tissue of obese, insulin-resistant individuals. *Diabetes*. **57**, 2438–2444
33. Alessi, D. R., James, S. R., Downes, C. P., Holmes, A. B., Gaffney, P. R., Reese, C. B., and Cohen, P. (1997) Characterization of a 3-phosphoinositide-dependent protein kinase which phosphorylates and activates protein kinase Balpha. *Curr. Biol.* **7**, 261–269
34. Sarbassov, D. D., Guertin, D. A., Ali, S. M., and Sabatini, D. M. (2005) Phosphorylation and regulation of Akt/PKB by the rictor-mTOR complex. *Science*. **307**, 1098–1101
35. Stephens, L., Anderson, K., Stokoe, D., Erdjument-Bromage, H., Painter, G. F., Holmes, A. B., Gaffney, P. R., Reese, C. B., McCormick, F., Tempst, P., Coadwell, J., and Hawkins, P. T. (1998) Protein kinase B kinases that mediate phosphatidylinositol 3,4,5-trisphosphate-dependent activation of protein kinase B. *Science*. **279**, 710–714
36. Manning, B. D., and Cantley, L. C. (2007) AKT/PKB signaling: navigating downstream. *Cell*. **129**, 1261–1274
37. Hay, N., and Sonenberg, N. (2004) Upstream and downstream of mTOR. *Genes Dev.* **18**, 1926–1945
38. Keith, C. T., and Schreiber, S. L. (1995) PIK-related kinases: DNA repair, recombination, and cell cycle checkpoints. *Science*. **270**, 50–51
39. Jacinto, E., Facchinetti, V., Liu, D., Soto, N., Wei, S., Jung, S. Y., Huang,

- Q., Qin, J., and Su, B. (2006) SIN1/MIP1 maintains rictor-mTOR complex integrity and regulates Akt phosphorylation and substrate specificity. *Cell*. **127**, 125–137
40. Kumar, A., Lawrence, J. C., Jung, D. Y., Ko, H. J., Keller, S. R., Kim, J. K., Magnuson, M. A., and Harris, T. E. (2010) Fat cell-specific ablation of rictor in mice impairs insulin-regulated fat cell and whole-body glucose and lipid metabolism. *Diabetes*. **59**, 1397–1406
 41. Yang, Q., Inoki, K., Ikenoue, T., and Guan, K.-L. (2006) Identification of Sin1 as an essential TORC2 component required for complex formation and kinase activity. *Genes Dev*. **20**, 2820–2832
 42. Cybulski, N., Zinzalla, V., and Hall, M. N. (2012) Inducible raptor and rictor knockout mouse embryonic fibroblasts. *Methods Mol. Biol.* **821**, 267–278
 43. Guertin, D. A., Stevens, D. M., Thoreen, C. C., Burds, A. A., Kalaany, N. Y., Moffat, J., Brown, M., Fitzgerald, K. J., and Sabatini, D. M. (2006) Ablation in Mice of the mTORC Components raptor, rictor, or mLST8 Reveals that mTORC2 Is Required for Signaling to Akt-FOXO and PKC α , but Not S6K1. *Dev. Cell*. **11**, 859–871
 44. Shiota, C., Woo, J.-T., Lindner, J., Shelton, K. D., and Magnuson, M. A. (2006) Multiallelic disruption of the rictor gene in mice reveals that mTOR complex 2 is essential for fetal growth and viability. *Dev. Cell*. **11**, 583–589
 45. Kumar, A., Harris, T. E., Keller, S. R., Choi, K. M., Magnuson, M. A., and Lawrence, J. C. (2007) Muscle-Specific Deletion of Rictor Impairs Insulin-Stimulated Glucose Transport and Enhances Basal Glycogen Synthase Activity. *Mol. Cell. Biol.* **28**, 61–70
 46. Cybulski, N., Polak, P., Auwerx, J., Ruegg, M. A., and Hall, M. N. (2009) mTOR complex 2 in adipose tissue negatively controls whole-body growth. *Proc. Natl. Acad. Sci. U.S.A.* **106**, 9902–9907
 47. Sarbassov, D. D., Ali, S. M., Kim, D.-H., Guertin, D. A., Latek, R. R., Erdjument-Bromage, H., Tempst, P., and Sabatini, D. M. (2004) Rictor, a novel binding partner of mTOR, defines a rapamycin-insensitive and raptor-independent pathway that regulates the cytoskeleton. *Curr. Biol.* **14**, 1296–1302
 48. Wang, R.-H., Kim, H.-S., Xiao, C., Xu, X., Gavrilova, O., and Deng, C.-X. (2011) Hepatic Sirt1 deficiency in mice impairs mTORC2/Akt signaling and results in hyperglycemia, oxidative damage, and insulin resistance. *J. Clin. Invest.* **121**, 4477–4490
 49. Miseta, A., and Csutora, P. (2000) Relationship between the occurrence of cysteine in proteins and the complexity of organisms. *Mol. Biol. Evol.* **17**, 1232–1239
 50. Imlay, J. A. (2003) Pathways of oxidative damage. *Annu. Rev. Microbiol.* **57**, 395–418
 51. Klomsiri, C., Nelson, K. J., Bechtold, E., Soito, L., Johnson, L. C., Lowther, W. T., Ryu, S.-E., King, S. B., Furdui, C. M., and Poole, L. B. (2010) Use of dimedone-based chemical probes for sulfenic acid detection evaluation of

- conditions affecting probe incorporation into redox-sensitive proteins. *Methods Enzymol.* **473**, 77–94
52. Nelson, K. J., Klomsiri, C., Codreanu, S. G., Soito, L., Liebler, D. C., Rogers, L. C., Daniel, L. W., and Poole, L. B. (2010) Use of dimedone-based chemical probes for sulfenic acid detection methods to visualize and identify labeled proteins. *Methods Enzymol.* **473**, 95–115
 53. Burgoyne, J. R., and Eaton, P. (2010) A rapid approach for the detection, quantification, and discovery of novel sulfenic acid or S-nitrosothiol modified proteins using a biotin-switch method. *Methods Enzymol.* **473**, 281–303
 54. Loewith, R., Jacinto, E., Wullschleger, S., Lorberg, A., Crespo, J. L., Bonenfant, D., Oppliger, W., Jenoe, P., and Hall, M. N. (2002) Two TOR Complexes, Only One of which Is Rapamycin Sensitive, Have Distinct Roles in Cell Growth Control. *Mol. Cell.* **10**, 457–468

CHAPTER FIVE

Perspectives and Conclusions

Joel Burrill wrote this chapter

The rise in the obesity epidemic over the last 50 years is responsible for the massive increase in obesity-related healthcare expenditures that account for more than \$114 billion annually in the United States (1). This represents costs only associated with obesity, not obesity-linked diseases that make up the metabolic syndrome. This rise in obesity is due to the average caloric intake being increased by 20% with no equivalent rise in energy expenditure (2, 3). This results in significant health risks such as cardiovascular disease, hepatic steatosis and type 2 diabetes. Weight loss provides improvements to metabolic health, however many people struggle with maintaining healthy body weights. For these people, one possible option is pharmacologic treatment. In order for effective therapies to be developed, a mechanistic understanding of the pathways behind metabolic syndrome is critical.

Whole body insulin sensitivity relies on coordination among metabolic tissues, such as β -cells, adipose tissue, liver and muscle. The adipocentric model sets forth the idea that adipose tissue biology is central in the development of obesity-linked diabetes. This dissertation has investigated the role of inflammation and oxidative stress in mitochondrial dynamics, metabolism and insulin signaling. The foundations of this work came from the studies on GSTA4 and its role in obesity-linked inflammation and mitochondrial function (4, 5). My research goals were two-fold; to identify how inflammation affects metabolism and mitochondrial function and to identify how mitochondrial ROS lead to the development of insulin

resistance. The hypothesis was that inflammation induced mitochondrial dysfunction resulting in increased oxidative stress and that this oxidative stress resulted in decreased metabolic function and insulin signaling.

The high-fat fed mouse has been ideal to study the adipocentric model of the development of insulin resistance as the visceral fat displays many signs of oxidative stress and is highly inflamed. However, this provides challenges in studying the mechanism behind insulin resistance as there are many compounding signaling pathways all active at once. In order to dissect this model, various 3T3-L1 adipocyte cell models can be used.

TNF α is a pro-inflammatory cytokine within adipose tissue that has been studied for many years. The cytokines IL-6 and IL-1 β , have been studied much less (6). As outlined in chapter two, TNF α and the interleukins, IL-6 and IL-1 β , have distinct effects on the adipocyte and the mitochondria. TNF α induces ROS formation and carbonylation whereas IL-6 and IL-1 β do not (Chapter 2, Fig 3). Furthermore, TNF α uniquely led to mitochondrial fragmentation (Chapter 2, Fig 6). Interestingly, the pro-inflammatory cytokines all led to a decrease in expression of the genes involved in mitochondrial biogenesis (Chapter 2, Fig 5A) and Gsta4 (Burrill data – unpublished). Changes to mitochondrial function, like what was seen with TNF α , perpetuate free radical production.

Obesity decreases the expression of the mitochondrial antioxidants (7). The data presented in Chapter 4, Fig 1 take this a step further and show that TNF α is capable of recapitulating the effect seen in obesity. In order to fully understand the role of oxidative stress in the adipocyte, ROS generation had to be decoupled from inflammation. The Prdx3 KD model is ideal for this type of study as it has increased levels of ROS and oxidative damage (Chapter 4, Fig 3 and 7D). mTORC2 is responsible for phosphorylation of Ser473 of AKT (8). The reduction of insulin signaling seen with obesity and oxidative stress tie directly to mTORC2 activity as phosphorylation levels of Ser473 on AKT are decreased (Chapter 4, Fig 5). This decrease in mTORC2 activity can be attributed to decreased complex formation through the oxidation of Rictor (Chapter 4, Fig 7). This provides a mechanism by which oxidative stress, independent of inflammation, can lead to the development of local adipose insulin resistance.

The role of inflammation obesity in controlling metabolism has been less well characterized for pathways outside of oxidative phosphorylation, such as BCAA metabolism. Circulating BCAAs are the best predictive biomarker of development of T2D, even preceding whole body insulin resistance (9). Adipose tissue has recently been identified as a major contributor to BCAA metabolism (10). Furthermore, the BCAA metabolism pathway is highly carbonylated in models of oxidative stress (5). The data presented in Chapter 3 show the role of inflammation in inhibiting BCAA metabolism in the adipocyte. This suggests that

during the development of obesity, BCAA uptake and metabolism in visceral adipose tissue is decreased due to the infiltration of macrophages. This reduction in uptake and metabolism could be responsible for the increase in circulating BCAAs observed with obesity and insulin resistance.

There are several interesting directions in which future work could proceed. Much has been studied about the role of carbonylation in the development of mitochondrial dysfunction, however direct protein oxidation has not been as highly characterized. As identified in Chapter 4, Rictor is oxidized leading to disrupted mTORC2 formation and decreased signaling. However, the site of oxidation is still unknown. To investigate this further, mass spectrometry can be used to identify the specific cysteine residues that are modified. Once the site of modification is identified, specific cysteine mutants can be made and re-expressed into 3T3-L1 cells to analyze its role in controlling mTORC2 function.

Additionally, there is a clear rise in protein oxidation with increases in oxidative stress (Chapter 4, Fig 7). The role of this modification has not been extensively studied. Using a labeling approach with sulfenic acid reactive probes, immunoprecipitation is possible for enrichment of those proteins and/or peptides that are oxidized. Subsequent mass spectrometry should allow for potential identification of redox sensitive proteins that play a role in central metabolic

processes. This identification could provide new targets for investigation for how oxidative stress induces insulin resistance.

BCAA metabolism is a critical mitochondrial metabolism pathway that provides a distinct biomarker of visceral adipose tissue dysfunction when altered in a whole-body context. This work investigated the role of inflammation in controlling BCAA uptake and metabolism in the adipocyte. However, further studies on the role of carbonylation in controlling this metabolic process could identify mechanisms of how inflammation and oxidative stress directly modulate metabolic pathways.

The culmination of this work portrays inflammation as a modulator of metabolism and oxidative stress as a cause of insulin resistance. The increased ROS production observed with TNF α is responsible for the increased oxidative damage observed with obesity. The increased oxidative stress leads to decreased mTORC2 formation and reduced S473 phosphorylation on AKT, and decreased insulin sensitivity. These studies for the first time have shown how inflammation causes insulin resistance through an oxidative stress-dependent mechanism.

References

1. Tsai, A. G., Williamson, D. F., and Glick, H. A. (2010) Direct medical cost of overweight and obesity in the USA: a quantitative systematic review. **12**, 50–61
2. Variyam, J. N. (2002) Patterns of Caloric Intake and Body Mass Index Among U.S. Adults. *FoodReview*. **25**, 16–20
3. Ogden, C. L., Carroll, M. D., Curtin, L. R., McDowell, M. A., Tabak, C. J., and Flegal, K. M. (2006) Prevalence of overweight and obesity in the United States, 1999-2004. *JAMA*. **295**, 1549–1555
4. Curtis, J. M., Grimsrud, P. A., Wright, W. S., Xu, X., Foncea, R. E., Graham, D. W., Brestoff, J. R., Wiczer, B. M., Ilkayeva, O., Cianflone, K., Muoio, D. E., Arriaga, E. A., and Bernlohr, D. A. (2010) Downregulation of adipose glutathione S-transferase A4 leads to increased protein carbonylation, oxidative stress, and mitochondrial dysfunction. *Diabetes*. **59**, 1132–1142
5. Curtis, J. M., Hahn, W. S., Stone, M. D., Inda, J. J., Drouillard, D. J., Kuzmich, J. P., Donoghue, M. A., Long, E. K., Armien, A. G., Lavandero, S., Arriaga, E., Griffin, T. J., and Bernlohr, D. A. (2012) Protein carbonylation and adipocyte mitochondrial function. *J. Biol. Chem*. **287**, 32967–32980
6. Hotamisligil, G. S., Shargill, N. S., and Spiegelman, B. M. (1993) Adipose expression of tumor necrosis factor- α : direct role in obesity-linked insulin resistance. *Science*. **259**, 87–91
7. Long, E. K., Olson, D. M., and Bernlohr, D. A. (2013) High-fat diet induces changes in adipose tissue trans-4-oxo-2-nonenal and trans-4-hydroxy-2-nonenal levels in a depot-specific manner. *Free Radical Biology and Medicine*. **63**, 390–398
8. Sarbassov, D. D., Guertin, D. A., Ali, S. M., and Sabatini, D. M. (2005) Phosphorylation and regulation of Akt/PKB by the rictor-mTOR complex. *Science*. **307**, 1098–1101
9. Wang, T. J., Larson, M. G., Vasan, R. S., Cheng, S., Rhee, E. P., McCabe, E., Lewis, G. D., Fox, C. S., Jacques, P. F., Fernandez, C., O'Donnell, C. J., Carr, S. A., Mootha, V. K., Florez, J. C., Souza, A., Melander, O., Clish, C. B., and Gerszten, R. E. (2011) Metabolite profiles and the risk of developing diabetes. *Nat. Med*. **17**, 448–453
10. Herman, M. A., She, P., Peroni, O. D., Lynch, C. J., and Kahn, B. B. (2010) Adipose tissue branched chain amino acid (BCAA) metabolism modulates circulating BCAA levels. *J. Biol. Chem*. **285**, 11348–11356

Complete Bibliography

- Abel ED, Peroni O, Kim JK, Kim Y-B, Boss O, Hadro E, et al. Adipose-selective targeting of the GLUT4 gene impairs insulin action in muscle and liver. *Nature*. Nature Publishing Group; 2001 Feb 8;409(6821):729–33.
- Adam-Vizi V. Production of reactive oxygen species in brain mitochondria: contribution by electron transport chain and non-electron transport chain sources. *Antioxid. Redox Signal.* Mary Ann Liebert, Inc. 2 Madison Avenue Larchmont, NY 10538 USA; 2005 Sep;7(9-10):1140–9.
- Ahmadian M, E Duncan R, Jaworski K, Sarkadi-Nagy E, Sul HS. Triacylglycerol metabolism in adipose tissue. *Future Lipidol.* 2007 Apr;2(2):229–37.
- Ahn B-H, Kim H-S, Song S, Lee IH, Liu J, Vassilopoulos A, et al. A role for the mitochondrial deacetylase Sirt3 in regulating energy homeostasis. *Proc. Natl. Acad. Sci. U.S.A.* 2008 Sep 23;105(38):14447–52. PMID: PMC2567183
- Alessi DR, James SR, Downes CP, Holmes AB, Gaffney PRJ, Reese CB, et al. Characterization of a 3-phosphoinositide-dependent protein kinase which phosphorylates and activates protein kinase B α . *Curr. Biol.* Elsevier; 1997 Apr;7(4):261–9.
- Alkhoury N, Gornicka A, Berk MP, Thapaliya S, Dixon LJ, Kashyap S, et al. Adipocyte apoptosis, a link between obesity, insulin resistance, and hepatic steatosis. *J. Biol. Chem.* American Society for Biochemistry and Molecular Biology; 2010 Jan 29;285(5):3428–38. PMID: PMC2823448
- Anderson EJ, Lustig ME, Boyle KE, Woodlief TL, Kane DA, Lin C-T, et al. Mitochondrial H₂O₂ emission and cellular redox state link excess fat intake to insulin resistance in both rodents and humans. *J. Clin. Invest.* 2009 Mar;119(3):573–81. PMID: PMC2648700
- Araki M, Nanri H, Ejima K, Murasato Y, Fujiwara T, Nakashima Y, et al. Antioxidant Function of the Mitochondrial Protein SP-22 in the Cardiovascular System. *Journal of Biological Chemistry.* American Society for Biochemistry and Molecular Biology; 1999 Jan 22;274(4):2271–8.
- Arkan MC, Hevener AL, Greten FR, Maeda S, Li Z-W, Long JM, et al. IKK- β links inflammation to obesity-induced insulin resistance. *Nat. Med.* Nature Publishing Group; 2005 Jan 30;11(2):191–8.
- Baregamian N, Song J, Bailey CE, Papaconstantinou J, Evers BM, Chung DH. Tumor Necrosis Factor- α and Apoptosis Signal-Regulating Kinase 1 Control Reactive Oxygen Species Release, Mitochondrial Autophagy and C-Jun N-

- Terminal Kinase/P38 Phosphorylation During Necrotizing Enterocolitis. *Oxid Med Cell Longev*. 2009;2(5):297–306.
- Baricault L, Ségui B, Guégand L, Olichon A, Valette A, Larminat F, et al. OPA1 cleavage depends on decreased mitochondrial ATP level and bivalent metals. *Exp. Cell Res*. 2007 Oct 15;313(17):3800–8.
- Barzilai A, Yamamoto K-I. DNA damage responses to oxidative stress. *DNA Repair (Amst.)*. 2004 Aug;3(8-9):1109–15.
- Batch BC, Shah SH, Newgard CB, Turer CB, Haynes C, Bain JR, et al. Branched chain amino acids are novel biomarkers for discrimination of metabolic wellness. *Metab. Clin. Exp*. 2013 Jul;62(7):961–9. PMID: PMC3691289
- Blachnio-Zabielska AU, Koutsari C, Tchkonja T, Jensen MD. Sphingolipid content of human adipose tissue: relationship to adiponectin and insulin resistance. *Obesity (Silver Spring)*. Blackwell Publishing Ltd; 2012a Dec;20(12):2341–7. PMID: PMC3443533
- Blachnio-Zabielska AU, Persson X-MT, Koutsari C, Zabielski P, Jensen MD. A liquid chromatography/tandem mass spectrometry method for measuring the in vivo incorporation of plasma free fatty acids into intramyocellular ceramides in humans. *Rapid Commun. Mass Spectrom*. John Wiley & Sons, Ltd; 2012b May 15;26(9):1134–40. PMID: PMC3370409
- Boden G, Duan X, Homko C, Molina EJ, Song W, Perez O, et al. Increase in endoplasmic reticulum stress-related proteins and genes in adipose tissue of obese, insulin-resistant individuals. *Diabetes*. American Diabetes Association; 2008 Sep;57(9):2438–44. PMID: PMC2518495
- Brand MD. The sites and topology of mitochondrial superoxide production. *Exp. Gerontol*. 2010 Aug;45(7-8):466–72.
- Brand MD, Nicholls DG. Assessing mitochondrial dysfunction in cells. *Biochem. J*. 3rd ed. 2011 Apr 15;435(2):297–312. PMID: PMC3076726
- Brandt C, Jakobsen AH, Adser H, Olesen J, Iversen N, Kristensen JM, et al. IL-6 regulates exercise and training-induced adaptations in subcutaneous adipose tissue in mice. *Acta Physiol (Oxf)*. Blackwell Publishing Ltd; 2012 Jun;205(2):224–35.
- Bremer AA, Jialal I. Adipose tissue dysfunction in nascent metabolic syndrome. *J Obes*. Hindawi Publishing Corporation; 2013;2013(19):393192–8. PMID: PMC3638696
- Breuleux M, Klopfenstein M, Stephan C, Doughty CA, Barys L, Maira SM, et al.

Increased AKT S473 phosphorylation after mTORC1 inhibition is rictor dependent and does not predict tumor cell response to PI3K/mTOR inhibition. *Mol. Cancer Ther.* American Association for Cancer Research; 2009 Apr 1;8(4):742–53.

Bruns CM, Hubatsch I, Ridderström M, Mannervik B, Tainer JA. Human glutathione transferase A4-4 crystal structures and mutagenesis reveal the basis of high catalytic efficiency with toxic lipid peroxidation products. *J. Mol. Biol.* 1999 May 7;288(3):427–39.

Bryk R, Griffin P, Nathan C. Peroxynitrite reductase activity of bacterial peroxiredoxins. *Nature.* Nature Publishing Group; 2000 Sep 14;407(6801):211–5.

Byerly MS, Swanson R, Wei Z, Seldin MM, McCulloh PS, Wong GW. A central role for C1q/TNF-related protein 13 (CTRP13) in modulating food intake and body weight. Smith W, editor. *PLoS ONE.* Public Library of Science; 2013;8(4):e62862. PMID: PMC3636217

Cabal-Hierro L, Lazo PS. Signal transduction by tumor necrosis factor receptors. *Cell. Signal.* 2012 Jun;24(6):1297–305.

Calvo SE, Mootha VK. The Mitochondrial Proteome and Human Disease. *Annu Rev Genomics Hum Genet.* Annual Reviews; 2010 Sep;11(1):25–44.

Carmean CM, Cohen RN, Brady MJ. Systemic regulation of adipose metabolism. *Biochim. Biophys. Acta.* 2014 Mar;1842(3):424–30.

Cecchini G. FUNCTION AND STRUCTURE OF COMPLEXES OF THE RESPIRATORY CHAIN*. *Annu. Rev. Biochem.* Annual Reviews 4139 El Camino Way, P.O. Box 10139, Palo Alto, CA 94303-0139, USA; 2003 Jun;72(1):77–109.

Chae HZ, Kim H-J, Kang SW, Rhee SG. Characterization of three isoforms of mammalian peroxiredoxin that reduce peroxides in the presence of thioredoxin. *Diabetes Res. Clin. Pract.* 1999 Sep;45(2-3):101–12.

Chawla A, Nguyen KD, Goh YPS. Macrophage-mediated inflammation in metabolic disease. *Nat. Rev. Immunol.* 2011 Nov;11(11):738–49. PMID: PMC3383854

Chen L, Na R, Gu M, Salmon AB, Liu Y, Liang H, et al. Reduction of mitochondrial H₂O₂ by overexpressing peroxiredoxin 3 improves glucose tolerance in mice. *Aging Cell.* 2008 Dec;7(6):866–78.

Chen X-H, Zhao Y-P, Xue M, Ji C-B, Gao C-L, Zhu J-G, et al. TNF- α induces

- mitochondrial dysfunction in 3T3-L1 adipocytes. *Mol. Cell. Endocrinol.* 2010 Oct 26;328(1-2):63–9.
- Chen Y, Dorn GW. PINK1-Phosphorylated Mitofusin 2 Is a Parkin Receptor for Culling Damaged Mitochondria. *Science.* 2013 Apr 25;340(6131):471–5.
- Cheng Z, Tseng Y, White MF. Insulin signaling meets mitochondria in metabolism. *Trends Endocrinol Metab.* Elsevier; 2010 Oct;21(10):589–98. PMID: PMC3994704
- Chi H, Flavell RA. Cutting edge: regulation of T cell trafficking and primary immune responses by sphingosine 1-phosphate receptor 1. *J. Immunol.* 2005 Mar 1;174(5):2485–8.
- Cho S-H, Lee C-H, Ahn Y, Kim H, Kim H, Ahn C-Y, et al. Redox regulation of PTEN and protein tyrosine phosphatases in H₂O₂ mediated cell signaling. *FEBS Letters.* Elsevier; 2004 Mar 17;560(1-3):7–13–13.
- Choi SM, Tucker DF, Gross DN, Easton RM, DiPilato LM, Dean AS, et al. Insulin Regulates Adipocyte Lipolysis via an Akt-Independent Signaling Pathway. *Mol. Cell. Biol.* American Society for Microbiology; 2010 Oct 11;30(21):5009–20.
- Cildir G, Akıncılar SC, Tergaonkar V. Chronic adipose tissue inflammation: all immune cells on the stage. *Trends in Molecular Medicine.* 2013 Aug;19(8):487–500.
- Crofts AR, Berry EA. Structure and function of the cytochrome bc₁ complex of mitochondria and photosynthetic bacteria. *Curr. Opin. Struct. Biol.* 1998 Sep 8;8(4):501–9.
- Cunningham JT, Rodgers JT, Arlow DH, Vazquez F, Mootha VK, Puigserver P. mTOR controls mitochondrial oxidative function through a YY1-PGC-1 α transcriptional complex. *Nature.* 2007 Nov 29;450(7170):736–40.
- Curtis JM, Grimsrud PA, Wright WS, Xu X, Foncea RE, Graham DW, et al. Downregulation of adipose glutathione S-transferase A4 leads to increased protein carbonylation, oxidative stress, and mitochondrial dysfunction. 2010 May;59(5):1132–42. PMID: PMC2857893
- Curtis JM, Hahn WS, Long EK, Burrill JS, Arriaga EA, Bernlohr DA. Protein carbonylation and metabolic control systems. *Trends Endocrinol Metab.* 2012a Aug;23(8):399–406. PMID: PMC3408802
- Curtis JM, Hahn WS, Stone MD, Inda JJ, Drouillard DJ, Kuzmicic JP, et al. Protein carbonylation and adipocyte mitochondrial function. *J. Biol. Chem.*

2012b Sep 21;287(39):32967–80. PMID: PMC3463318

Cybulski N, Polak P, Auwerx J, Ruegg MA, Hall MN. mTOR complex 2 in adipose tissue negatively controls whole-body growth. *Proc. Natl. Acad. Sci. U.S.A.* 2009 Jun 16;106(24):9902–7. PMID: PMC2700987

Cybulski N, Zinzalla V, Hall MN. Inducible raptor and rictor knockout mouse embryonic fibroblasts. *Methods Mol. Biol.* Totowa, NJ: Humana Press; 2012;821(Chapter 16):267–78.

Dashty M. A quick look at biochemistry: Carbohydrate metabolism. *Clin. Biochem.* 2013 Oct;46(15):1339–52.

DeFronzo RA. Lilly lecture 1987. The triumvirate: beta-cell, muscle, liver. A collusion responsible for NIDDM. *Diabetes.* 1988 Jun;37(6):667–87.

Deng Y, Scherer PE. Adipokines as novel biomarkers and regulators of the metabolic syndrome. *Ann. N. Y. Acad. Sci.* Blackwell Publishing Inc; 2010 Nov;1212(1):E1–E19. PMID: PMC3075414

Denu JM, Tanner KG. Specific and reversible inactivation of protein tyrosine phosphatases by hydrogen peroxide: evidence for a sulfenic acid intermediate and implications for redox regulation. *Biochemistry.* American Chemical Society; 1998 Apr 21;37(16):5633–42.

Dominy JE, Puigserver P. Mitochondrial Biogenesis through Activation of Nuclear Signaling Proteins. *Cold Spring Harb Perspect Biol.* 2013 Jul 1;5(7):a015008–8.

Emerling BM, Plataniias LC, Black E, Nebreda AR, Davis RJ, Chandel NS. Mitochondrial reactive oxygen species activation of p38 mitogen-activated protein kinase is required for hypoxia signaling. *Mol. Cell. Biol.* American Society for Microbiology; 2005 Jun;25(12):4853–62. PMID: PMC1140591

Engle MR, Singh SP, Czernik PJ, Gaddy D, Montague DC, Ceci JD, et al. Physiological role of mGSTA4-4, a glutathione S-transferase metabolizing 4-hydroxynonenal: generation and analysis of mGsta4 null mouse. *Toxicol. Appl. Pharmacol.* 2004 Feb 1;194(3):296–308.

Esser N, Legrand-Poels S, Piette J, Scheen AJ, Paquot N. Inflammation as a link between obesity, metabolic syndrome and type 2 diabetes. *Diabetes Res. Clin. Pract.* Elsevier; 2014 Aug;105(2):141–50.

Esterbauer H, Zollner H, Schaur RJ. Aldehydes Formed by Lipid Peroxidation: Mechanisms of Formation, Occurrence and Determination. Vigo-Pelfrey C, editor. *Membrane Lipid Oxidation.* Boca Raton, Florida; 1990. p. 239–68.

- Evans MD, Dizdaroglu M, Cooke MS. Oxidative DNA damage and disease: induction, repair and significance. *Mutation Research/Reviews in Mutation Research*. 2004 Sep;567(1):1–61.
- Fernández-Sánchez A, Madrigal-Santillán E, Bautista M, Esquivel-Soto J, Morales-González A, Esquivel-Chirino C, et al. Inflammation, oxidative stress, and obesity. *Int J Mol Sci. Molecular Diversity Preservation International*; 2011;12(5):3117–32. PMID: PMC3116179
- Finkel T. Signal transduction by reactive oxygen species. *J. Cell Biol. Rockefeller University Press*; 2011 Jul 13;194(1):7–15–15.
- Flint DH, Tuminello JF, Emptage MH. The inactivation of Fe-S cluster containing hydro-lyases by superoxide. *Journal of Biological Chemistry*. 1993 Oct 25;268(30):22369–76.
- Ford ES, Li C, Sattar N. Metabolic Syndrome and Incident Diabetes: Current state of the evidence. *American Diabetes Association*; 2008 Aug 27;31(9):1898–904.
- Fotiadis D, Kanai Y, Palacín M. The SLC3 and SLC7 families of amino acid transporters. *Mol. Aspects Med*. 2013 Apr;34(2-3):139–58.
- Frame S, Cohen P. GSK3 takes centre stage more than 20 years after its discovery. *Biochem. J*. 2001 Sep 21;359(Pt 1):1–16.
- Frezza C, Cipolat S, Scorrano L. Organelle isolation: functional mitochondria from mouse liver, muscle and cultured fibroblasts. *Nat Protoc*. 2007;2(2):287–95.
- Fridovich I. Superoxide Radical and Superoxide Dismutases. *Annu. Rev. Biochem. Annual Reviews* 4139 El Camino Way, P.O. Box 10139, Palo Alto, CA 94303-0139, USA; 1995 Jun;64(1):97–112.
- Frohnert BI, Long EK, Hahn WS, Bernlohr DA. Glutathionylated lipid aldehydes are products of adipocyte oxidative stress and activators of macrophage inflammation. *Diabetes. American Diabetes Association*; 2014 Jan;63(1):89–100. PMID: PMC3868039
- Frohnert BI, Sinaiko AR, Serrot FJ, Foncea RE, Moran A, Ikramuddin S, et al. Increased adipose protein carbonylation in human obesity. *Obesity*. 2011 Sep;19(9):1735–41.
- Fuchs BC, Bode BP. Amino acid transporters ASCT2 and LAT1 in cancer: partners in crime? *Semin. Cancer Biol*. 2005 Aug;15(4):254–66.

- Furukawa S, Fujita T, Shimabukuro M, Iwaki M, Yamada Y, Nakajima Y, et al. Increased oxidative stress in obesity and its impact on metabolic syndrome. *J. Clin. Invest.* 2004 Dec;114(12):1752–61. PMID: PMC535065
- Gaidhu MP, Anthony NM, Patel P, Hawke TJ, Ceddia RB. Dysregulation of lipolysis and lipid metabolism in visceral and subcutaneous adipocytes by high-fat diet: role of ATGL, HSL, and AMPK. *Am. J. Physiol., Cell Physiol.* 2010 Apr;298(4):C961–71.
- Galic S, Oakhill JS, Steinberg GR. Adipose tissue as an endocrine organ. *Mol. Cell. Endocrinol.* 2010 Mar 25;316(2):129–39.
- Ganesan V, Perera MN, Colombini D, Datskovskiy D, Chadha K, Colombini M. Ceramide and activated Bax act synergistically to permeabilize the mitochondrial outer membrane. *Apoptosis.* Springer US; 2010 May;15(5):553–62.
- Gregor MF, Hotamisligil GS. Inflammatory mechanisms in obesity. *Annu. Rev. Immunol. Annual Reviews;* 2011;29(1):415–45.
- Grimsrud PA, Picklo MJ, Griffin TJ, Bernlohr DA. Carbonylation of adipose proteins in obesity and insulin resistance: identification of adipocyte fatty acid-binding protein as a cellular target of 4-hydroxynonenal. *Molecular & Cellular Proteomics.* American Society for Biochemistry and Molecular Biology; 2007 Apr;6(4):624–37.
- Griparic L, Kanazawa T, van der Blik AM. Regulation of the mitochondrial dynamin-like protein Opa1 by proteolytic cleavage. *J. Cell Biol. Rockefeller Univ Press;* 2007 Aug 27;178(5):757–64. PMID: PMC2064541
- Guertin DA, Stevens DM, Thoreen CC, Burds AA, Kalaany NY, Moffat J, et al. Ablation in Mice of the mTORC Components raptor, rictor, or mLST8 Reveals that mTORC2 Is Required for Signaling to Akt-FOXO and PKC α , but Not S6K1. *Dev. Cell. Elsevier;* 2006 Dec;11(6):859–71.
- Guilherme A, Virbasius JV, Puri V, Czech MP. Adipocyte dysfunctions linking obesity to insulin resistance and type 2 diabetes. *Nat. Rev. Mol. Cell Biol.* 2008 May;9(5):367–77. PMID: PMC2886982
- Guo S. Insulin signaling, resistance, and the metabolic syndrome: insights from mouse models into disease mechanisms. *J. Endocrinol. BioScientifica;* 2014 Jan 8;220(2):T1–T23.
- Hahn WS, Kuzmicic J, Burrill JS, Donoghue MA, Foncea R, Jensen MD, et al. Proinflammatory cytokines differentially regulate adipocyte mitochondrial metabolism, oxidative stress, and dynamics. *Am. J. Physiol. Endocrinol.*

- Metab. 2014 May 1;306(9):E1033–45. PMID: PMC4010657
- Hamanaka RB, Chandel NS. Mitochondrial reactive oxygen species regulate cellular signaling and dictate biological outcomes. *Trends Biochem. Sci.* Elsevier; 2010 Sep;35(9):505–13.
- Hamman RF, Wing RR, Edelstein SL, Lachin JM, Bray GA, Delahanty L, et al. Effect of Weight Loss With Lifestyle Intervention on Risk of Diabetes. *American Diabetes Association*; 2006 Aug 25;29(9):2102–7.
- Harris TE, Lawrence JC. TOR Signaling. *Sci Signal. Science Signaling*; 2003 Dec 9;2003(212):re15–5.
- Hay N, Sonenberg N. Upstream and downstream of mTOR. *Genes Dev.* 2004 Aug 15;18(16):1926–45.
- Herman MA, She P, Peroni OD, Lynch CJ, Kahn BB. Adipose tissue branched chain amino acid (BCAA) metabolism modulates circulating BCAA levels. *J. Biol. Chem.* 2010 Apr 9;285(15):11348–56. PMID: PMC2857013
- Herold C, Rennekampff HO, Engeli S. Apoptotic pathways in adipose tissue. *Apoptosis.* Springer US; 2013 Aug;18(8):911–6.
- Hofmann C, Lorenz K, Braithwaite SS, Colca JR, Palazuk BJ, Hotamisligil GS, et al. Altered gene expression for tumor necrosis factor-alpha and its receptors during drug and dietary modulation of insulin resistance. *Endocrinology.* 1994 Jan;134(1):264–70.
- Holland WL, Brozinick JT, Wang L-P, Hawkins ED, Sargent KM, Liu Y, et al. Inhibition of ceramide synthesis ameliorates glucocorticoid-, saturated-fat-, and obesity-induced insulin resistance. *Cell Metab.* 2007 Mar;5(3):167–79.
- Hotamisligil GS, Shargill NS, Spiegelman BM. Adipose expression of tumor necrosis factor-alpha: direct role in obesity-linked insulin resistance. *Science.* 1993 Jan 1;259(5091):87–91.
- Houstis N, Rosen ED, Lander ES. Reactive oxygen species have a causal role in multiple forms of insulin resistance. *Nature.* 2006 Apr 13;440(7086):944–8.
- Hu F, Liu F. Mitochondrial stress: A bridge between mitochondrial dysfunction and metabolic diseases? *Cell. Signal.* 2011 Oct;23(10):1528–33.
- Hubatsch I, Ridderström M, Mannervik B. Human glutathione transferase A4-4: an alpha class enzyme with high catalytic efficiency in the conjugation of 4-hydroxynonenal and other genotoxic products of lipid peroxidation. *Biochem. J.* 1998 Feb 15;330 (Pt 1):175–9. PMID: PMC1219124

- Ikramuddin S, Korner J, Lee W-J, Connett JE, Inabnet WB, Billington CJ, et al. Roux-en-Y Gastric Bypass vs Intensive Medical Management for the Control of Type 2 Diabetes, Hypertension, and Hyperlipidemia. *JAMA. American Medical Association*; 2013 Jun 5;309(21):2240–9.
- Imlay JA. Pathways of oxidative damage. *Annu. Rev. Microbiol.* 2003;57(1):395–418.
- Inoki K, Li Y, Zhu T, Wu J, Guan K-L. TSC2 is phosphorylated and inhibited by Akt and suppresses mTOR signalling. *Nat. Cell Biol. Nature Publishing Group*; 2002 Aug 12;4(9):648–57.
- Jacinto E, Facchinetti V, Liu D, Soto N, Wei S, Jung SY, et al. SIN1/MIP1 maintains rictor-mTOR complex integrity and regulates Akt phosphorylation and substrate specificity. *Cell.* 2006 Oct 6;127(1):125–37.
- Jo J, Shreif Z, Periwal V. Quantitative dynamics of adipose cells. *Adipocyte. Taylor & Francis*; 2012 Apr 1;1(2):80–8. PMID: PMC3609080
- Kanai Y, Segawa H, Miyamoto KI, Uchino H, Takeda E, Endou H. Expression cloning and characterization of a transporter for large neutral amino acids activated by the heavy chain of 4F2 antigen (CD98). *J. Biol. Chem.* 1998 Sep 11;273(37):23629–32.
- Kansanen E, Kuosmanen SM, Leinonen H, Levonen A-L. The Keap1-Nrf2 pathway: Mechanisms of activation and dysregulation in cancer. *Redox Biol.* 2013;1(1):45–9.
- Keith CT, Schreiber SL. PIK-related kinases: DNA repair, recombination, and cell cycle checkpoints. *Science.* 1995 Oct 6;270(5233):50–1.
- Keller MP, Choi Y, Wang P, Davis DB, Rabaglia ME, Oler AT, et al. A gene expression network model of type 2 diabetes links cell cycle regulation in islets with diabetes susceptibility. *Genome Res.* 2008 May;18(5):706–16. PMID: PMC2336811
- Kim SJ, DeStefano MA, Oh WJ, Wu C-C, Vega-Cotto NM, Finlan M, et al. mTOR complex 2 regulates proper turnover of insulin receptor substrate-1 via the ubiquitin ligase subunit Fbw8. *Mol. Cell.* 2012 Dec 28;48(6):875–87. PMID: PMC3534931
- Klok MD, Jakobsdottir S, Drent ML. The role of leptin and ghrelin in the regulation of food intake and body weight in humans: a review. *Blackwell Publishing Ltd*; 2007 Jan;8(1):21–34.
- Klomsiri C, Nelson KJ, Bechtold E, Soito L, Johnson LC, Lowther WT, et al. Use

- of dimedone-based chemical probes for sulfenic acid detection evaluation of conditions affecting probe incorporation into redox-sensitive proteins. *Methods Enzymol.* Elsevier; 2010;473:77–94.
- Knoops B, Loumaye E, Van Der Eecken V. Evolution of the peroxiredoxins. *Subcell. Biochem.* 2007;44:27–40.
- Kobayashi H, Matsuda M, Fukuhara A, Komuro R, Shimomura I. Dysregulated glutathione metabolism links to impaired insulin action in adipocytes. *Am. J. Physiol. Endocrinol. Metab.* 2009 Jun;296(6):E1326–34.
- Kotsias F, Hoffmann E, Amigorena S, Savina A. Reactive oxygen species production in the phagosome: impact on antigen presentation in dendritic cells. *Antioxid. Redox Signal.* Mary Ann Liebert, Inc. 140 Huguenot Street, 3rd Floor New Rochelle, NY 10801 USA; 2013 Feb 20;18(6):714–29.
- Kumar A, Harris TE, Keller SR, Choi KM, Magnuson MA, Lawrence JC. Muscle-Specific Deletion of Rictor Impairs Insulin-Stimulated Glucose Transport and Enhances Basal Glycogen Synthase Activity. *Mol. Cell. Biol.* American Society for Microbiology; 2007 Dec 18;28(1):61–70.
- Kumar A, Lawrence JC, Jung DY, Ko HJ, Keller SR, Kim JK, et al. Fat cell-specific ablation of rictor in mice impairs insulin-regulated fat cell and whole-body glucose and lipid metabolism. *Diabetes.* American Diabetes Association; 2010 Jun;59(6):1397–406. PMID: PMC2874700
- Kuzmicic J, Del Campo A, López-Crisosto C, Morales PE, Pennanen C, Bravo-Sagua R, et al. [Mitochondrial dynamics: a potential new therapeutic target for heart failure]. *Rev Esp Cardiol.* 2011 Oct;64(10):916–23.
- Lackey DE, Lynch CJ, Olson KC, Mostaedi R, Ali M, Smith WH, et al. Regulation of adipose branched-chain amino acid catabolism enzyme expression and cross-adipose amino acid flux in human obesity. *Am. J. Physiol. Endocrinol. Metab.* 2013 Jun 1;304(11):E1175–87. PMID: PMC3680678
- Langin D. Control of fatty acid and glycerol release in adipose tissue lipolysis. *C. R. Biol.* 2006 Aug;329(8):598–607.
- Langin D, Arner P. Importance of TNF α and neutral lipases in human adipose tissue lipolysis. *Trends in Endocrinology & Metabolism.* Elsevier; 2006 Oct;17(8):314–20.
- Langin D, Dicker A, Tavernier G, Hoffstedt J, Mairal A, Rydén M, et al. Adipocyte lipases and defect of lipolysis in human obesity. *Diabetes.* 2005 Nov;54(11):3190–7.

- Laplante M, Sabatini DM. mTOR Signaling in Growth Control and Disease. *Cell*. Elsevier; 2012 Apr;149(2):274–93.
- Lee B-C, Lee J. Cellular and molecular players in adipose tissue inflammation in the development of obesity-induced insulin resistance. *Biochim. Biophys. Acta*. 2014 Mar;1842(3):446–62.
- Lee H, Lee YJ, Choi H, Ko EH, Kim JW. Reactive Oxygen Species Facilitate Adipocyte Differentiation by Accelerating Mitotic Clonal Expansion. *Journal of Biological Chemistry*. American Society for Biochemistry and Molecular Biology; 2009 Feb 23;284(16):10601–9.
- Lim JH, Lee HJ, Ho Jung M, Song J. Coupling mitochondrial dysfunction to endoplasmic reticulum stress response: a molecular mechanism leading to hepatic insulin resistance. *Cell. Signal*. 2009 Jan;21(1):169–77.
- Lim S-Y, Doherty JD, Salem N. Lead exposure and (n-3) fatty acid deficiency during rat neonatal development alter liver, plasma, and brain polyunsaturated fatty acid composition. *J. Nutr*. 2005 May;135(5):1027–33.
- Liochev SI, Fridovich I. The role of O₂⁻ in the production of HO₂·: in vitro and in vivo. *Free Radical Biology and Medicine*. 1994 Jan 1;16(1):29–33.
- Liochev SI, Fridovich I. The effects of superoxide dismutase on H₂O₂ formation. *Free Radical Biology and Medicine*. 2007 May;42(10):1465–9.
- Liu Q, Smith MA, Avilá J, DeBernardis J, Kansal M, Takeda A, et al. Alzheimer-specific epitopes of tau represent lipid peroxidation-induced conformations. *Free Radical Biology and Medicine*. 2005 Mar;38(6):746–54.
- Lloyd RV, Hanna PM, Mason RP. The origin of the hydroxyl radical oxygen in the Fenton reaction. *Free Radical Biology and Medicine*. 1997 Jan 1;22(5):885–8.
- Lobo S, Wiczler BM, Smith AJ, Hall AM, Bernlohr DA. Fatty acid metabolism in adipocytes: functional analysis of fatty acid transport proteins 1 and 4. *J. Lipid Res*. 2007 Mar;48(3):609–20.
- Loewith R, Jacinto E, Wullschleger S, Lorberg A, Crespo JL, Bonenfant D, et al. Two TOR Complexes, Only One of which Is Rapamycin Sensitive, Have Distinct Roles in Cell Growth Control. *Mol. Cell*. Elsevier; 2002 Sep;10(3):457–68.
- Loh K, Deng H, Fukushima A, Cai X, Boivin B, Galic S, et al. Reactive oxygen species enhance insulin sensitivity. *Cell Metab*. 2009 Oct;10(4):260–72. PMID: PMC2892288

- Long EK, Murphy TC, Leiphon LJ, Watt J, Morrow JD, Milne GL, et al. Trans-4-hydroxy-2-hexenal is a neurotoxic product of docosahexaenoic (22:6; n-3) acid oxidation. *J. Neurochem.* Blackwell Publishing Ltd; 2008 May;105(3):714–24.
- Long EK, Olson DM, Bernlohr DA. High-fat diet induces changes in adipose tissue trans-4-oxo-2-nonenal and trans-4-hydroxy-2-nonenal levels in a depot-specific manner. *Free Radical Biology and Medicine.* 2013 Oct;63:390–8. PMID: PMC3737572
- Lumeng CN, Bodzin JL, Saltiel AR. Obesity induces a phenotypic switch in adipose tissue macrophage polarization. *J. Clin. Invest.* American Society for Clinical Investigation; 2007 Jan;117(1):175–84.
- Lumeng CN, DelProposto JB, Westcott DJ, Saltiel AR. Phenotypic switching of adipose tissue macrophages with obesity is generated by spatiotemporal differences in macrophage subtypes. *Diabetes.* 2008 Dec;57(12):3239–46. PMID: PMC2584129
- Magkos F, Bradley D, Schweitzer GG, Finck BN, Eagon JC, Ilkayeva O, et al. Effect of Roux-en-Y gastric bypass and laparoscopic adjustable gastric banding on branched-chain amino acid metabolism. 2013 Aug;62(8):2757–61. PMID: PMC3717831
- Malcom GT, Bhattacharyya AK, Velez-Duran M, Guzman MA, Oalman MC, Strong JP. Fatty acid composition of adipose tissue in humans: differences between subcutaneous sites. *Am. J. Clin. Nutr.* 1989 Aug;50(2):288–91.
- Manning BD, Cantley LC. AKT/PKB signaling: navigating downstream. *Cell.* 2007 Jun 29;129(7):1261–74. PMID: PMC2756685
- Manning BD, Tee AR, Logsdon MN, Blenis J, Cantley LC. Identification of the Tuberous Sclerosis Complex-2 Tumor Suppressor Gene Product Tuberin as a Target of the Phosphoinositide 3-Kinase/Akt Pathway. *Mol. Cell.* Elsevier; 2002 Jul;10(1):151–62.
- Matsuzawa Y. The metabolic syndrome and adipocytokines. *FEBS Letters.* 2006 May 22;580(12):2917–21.
- Maury E, Brichard SM. Adipokine dysregulation, adipose tissue inflammation and metabolic syndrome. *Mol. Cell. Endocrinol.* 2010 Jan 15;314(1):1–16.
- McCormack SE, Shaham O, McCarthy MA, Deik AA, Wang TJ, Gerszten RE, et al. Circulating branched-chain amino acid concentrations are associated with obesity and future insulin resistance in children and adolescents. *Pediatr Obes.* 2012 Sep 7.

- Meister A. Glutathione metabolism and its selective modification. *Journal of Biological Chemistry*. American Society for Biochemistry and Molecular Biology; 1988 Nov 25;263(33):17205–8–17208.
- Michel H, Behr J, Harrenga A, Kannt A. CYTOCHROME COXIDASE: Structure and Spectroscopy. *Annu Rev Biophys Biomol Struct*. Annual Reviews 4139 El Camino Way, P.O. Box 10139, Palo Alto, CA 94303-0139, USA; 1998 Jun;27(1):329–56.
- Miller A-F. Superoxide dismutases: ancient enzymes and new insights. *FEBS Letters*. 2012 Mar 9;586(5):585–95.
- Miseta A, Csutora P. Relationship between the occurrence of cysteine in proteins and the complexity of organisms. *Mol. Biol. Evol*. 2000 Aug;17(8):1232–9.
- Mizuhara H, O'Neill E, Seki N, Ogawa T, Kusunoki C, Otsuka K, et al. T cell activation-associated hepatic injury: mediation by tumor necrosis factors and protection by interleukin 6. *J. Exp. Med*. 1994 May 1;179(5):1529–37. PMID: PMC2191474
- Monteiro R, Azevedo I. Chronic inflammation in obesity and the metabolic syndrome. *Mediators of Inflammation*. 2010;2010(18):1–10. PMID: PMC2913796
- Mootha VK, Lindgren CM, Eriksson K-F, Subramanian A, Sihag S, Lehar J, et al. PGC-1alpha-responsive genes involved in oxidative phosphorylation are coordinately downregulated in human diabetes. *Nat. Genet*. 2003 Jul;34(3):267–73.
- Muoio DM, Newgard CB. Mechanisms of disease: Molecular and metabolic mechanisms of insulin resistance and beta-cell failure in type 2 diabetes. *Nat. Rev. Mol. Cell Biol*. 2008 Mar;9(3):193–205.
- Murphy MP. How mitochondria produce reactive oxygen species. *Biochem. J*. 2009 Jan 1;417(1):1–13. PMID: PMC2605959
- Nakatani Y, Kaneto H, Kawamori D, Yoshiuchi K, Hatazaki M, Matsuoka TA, et al. Involvement of Endoplasmic Reticulum Stress in Insulin Resistance and Diabetes. *Journal of Biological Chemistry*. American Society for Biochemistry and Molecular Biology; 2004 Dec 29;280(1):847–51.
- Nelson KJ, Klomsiri C, Codreanu SG, Soito L, Liebler DC, Rogers LC, et al. Use of dimedone-based chemical probes for sulfenic acid detection methods to visualize and identify labeled proteins. *Methods Enzymol*. Elsevier; 2010;473:95–115. PMID: PMC3835715

- Newgard CB. Interplay between Lipids and Branched-Chain Amino Acids in Development of Insulin Resistance. *Cell Metab.* 2012 May;15(5):606–14.
- Newgard CB, An J, Bain JR, Muehlbauer MJ, Stevens RD, Lien LF, et al. A branched-chain amino acid-related metabolic signature that differentiates obese and lean humans and contributes to insulin resistance. *Cell Metab.* 2009 Apr;9(4):311–26.
- O'Neill LAJ. The interleukin-1 receptor/Toll-like receptor superfamily: 10 years of progress. *Immunol. Rev.* Blackwell Publishing Ltd; 2008 Dec;226(1):10–8.
- Odegaard JI, Chawla A. Connecting Type 1 and Type 2 Diabetes through Innate Immunity. *Cold Spring Harbor Perspectives in Medicine.* Cold Spring Harbor Laboratory Press; 2012 Mar 1;2(3):a007724–4.
- Ogden CL, Carroll MD, Curtin LR, McDowell MA, Tabak CJ, Flegal KM. Prevalence of overweight and obesity in the United States, 1999-2004. *JAMA.* 2006 Apr 5;295(13):1549–55.
- Ogden CL, Carroll MD, Kit BK, Flegal KM. Prevalence of Obesity and Trends in Body Mass Index Among US Children and Adolescents, 1999-2010. *JAMA.* American Medical Association; 2012 Feb 1;307(5):483–90.
- Ozcan U, Cao Q, Yilmaz E, Lee A-H, Iwakoshi NN, Ozdelen E, et al. Endoplasmic reticulum stress links obesity, insulin action, and type 2 diabetes. *Science.* American Association for the Advancement of Science; 2004 Oct 15;306(5695):457–61.
- Parra V, Eisner V, Chiong M, Criollo A, Moraga F, Garcia A, et al. Changes in mitochondrial dynamics during ceramide-induced cardiomyocyte early apoptosis. *Cardiovasc. Res.* 2008 Jan 15;77(2):387–97.
- Parra V, Moraga F, Kuzmicic J, López-Crisosto C, Troncoso R, Torrealba N, et al. Calcium and mitochondrial metabolism in ceramide-induced cardiomyocyte death. *Biochim. Biophys. Acta.* 2013 Aug;1832(8):1334–44. PMID: PMC4118291
- Parra V, Verdejo H, Del Campo A, Pennanen C, Kuzmicic J, Iglewski M, et al. The complex interplay between mitochondrial dynamics and cardiac metabolism. *J. Bioenerg. Biomembr.* 2011 Feb;43(1):47–51. PMID: PMC3286637
- Patsouris D, Li P-P, Thapar D, Chapman J, Olefsky JM, Neels JG. Ablation of CD11c-Positive Cells Normalizes Insulin Sensitivity in Obese Insulin Resistant Animals. *Cell Metab.* Elsevier; 2008 Oct;8(4):301–9.

- Pawlosky RJ, Bacher J, Salem N. Ethanol consumption alters electroretinograms and depletes neural tissues of docosahexaenoic acid in rhesus monkeys: nutritional consequences of a low n-3 fatty acid diet. *Alcohol. Clin. Exp. Res.* 2001 Dec;25(12):1758–65.
- Peraldi P, Spiegelman B. TNF-alpha and insulin resistance: summary and future prospects. *Mol. Cell. Biochem.* 1998 May;182(1-2):169–75.
- Perluigi M, Fai Poon H, Hensley K, Pierce WM, Klein JB, Calabrese V, et al. Proteomic analysis of 4-hydroxy-2-nonenal-modified proteins in G93A-SOD1 transgenic mice—A model of familial amyotrophic lateral sclerosis. *Free Radical Biology and Medicine.* 2005 Apr;38(7):960–8.
- Petersen KF, Befroy D, Dufour S, Dziura J, Ariyan C, Rothman DL, et al. Mitochondrial dysfunction in the elderly: possible role in insulin resistance. *Science.* 2003 May 16;300(5622):1140–2. PMID: PMC3004429
- Pidoux G, Witczak O, Jarnæss E, Myrvold L, Urlaub H, Stokka AJ, et al. Optic atrophy 1 is an A-kinase anchoring protein on lipid droplets that mediates adrenergic control of lipolysis. *EMBO J.* 2011 Nov 2;30(21):4371–86. PMID: PMC3230380
- Poitout V, Robertson RP. Minireview: Secondary β -Cell Failure in Type 2 Diabetes—A Convergence of Glucotoxicity and Lipotoxicity. *Endocrinology. Endocrine Society;* 2002 Feb;143(2):339–42.
- Polak P, Cybulski N, Feige JN, Auwerx J, Ruegg MA, Hall MN. Adipose-Specific Knockout of raptor Results in Lean Mice with Enhanced Mitochondrial Respiration. *Cell Metab. Elsevier;* 2008 Nov;8(5):399–410.
- Poole LB, Karplus PA, Claiborne AI. Protein sulfenic acids in redox signaling. *Annu. Rev. Pharmacol. Toxicol. Annual Reviews;* 2004 Jan 28;44:325–47.
- Potashnik R, Bloch-Damti A, Bashan N, Rudich A. IRS1 degradation and increased serine phosphorylation cannot predict the degree of metabolic insulin resistance induced by oxidative stress. *Diabetologia.* 2003 May 15;46(5):639–48.
- Potter CJ, Pedraza LG, Xu T. Akt regulates growth by directly phosphorylating Tsc2. *Nat. Cell Biol. Nature Publishing Group;* 2002 Aug 12;4(9):658–65.
- Raes G, De Baetselier P, Noël W, Beschin A, Brombacher F, Gh GH. Differential expression of FIZZ1 and Ym1 in alternatively versus classically activated macrophages. *J. Leukoc. Biol. Society for Leukocyte Biology;* 2002 Apr 3;71(4):597–602–602.

- Rasbach KA, Gupta RK, Ruas JL, Wu J, Naseri E, Estall JL, et al. PGC-1 regulates a HIF2 -dependent switch in skeletal muscle fiber types. *Proceedings of the National Academy of Sciences. National Academy of Sciences*; 2010 Dec 14;107(50):21866–71.
- Raza H, John A, Howarth FC. Increased oxidative stress and mitochondrial dysfunction in zucker diabetic rat liver and brain. *Cell. Physiol. Biochem.* Karger Publishers; 2015;35(3):1241–51.
- Rhee SG, Bae YS, Lee SR, Kwon J. Hydrogen peroxide: a key messenger that modulates protein phosphorylation through cysteine oxidation. *Sci Signal. Science Signaling*; 2000 Oct 10;2000(53):pe1–pe1.
- Roth Flach RJ, Matevossian A, Akie TE, Negrin KA, Paul MT, Czech MP. β 3-Adrenergic receptor stimulation induces E-selectin-mediated adipose tissue inflammation. *J. Biol. Chem. American Society for Biochemistry and Molecular Biology*; 2013 Jan 25;288(4):2882–92. PMID: PMC3554952
- Salem N, Litman B, Kim HY, Gawrisch K. Mechanisms of action of docosahexaenoic acid in the nervous system. *Lipids*. 2001 Sep;36(9):945–59.
- Saltiel AR. Insulin resistance in the defense against obesity. *Cell Metab.* 2012 Jun 6;15(6):798–804.
- Sano H, Kane S, Sano E, Miinea CP, Asara JM, Lane WS, et al. Insulin-stimulated Phosphorylation of a Rab GTPase-activating Protein Regulates GLUT4 Translocation. *Journal of Biological Chemistry. American Society for Biochemistry and Molecular Biology*; 2003 Apr 25;278(17):14599–602.
- Sarbassov DD, Ali SM, Kim D-H, Guertin DA, Latek RR, Erdjument-Bromage H, et al. Rictor, a novel binding partner of mTOR, defines a rapamycin-insensitive and raptor-independent pathway that regulates the cytoskeleton. *Curr. Biol.* 2004 Jul 27;14(14):1296–302.
- Sarbassov DD, Guertin DA, Ali SM, Sabatini DM. Phosphorylation and regulation of Akt/PKB by the rictor-mTOR complex. *Science. American Association for the Advancement of Science*; 2005 Feb 18;307(5712):1098–101.
- Sazanov LA. A giant molecular proton pump: structure and mechanism of respiratory complex I. *Nat. Rev. Mol. Cell Biol. Nature Publishing Group*; 2015 May 20;16(6):375–88.
- Scarpulla RC. Transcriptional Paradigms in Mammalian Mitochondrial Biogenesis and Function. *Physiol. Rev. American Physiological Society*; 2008 Apr 1;88(2):611–38.

- Schaur RJ. Basic aspects of the biochemical reactivity of 4-hydroxynonenal. *Mol. Aspects Med.* 2003 Aug;24(4-5):149–59.
- Schipper HS, Prakken B, Kalkhoven E, Boes M. Adipose tissue-resident immune cells: key players in immunometabolism. *Trends Endocrinol Metab.* Elsevier; 2012 Aug;23(8):407–15.
- Sears DD, Hsiao G, Hsiao A, Yu JG, Courtney CH, Ofrecio JM, et al. Mechanisms of human insulin resistance and thiazolidinedione-mediated insulin sensitization. *Proc. Natl. Acad. Sci. U.S.A.* 2009 Nov 3;106(44):18745–50. PMID: PMC2763882
- Segawa H, Fukasawa Y, Miyamoto K, Takeda E, Endou H, Kanai Y. Identification and functional characterization of a Na⁺-independent neutral amino acid transporter with broad substrate selectivity. *Journal of Biological Chemistry.* 1999 Jul 9;274(28):19745–51.
- Seki S, Kitada T, Sakaguchi H, Nakatani K, Wakasa K. Pathological significance of oxidative cellular damage in human alcoholic liver disease. *Histopathology.* Blackwell Science Ltd; 2003 Apr;42(4):365–71.
- Senft D, Ronai ZA. UPR, autophagy, and mitochondria crosstalk underlies the ER stress response. *Trends Biochem. Sci.* Elsevier; 2015 Mar;40(3):141–8.
- She P, Reid TM, Bronson SK, Vary TC, Hajnal A, Lynch CJ, et al. Disruption of BCATm in mice leads to increased energy expenditure associated with the activation of a futile protein turnover cycle. *Cell Metab.* 2007 Sep;6(3):181–94. PMID: PMC2693888
- She P, Zhou Y, Zhang Z, Griffin K, Gowda K, Lynch CJ. Disruption of BCAA metabolism in mice impairs exercise metabolism and endurance. *J. Appl. Physiol.* 2010 Apr;108(4):941–9. PMID: PMC2853195
- Shi H, Kokoeva MV, Inouye K, Tzameli I, Yin H, Flier JS. TLR4 links innate immunity and fatty acid-induced insulin resistance. *J. Clin. Invest.* American Society for Clinical Investigation; 2006 Oct 19;116(11):3015–25–3025.
- Shi Y, Burn P. Lipid metabolic enzymes: emerging drug targets for the treatment of obesity. *Nat Rev Drug Discov.* Nature Publishing Group; 2004 Aug;3(8):695–710.
- Shimoda K, van Deursen J, Sangster MY, Sarawar SR, Carson RT, Tripp RA, et al. Lack of IL-4-induced Th2 response and IgE class switching in mice with disrupted Stat6 gene. *Nature.* Nature Publishing Group; 1996 Apr 18;380(6575):630–3.

- Shimomura I, Funahashi T, Takahashi M, Maeda K, Kotani K, Nakamura T, et al. Enhanced expression of PAI-1 in visceral fat: possible contributor to vascular disease in obesity. *Nat. Med.* 1996 Jul 1;2(7):800–3.
- Shiota C, Woo J-T, Lindner J, Shelton KD, Magnuson MA. Multiallelic disruption of the rictor gene in mice reveals that mTOR complex 2 is essential for fetal growth and viability. *Dev. Cell.* 2006 Oct;11(4):583–9.
- Siddle K. Signalling by insulin and IGF receptors: supporting acts and new players. *J. Mol. Endocrinol. BioScientifica*; 2011 Jun 17;47(1):R1–R10.
- Sies H. Role of metabolic H₂O₂ generation: redox signaling and oxidative stress. *J. Biol. Chem. American Society for Biochemistry and Molecular Biology*; 2014 Mar 28;289(13):8735–41. PMID: PMC3979367
- Steinberg GR, Michell BJ, van Denderen BJW, Watt MJ, Carey AL, Fam BC, et al. Tumor necrosis factor alpha-induced skeletal muscle insulin resistance involves suppression of AMP-kinase signaling. *Cell Metab.* 2006 Dec;4(6):465–74.
- Stephens L, Anderson K, Stokoe D, Erdjument-Bromage H, Painter GF, Holmes AB, et al. Protein kinase B kinases that mediate phosphatidylinositol 3,4,5-trisphosphate-dependent activation of protein kinase B. *Science.* 1998 Jan 30;279(5351):710–4.
- Student AK, Hsu RY, Lane MD. Induction of fatty acid synthetase synthesis in differentiating 3T3-L1 preadipocytes. *J. Biol. Chem.* 1980 May 25;255(10):4745.
- Sun K, Wernstedt Asterholm I, Kusminski CM, Bueno AC, Wang ZV, Pollard JW, et al. Dichotomous effects of VEGF-A on adipose tissue dysfunction. *Proc. Natl. Acad. Sci. U.S.A.* 2012 Apr 10;109(15):5874–9. PMID: PMC3326476
- Surh Y-J, Kundu JK, Na H-K. Nrf2 as a master redox switch in turning on the cellular signaling involved in the induction of cytoprotective genes by some chemopreventive phytochemicals. *Planta Med.* 2008 Oct;74(13):1526–39.
- Surwit RS, Kuhn CM, Cochrane C, McCubbin JA, Feinglos MN. **Diet-Induced Type II Diabetes in C57BL/6J Mice.** 1988 Sep;37(9):1163.
- Takeda K, Kamanaka M, Tanaka T, Kishimoto T, Akira S. Impaired IL-13-mediated functions of macrophages in STAT6-deficient mice. *J. Immunol.* 1996 Oct 15;157(8):3220–2.
- Tang X, Powelka AM, Soriano NA, Czech MP, Guilherme A. PTEN, but not SHIP2, suppresses insulin signaling through the phosphatidylinositol 3-

- kinase/Akt pathway in 3T3-L1 adipocytes. *Journal of Biological Chemistry*. American Society for Biochemistry and Molecular Biology; 2005 Apr 11;280(23):22523–9–22529.
- Taniguchi CM, Emanuelli B, Kahn CR. Critical nodes in signalling pathways: insights into insulin action. *Nat. Rev. Mol. Cell Biol.* 2006 Feb;7(2):85–96.
- Thannickal VJ, Fanburg BL. Reactive oxygen species in cell signaling. *Am. J. Physiol. Lung Cell Mol. Physiol.* American Physiological Society; 2000 Nov 15;279(6):L1005–28–L1028.
- Thomas RL, Gustafsson AB. Mitochondrial autophagy--an essential quality control mechanism for myocardial homeostasis. *Circ. J.* 2013 Aug 27;77(10):2449–54.
- Todd DJ, Lee A-H, Glimcher LH. The endoplasmic reticulum stress response in immunity and autoimmunity. *Nat. Rev. Immunol.* Nature Publishing Group; 2008 Sep;8(9):663–74.
- Tretter L, Adam-Vizi V. Alpha-ketoglutarate dehydrogenase: a target and generator of oxidative stress. *Philos. Trans. R. Soc. Lond., B, Biol. Sci.* 2005 Dec 29;360(1464):2335–45. PMID: PMC1569585
- Tsai AG, Williamson DF, Glick HA. Direct medical cost of overweight and obesity in the USA: a quantitative systematic review. *Blackwell Publishing Ltd*; 2010 Dec 24;12(1):50–61.
- Uldry M, Yang W, St-Pierre J, Lin J, Seale P, Spiegelman BM. Complementary action of the PGC-1 coactivators in mitochondrial biogenesis and brown fat differentiation. *Cell Metab.* Elsevier; 2006 May;3(5):333–41.
- Um SH, Frigerio F, Watanabe M, Picard F, Joaquin M, Sticker M, et al. Absence of S6K1 protects against age- and diet-induced obesity while enhancing insulin sensitivity. *Nature.* Nature Publishing Group; 2004 Aug 11;431(7005):200–5.
- Upadhyay M, Samal J, Kandpal M, Singh OV, Vivekanandan P. The Warburg effect: insights from the past decade. *Pharmacol. Ther.* 2013 Mar;137(3):318–30.
- Utsunomiya-Tate N, Endou H, Kanai Y. Cloning and functional characterization of a system ASC-like Na⁺-dependent neutral amino acid transporter. *J. Biol. Chem.* 1996 Jun 21;271(25):14883–90.
- Uysal KT, Wiesbrock SM, Marino MW, Hotamisligil GS. Protection from obesity-induced insulin resistance in mice lacking TNF- α function. *Nature.* 1997

Oct 9;389(6651):610–4.

Valerio A, Cardile A, Cozzi V, Bracale R, Tedesco L, Pisconti A, et al. TNF-alpha downregulates eNOS expression and mitochondrial biogenesis in fat and muscle of obese rodents. *J. Clin. Invest.* 2006 Oct;116(10):2791–8. PMID: PMC1564431

van den Borst B, Schols AMWJ, de Theije C, Boots AW, Köhler SE, Goossens GH, et al. Characterization of the inflammatory and metabolic profile of adipose tissue in a mouse model of chronic hypoxia. *J. Appl. Physiol.* 2013 Jun;114(11):1619–28.

van der Blik AM, Shen Q, Kawajiri S. Mechanisms of mitochondrial fission and fusion. *Cold Spring Harb Perspect Biol.* Cold Spring Harbor Lab; 2013 Jun;5(6):a011072–2.

Varela L, Horvath TL. Leptin and insulin pathways in POMC and AgRP neurons that modulate energy balance and glucose homeostasis. *EMBO Rep.* 2012 Dec;13(12):1079–86. PMID: PMC3512417

Variyam JN. Patterns of Caloric Intake and Body Mass Index Among U.S. Adults. *FoodReview.* 2002;25(3):16–20.

Wang R-H, Kim H-S, Xiao C, Xu X, Gavrilova O, Deng C-X. Hepatic Sirt1 deficiency in mice impairs mTorc2/Akt signaling and results in hyperglycemia, oxidative damage, and insulin resistance. *J. Clin. Invest. American Society for Clinical Investigation;* 2011a Nov;121(11):4477–90. PMID: PMC3204833

Wang TJ, Larson MG, Vasan RS, Cheng S, Rhee EP, McCabe E, et al. Metabolite profiles and the risk of developing diabetes. *Nat. Med.* 2011b Apr;17(4):448–53. PMID: PMC3126616

Wannamethee SG, Shaper AG, Lennon L, Morris RW. Metabolic Syndrome vs Framingham Risk Score for Prediction of Coronary Heart Disease, Stroke, and Type 2 Diabetes Mellitus. *Archives of Internal Medicine. American Medical Association;* 2005 Dec 12;165(22):2644–50.

WARBURG O. On the origin of cancer cells. *Science.* 1956 Feb 24;123(3191):309–14.

Watanabe Y, Nagai Y, Takatsu K. Activation and regulation of the pattern recognition receptors in obesity-induced adipose tissue inflammation and insulin resistance. *Nutrients. Multidisciplinary Digital Publishing Institute;* 2013 Sep 23;5(9):3757–78–3778.

Watt IN, Montgomery MG, Runswick MJ, Leslie AGW, Walker JE. Bioenergetic

cost of making an adenosine triphosphate molecule in animal mitochondria. *Proceedings of the National Academy of Sciences*. National Academy of Sciences; 2010 Sep 28;107(39):16823–7.

Weisberg SP, McCann D, Desai M, Rosenbaum M, Leibel RL, Ferrante AW. Obesity is associated with macrophage accumulation in adipose tissue. *J. Clin. Invest.* American Society for Clinical Investigation; 2003 Dec;112(12):1796–808. PMID: PMC296995

Westermann B. Mitochondrial fusion and fission in cell life and death. *Nat. Rev. Mol. Cell Biol.* Nature Publishing Group; 2010 Dec;11(12):872–84.

Wolsk E, Mygind H, Grøndahl TS, Pedersen BK, van Hall G. IL-6 selectively stimulates fat metabolism in human skeletal muscle. *Am. J. Physiol. Endocrinol. Metab.* 2010 Nov;299(5):E832–40.

Xu H, Barnes GT, Yang Q, Tan G, Yang D, Chou CJ, et al. Chronic inflammation in fat plays a crucial role in the development of obesity-related insulin resistance. *J. Clin. Invest.* American Society for Clinical Investigation; 2003 Dec 15;112(12):1821–30.

Xu X, Arriaga EA. Chemical cytometry quantitates superoxide levels in the mitochondrial matrix of single myoblasts. *Anal. Chem.* American Chemical Society; 2010 Aug 15;82(16):6745–50. PMID: PMC2929569

Xue X, Piao J-H, Nakajima A, Sakon-Komazawa S, Kojima Y, Mori K, et al. Tumor necrosis factor alpha (TNFalpha) induces the unfolded protein response (UPR) in a reactive oxygen species (ROS)-dependent fashion, and the UPR counteracts ROS accumulation by TNFalpha. *J. Biol. Chem.* American Society for Biochemistry and Molecular Biology; 2005 Oct 7;280(40):33917–25.

Yang B, Rizzo V. TNF-alpha potentiates protein-tyrosine nitration through activation of NADPH oxidase and eNOS localized in membrane rafts and caveolae of bovine aortic endothelial cells. *Am. J. Physiol. Heart Circ. Physiol.* 2007 Feb;292(2):H954–62.

Yang G, Badeanlou L, Bielawski J, Roberts AJ, Hannun YA, Samad F. Central role of ceramide biosynthesis in body weight regulation, energy metabolism, and the metabolic syndrome. *Am. J. Physiol. Endocrinol. Metab.* 2009 Jul;297(1):E211–24. PMID: PMC2711669

Yang Q, Inoki K, Ikenoue T, Guan K-L. Identification of Sin1 as an essential TORC2 component required for complex formation and kinase activity. *Genes Dev.* Cold Spring Harbor Lab; 2006 Oct 15;20(20):2820–32. PMID: PMC1619946

- Yoshida M, Muneyuki E, Hisabori T. ATP synthase--a marvellous rotary engine of the cell. *Nat. Rev. Mol. Cell Biol.* Nature Publishing Group; 2001 Sep 1;2(9):669–77.
- Youle RJ, van der Bliek AM. Mitochondrial fission, fusion, and stress. *Science.* American Association for the Advancement of Science; 2012 Aug 31;337(6098):1062–5.
- Yuzefovych LV, Musiyenko SI, Wilson GL, Rachek LI. Mitochondrial DNA Damage and Dysfunction, and Oxidative Stress Are Associated with Endoplasmic Reticulum Stress, Protein Degradation and Apoptosis in High Fat Diet-Induced Insulin Resistance Mice. Santos J, editor. *PLoS ONE.* Public Library of Science; 2013 Jan 16;8(1):e54059.
- Zhou Y, Jetton TL, Goshorn S, Lynch CJ, She P. Transamination is required for α -ketoisocaproate but not leucine to stimulate insulin secretion. *J. Biol. Chem.* American Society for Biochemistry and Molecular Biology; 2010 Oct 29;285(44):33718–26. PMID: PMC2962470